DISSERTATION

THERMALLY-ASSISTED FRONTAL POLYMERIZATION FOR RAPID CURING OF FIBER-REINFORCED POLYMER COMPOSITES

Submitted by

Iman Naseri

Department of Mechanical Engineering

In partial fulfillment of the requirements

For the Degree of Doctor of Philosophy

Colorado State University

Fort Collins, Colorado

Spring 2024

Doctoral Committee:

Advisor: Susan James

Margarita Herrera-Alonso
Kaka Ma
Travis Bailey

ABSTRACT

THERMALLY-ASSISTED FRONTAL POLYMERIZATION FOR RAPID CURING OF FIBER-REINFORCED POLYMER COMPOSITES

Fiber-reinforced polymer composites (FRPCs) are widely used in a variety of applications owing to their excellent specific mechanical properties, chemical stability, and fatigue resistance. However, the state-of-the-art technologies for manufacturing FRPCs are intensive in terms of time and energy, generate a significant carbon footprint, and require costly resources. In addition, FRPCs lack key non-structural functionalities (e.g., de-icing, damage sensing) required for many applications. Despite the enormous efforts made to improve the manufacturability of FRPCs and address the shortcomings associated with the performance of FRPCs, there is still a pressing need for alternative manufacturing technologies to enable the rapid, energy-efficient, and low-cost manufacturing of multifunctional fiber-reinforced polymer composites.

In this dissertation, a novel technique for rapid and cost-effective manufacturing of multifunctional fiber-reinforced polymer composites is developed by exploiting the frontal polymerization concept and joule heating of nanostructured materials. A nanostructured paper or fabric is integrated into the composite layup to supply the energy required to trigger frontal polymerization via the Joule heating effect. In addition, the nanostructured paper remains advantageous in in-service conditions and imparts new functionalities to the host composite structure. In the first chapter, the recent developments in material systems, as well as heating techniques reported for improving the manufacturability of FRPCs, are reviewed, and frontal polymerization (FP) as a rapid and energy-

efficient technique for curing thermoset matrix composites is introduced. In the second chapter, frontal curing of multifunctional composites via a commercial nanostructured heater (buckypaper) is demonstrated, and the curing behavior of composite laminate is studied under various layup conditions. It is demonstrated that the through-thickness FP manufacturing strategy using an embedded buckypaper surface heater allows for rapid and energy-efficient manufacturing of fully cured composite panels using the conventional tooling materials utilized in the composite industry. However, the temperature profiles developed during the cure cycle, as well as the degree of cure of resin in produced composites, are greatly affected by the thermal properties of the tooling materials, where lower front temperatures and degree of cure are measured for composite panels manufactured using thermally conductive tooling materials such as aluminum. This issue can be effectively addressed by preheating the dry composite layup for a few minutes. Despite the relatively uniform heat generation in nanostructured buckypaper heaters, the infrared thermal imaging of the curing process reveals that the front initiates from multiple locations and propagates in both the through-thickness and in-plane directions. In addition, the de-icing functionality is demonstrated in the cured composite as one of the several possible functionalities imparted to composite structures due to the presence of a buckypaper layer. In the third chapter, a fabric heater is developed by writing laser-induced graphene on aramid fabric using a CO_2 laser and used as an integrated heater for manufacturing FRPCs via the through-thickness FP manufacturing technique. A 10 cm × 10 cm composite panel is successfully cured within only 1 minute with a total energy consumption of 4.13 KJ, which is comparable to the time and energy required for producing a similar composite panel using a buckypaper heater. In addition to composite manufacturing, flexible heaters are prepared with the addition of silicone rubber to fabric heaters. Although the addition of electrically insulating rubber negatively affects the electrothermal performance of

fabric heaters, it greatly improves the durability of fabric heaters. In the fourth chapter, a facile and rapid technique for the preparation of mechanically robust nanocomposite film heaters is developed based on a frontally polymerizable resin system. The mechanical and electrothermal properties of the nanocomposite film heaters are characterized, and the produced heaters are used for out-of-oven manufacturing composite laminates. In the final chapter, the main research findings are summarized, and the recommendations for future studies are presented.

.

ACKNOWLEDGMENTS

I couldn't have reached this goal without the help of many people in my life. I'd like to take this opportunity to thank them for their support. I cannot thank enough my advisor, Dr. James, for all the support she offered me in the toughest moments of my life.

I would like to thank my research committee, Dr. Travis Bailey, Dr. Kaka Ma, and Dr. Margarita Herrera-Alonso, for their precious feedback, which helped me to greatly improve the quality of my research. I also need to thank Dr. Herrera-Alonso for all the time and effort she put into resolving the issues I had during my Ph.D. program.

I also owe the Dean of the Graduate School, Dr. Colleen Webb, and the Deputy General Counsel of the CSU board, Jannine Mohr, a debt of gratitude, who offered me full support. Additionally, I would like to thank Dr. Quynn for her precious feedback on writing my dissertation.

I would like to thank my wife, Mahsa, for her unconditional love and support throughout my PhD program. I would also like to thank my parents, brother, sister-in-law, and Benita for all the encouragement and support they provided me with throughout my studies.

I would also like to extend my thanks to my laboratory members. Finally, I would like to thank the co-authors of my papers, especially Dr. Yourdkhani, which make up chapters 2, 3, and 4 of this dissertation. I would not be able to publish these three papers without the help of my co-authors.

DEDICATION

I dedicate this dissertation to Mahsa, my other half. I will never be able to thank you enough for your support and sacrifices that have allowed me to earn my Ph.D.

TABLE OF CONTENTS

LIST OF TABLES

LIST OF FIGURES

CHAPTER 1: INTRODUCTION

1.1 Fiber-reinforced polymer composites

Fiber-reinforced polymer composites (FRPCs) are increasingly used in a wide variety of industries, including defense, aerospace, wind energy, construction, and architecture, owing to their excellent specific mechanical properties, corrosion resistance, and good fatigue performance.[1–3] The current technology for manufacturing FRPCs involves bulk polymerization of the matrix thermoset resin at elevated temperatures (ca. 180 °C) for several hours (up to 24 h) under combined external pressure and internal vacuum using large autoclaves, ovens, or heated molds that scale in size with the component. This technology is slow and energy intensive, has a large carbon footprint, and involves significant capital investment, leading to a high cost of manufacturing and low production rates.[4,5] In addition to the manufacturing challenges, FRPCs lack key non-structural functionalities (e.g., electrical conductivity) required for a given application.[6] External sub-systems are required to impart additional functionalities into composite structures, which are not ideal as they add to the cost and complexity of design.

1.2 Recent developments in manufacturing of FRPCs

The slow kinetics of the curing reactions during bulk polymerization, along with the inefficient convective heat transfer mechanism inside an autoclave/oven, are the main contributing factors that make existing technologies for manufacturing polymer composites time- and energy-intensive. The growing need for FRPCs in many industries has created a demand for alternative technologies that enable low-cost and high-throughput manufacturing of fiber-reinforced polymer

composites. Formulating new material systems with improved cure characteristics and developing efficient heating techniques are two of the predominant methods of improving the manufacturability of FRPCs. In the following sections, several important developments made in the composite industry over two past decades are briefly reviewed.

1.2.1 Alternative heating methods

A composite layup inside an autoclave or oven is heated via convection, which is inefficient with regards to energy consumption since it requires heating the whole volume of the oven or autoclave.[7] Radiation and conductive heating techniques have been proposed as alternative heating approaches to enable the manufacture of FRPCs at a reduced cost, energy input, and manufacturing time.[8,9]

1.2.1.1 Radiation curing

Radiation heating is an alternative method of curing a composite part, where the energy required for curing the material is supplied via an electromagnetic wave. Electromagnetic radiation (EMR), including ultraviolet (UV), microwave (MW), infrared (IR), gamma, and radio frequency (RF), have been used to heat and cure composites.[10–15] Infrared and microwave heating techniques have been widely studied as promising heating techniques for out-of-oven composite manufacturing and will be discussed in more detail. Infrared radiation heating relies on the conversion of electromagnetic energy to heat by resonance vibration of molecules. Materials containing couplings such as CH, CH_2, and CH_3 in their chemical structure can be effectively heated via infrared radiation. These molecules vibrate at specific frequencies. The large majority of the vibration frequencies of these molecules correspond to the short and medium wavelength infrared region above 1.5 μm. When irradiated by infrared light, the vibrations intensify and produce thermal energy.[16] Infrared heating is efficient, controllable, safe, cost-efficient, and scalable.

However, the successful integration of the infrared heating method into composite processing techniques requires optimizing the heating process parameters as the interaction between infrared radiation and composite layup is quite complex. The efficiency of the heating process depends on various factors, including the radiative properties of the matrix and reinforcement and their volume fractions, the orientation of the part with respect to the heater, the layup volume, the heater-layup distance, the heater power, and the wavelength of the incoming infrared radiation.[17–19] Experimental studies have shown that heater-layup distance is a key factor that greatly affects the in-plane as well as through-thickness temperature gradient formed in the composite layup during the cure cycle. When the distance between the heater and layup is too short, the formation of large temperature gradients along the surface and across the thickness of the composite layup occurs, where a temperature difference of ~9 °C was measured across the thickness of a thin carbon panel consisting of only four plies of fabric.[20] Radiative properties of the matrix and reinforcement have a profound impact on the efficiency of the heating process. For example, while carbon fibers are opaque and absorb most of the incoming infrared radiation, glass fibers mainly transmit infrared radiation. Similarly, infrared curing of geometrically complex parts is more challenging than infrared curing of flat parts as a high portion of incoming radiation is reflected. Numerical simulations are typically performed to identify optimum process parameters to ensure uniform curing of complex parts. For example, mathematical models were developed to predetermine optimum process parameters for manufacturing an aerospace wing stiffener.[21] Similarly, mathematical models were developed to identify appropriate process parameter settings, such as winding speed and heater power, for continuous infrared curing of hoop-wound glass and carbon cylinders.[22]

Microwave heating is an efficient technique for the volumetric heating of polymers, which has been used for various purposes in the polymer industry such as in the vulcanization of rubbers and the curing of thermoset resins and their composites.[23,24] The mechanism of heat generation in polymers when they are irradiated by microwave radiation is dipole reorientation. Dipoles realign themselves with the oscillating electric field in order to be in phase with the field. These frequent reorientations of the dipoles are resisted by the inertial, frictional, elastic, and molecular interaction forces, leading to the generation of heat in polymers.[25] Microwave heating enables energy-efficient curing of FRPCs, where a 36-fold reduction in energy required for manufacturing FRPCs was reported.[26] Although the microwave curing technique shows promise for energy-efficient manufacturing of FRPCs, the adoption of this heating technique for processing fiber-reinforced polymer composites at industrial scales faces several challenges. Conventional metal tools that are used for the thermal curing of composites are not ideal for microwave processing of FRPCs since they reflect electromagnetic radiation, and this reflection can lead to the formation of an arc.[27] The uneven temperature distribution and the formation of hot spots in composite layups due to non-uniformity within the electromagnetic field are other major concerns in the microwave curing of polymer composites.[28] Another issue is the formation of an arc in carbon fiber-reinforced composites due to the high microwave absorption characteristics of carbon fiber, which negatively affects the mechanical properties of cured composites.[29,30] In addition, microwave ovens are costly to acquire and maintain.

There are also a few reports on using electromagnetic radiation in the ultraviolet and radio frequency ranges for curing composites. UV curing requires the use of special resin formulations and has been mainly utilized in combination with the filament winding process for manufacturing glass fiber-reinforced composites due to the very short penetration depth of UV radiation in aramid

and carbon fabrics.[31,32] Radio frequency heating has been used for supplying the energy required for partial curing of the matrix thermoset resin in continuous processing of carbon fiber prepregs.[33] The RF heating technique was also used to cure carbon fiber panels, and the effect of RF heating on the quality of matrix-fiber bonding was studied. The results showed that the RF heating technique had no detrimental effect on the quality of interfacial bonds formed between the matrix and fiber.[34]

1.2.1.2 Direct conductive curing

Direct conductive heating is an alternative curing method, which significantly reduces the energy demand of the curing process while eliminating the need for using expensive autoclaves/ovens. In this curing approach, heat is directly supplied to the composite layup via conduction, either from a heated mold or direct resistive heating of a conductive material.[35,36] The latter approach is advantageous as the acquisition and maintenance of heated tools is costly. In direct resistive heating, the heat required for curing the thermoset resin is supplied by passing a small amount of electric current through a conductor, where electric energy is converted into heat via Joule's effect. A wide range of conductive materials, including carbon fiber, metal meshes, and carbon nanomaterials, have been used as resistive elements for directly heating composite laminates.[37–39] Carbon nanomaterials resistive heaters are particularly attractive for energy-efficient and low-cost manufacturing of FRPCs due to their low thermal mass, excellent heat generation capabilities, uniformity of heat generation, and ease of integration into the composite layup.[40,41] Nanomaterial-based heaters can be either used as detachable/reusable external heaters on the surface of the composite layup or be integrated into the layup and be co-cured with the composite. In the latter case, the nanostructured layer can impart new functionalities (e.g., de-icing, damage sensing) into a composite structure in service conditions.[42–44] Fabrication of a resistive heater based on

nanomaterials requires forming a continuous network of conductive nanoparticles to enable the flow of electrons. Broadly speaking, carbon nanomaterials have been used in three main forms as a Joule heater for manufacturing FRPCs: 1) nanostructured paper or fabric, 2) nanocomposite films, and 3) coated on glass fabrics.

Buckypaper (BP) and Laser-induced graphene (LIG) are two nanostructured materials of importance which have been used for various purposes in composite research (e.g., damage sensing, composite curing, and fire retardancy). Buckypaper is a thin sheet of carbon nanotube aggregates (Figure 1-1 a, b). The excellent electrothermal efficiency of BP (Figure 1-1 c, d) coupled with its porous microstructure, low density, high electrical conductivity, good thermal and chemical resistance, and high flexibility make it an ideal material for the electrical curing of multifunctional composites.[42,45,46] Electrical curing of FRPCs using buckypaper was first demonstrated in 2014, where an aligned carbon nanotube film was used for curing a carbon fiber laminate. The produced laminate showed a comparable degree of cure to that measured for a similar oven-cured laminate while consuming several orders of magnitude less energy.[47] Similarly, multi-walled carbon nanotube buckypaper was used as a resistive element for out-of-oven curing glass fiber/epoxy resin composites. Compared to a similar panel fabricated using the hot compression molding process, 98% less energy was used in the direct conductive curing method.[48] The comparison of the mechanical properties of two series of composite panels cured using direct conductive heating and conventional oven curing methods revealed that there was no significant difference in the short beam shear, dynamic mechanical analysis, and double-edge notch tensile tests, indicating the capabilities of the direct conductive curing method for energy-efficient manufacturing high-quality FRPCs. In addition to energy saving, an integrated nanostructured paper can impart new functionalities to the host composite structure, eliminating the need for using

external subsystems.[49] For instance, Figure 1-1 e, f shows the de-icing functionality in a composite wing.

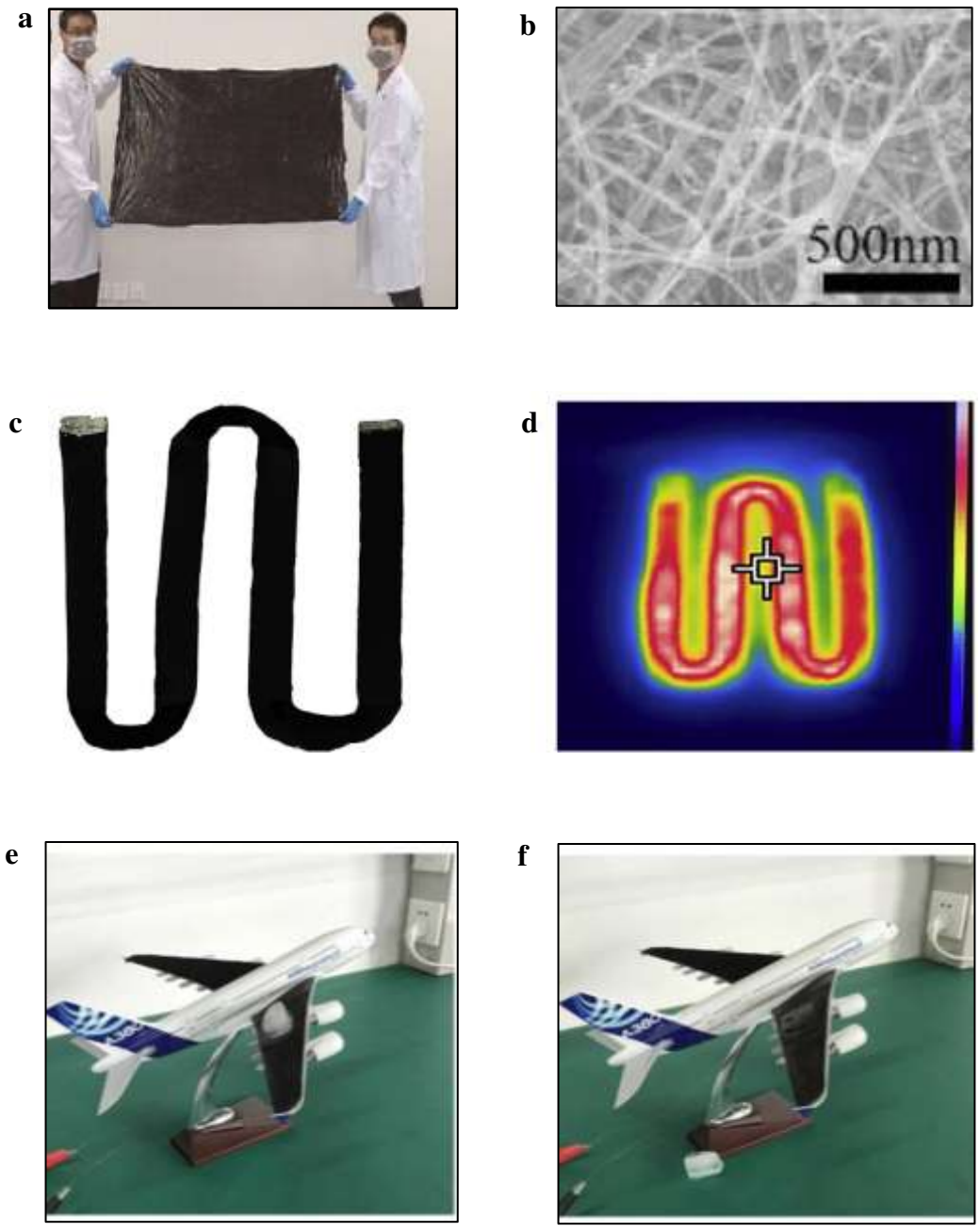

Figure 1-1. Energy-efficient manufacture of multifunctional composites using an integrated buckypaper heater. (a) Digital image of a roll of buckypaper.[5] (b) Microstructure of buckypaper.[5] Copyright (2017) Elsevier (c, d) Digital and infrared images of a buckypaper heater.[46] Copyright (2016) Elsevier (e, f) Demonstrating the de-icing functionality in a composite panel containing an integrated buckypaper surface layer.[5] Copyright (2017) Elsevier. All figures are reprinted with permission from publishers.

Although the direct conductive heating method enables low-cost and energy-efficient manufacturing of FRPCs, uniform heating of composite laminates across the thickness remains challenging. For example, a temperature difference of 15 °C was measured between the top and bottom surfaces of a 3.3 mm thick composite layup.[5] The formation of a large temperature gradient across the thickness can cause non-uniform curing composite laminates and buildup of a high level of residual stresses. An effective strategy for mitigating this issue is embedding several buckypaper interlayers in the layup to enable heating of the layup from the inside. However, dynamic mechanical measurements revealed that electrically cured laminates containing buckypaper interplies exhibited an inferior storage modulus compared to that measured for an autoclave-cured laminate due to the formation of void at buckypaper interfaces with composite plies.[50]

Laser-induced graphene, commonly known as LIG, is another conductive nanostructured material of importance for composite manufacturing. LIG is a porous form of graphene, which is produced by direct laser writing on a carbon material at ambient conditions. Upon irradiation of an appropriate precursor material using a laser source, the precursor is converted into graphene via a photothermal or photochemical effect (Figure 1-2 a).[51–53] The morphology and properties of the LIG can be easily tailored by controlling the process parameters: primarily the laser input power, scanning speed, and composition of the precursor. LIG shows excellent thermal and electrical properties, tunable properties, and mechanical flexibility. In addition, the production process of LIG is scalable, inexpensive, and fast.[54] LIG can be written on various precursors including polyimide (PI),[55] Polyetheretherketone (PEEK),[56] aramid fabric,[57] and wood.[58] LIG shows more uniform heat generation as compared to traditional metallic resistive heaters (Figure 1-2 b).[59]

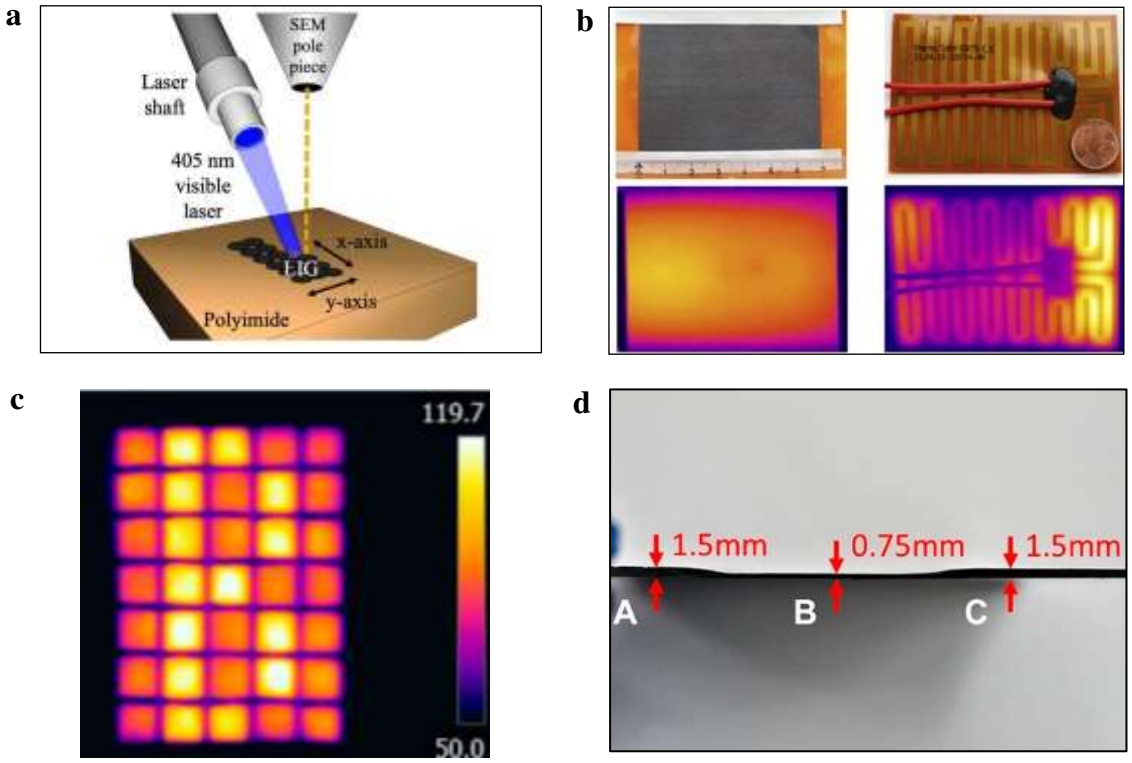

Figure 1-2. Laser-induced graphene. (a) Direct writing of LIG on a polyimide film using a 405 nm blue laser.[52] Copyright (2020) American Chemical Society (b) Heat generation via the electrothermal effect in a LIG heater and a conventional metallic resistive heater.[59] Copyright (2019) Elsevier. (c) Creation of a heater with multiple heating zones by tuning the lasing process parameters.[60] (d) Uniform curing of a part of varying thickness using a LIG heater with multiple heating zones.[60] Copyright (2020) American Chemical society. All figures are reprinted with permission from publishers.

Free-standing LIG-PI heaters were prepared using a PI paper as a precursor and utilized for direct conductive curing of FRPCs. Energy savings of 85% were reported compared to the oven curing approach. Additionally, laminates cured using the LIG heater showed the same degree of cure and mechanical properties compared to those measured in a reference oven-cured panel.[60] Another key advantage of LIG-based heaters is the ability to create multiple heating zones in a single heater via tuning the lasing process parameters during the production process (Figure 1-2 c). This unique characteristic of LIG-based resistive heaters has been used to uniformly cure composites with variable thickness (Figure 1-2 d), which is quite challenging to achieve using heaters with a single

heating zone. In another study, a free-standing laser-induced graphene heater was obtained by one-step laser irradiation on polybenzoxazine resin followed by rapid quench-peeling.[61] The produced paper was then used as a resistive element for direct conductive curing of composite laminates. Energy savings of 45% were realized while no adverse effect on the mechanical properties of produced composites was measured.

Nanocomposite film heaters are another form of nanomaterial-based resistive heaters that have found applications in composite manufacturing. Nanocomposite film heaters consist of a conductive nanomaterial dispersed in a polymer matrix. Nanocomposite film heaters typically show lower electrical conductivity and electrothermal efficiency compared to buckypaper and LIG due to the lower nanoparticle content. A unique feature of nanocomposite film heaters is the ability to design and create heaters with intrinsic self-regulating heating capabilities.[62] This feature allows for the safe curing of FRPCs without the risk of overheating. The large volume expansion that occurs in the thermoplastic matrix at the transition temperature results in a sudden increase in inter-particle distance between conductive particles, leading to a significant drop in the heat generation capabilities of the heating element. Upon cooling, the conductive network is re-formed, and the heat generation capability of the nanocomposite film is restored.[63] The thermoplastic nature of the nanocomposite film allows for easy fabrication of flexible heaters with complex shapes. In 2020, direct conductive curing of FRPCs using a nanocomposite film heater based on graphene nanoplates and high-density polyethylene with intrinsic self-regulating heating capabilities was reported.[64] Compared to conventional thermal processing methods, only 1% of the energy was consumed, and no drop in mechanical properties or degree of cure was measured. Similarly, bio-based nanocomposite films with intrinsic self-regulating heating capabilities were prepared and

embedded in composite layups to fabricate natural fiber-reinforced composites with integrated real-time deformation and damage sensing capabilities, and enhanced water barrier properties.[65]

The third approach for creating nanostructured Joule heaters is the direct deposition of carbon nanomaterials on conventional fabrics used in the composites industry. This technique allows for the creation of efficient fabric heaters that can be easily integrated into the composite layups. However, production processes for this type of heater typically involve multiple steps, making large-scale and low-cost manufacturing of this type of heater quite challenging. Unidirectional glass fiber-carbon nanotube Joule heaters were fabricated using a mask-assisted wet chemical deposition/printing process and were embedded in carbon fiber composite laminates to supply the energy required for composite manufacturing.[66] Three-point bending tests revealed a drop of 75 MPa in the bending strength of produced composites compared to oven-cured laminates, whereas the glass transition temperature was almost the same. The de-icing functionality in manufactured laminates was also demonstrated, where an ice cube with a volume of 16 mL was completely melted within 8 min. In another study, LIG was first created on a polyimide substrate before then being transfer-printed onto a fiberglass prepreg to form a uniform surface coating.[67] LIG-coated FRPCs cured through Joule heating (LIG-cured FRCs) were found to have a high degree of cure of 96%, comparable to oven-cured ones, while requiring 89% less specific energy.

1.2.2 New material systems

While previously described heating methods can improve the energy efficiency of the curing process of composites, they have a small impact on the cure times, as the cure cycle time is mainly controlled by the kinetics of bulk polymerization. An important direction for improving the manufacturability of FRPCs has been focused on developing new material systems with improved cure characteristics.

1.2.2.1 Out-of-autoclave prepregs

Out-of-autoclave (OoA) prepregs are a new generation of prepregs, which have gained popularity in the composite industry in recent years. These prepregs enable manufacturing of autoclave-quality composite components through vacuum-bag-only cure in an oven at ambient pressure when processed under optimal conditions.[68] Out-of-autoclave prepregs possess unique microstructure, allowing for the evacuation of entrapped air, vaporized moisture, or any other form of volatile prior to resin gelation under a low atmospheric pressure (1 atm). Unlike traditional prepregs, OoA prepregs are only partially impregnated and there are dry areas in the prepreg intended to create paths for air evacuation at the beginning of the cure cycle. During processing, dry regions are progressively infiltrated with resin to produce a uniform, void-free structure.[69,70] Although the use of OoA prepregs reduces costs associated with the acquisition and operation of autoclaves, processing of OoA prepregs requires using an oven or a heated mold which is still time- and energy-intensive.

1.2.2.2 Fast curing resins

The conventional resin systems used in the composite industry are solidified via bulk polymerization. The kinetic of crosslinking reactions in these bulk polymerizable resin systems is slow, necessitating prolonged curing at elevated temperatures to ensure full cure of resins. One approach for improving the manufacturability of polymer composites is developing new resin chemistries with fast cure rates. New generation of curing agents, such as imidazole family, have been used to formulate resin systems with cure times less than 20 min.[71] While these snap-cure resin systems are promising for applications where mass production of polymer composites is required (e.g., automotive industry), widespread use of these resin systems is limited by two issues. The short pot life of such resin systems makes fabrication of large composite components

challenging. In addition, exothermic energy released during the short cure process is large, leading to the generation of a large temperature gradient across the thickness of the laminate. Warpage and shape distortion are common processing issues observed during the manufacturing of FRPCs using fast-curing resin systems.[72]

1.2.2.3 Frontally polymerizable resins

Frontal polymerization (FP) offers a fast and energy-efficient route for curing thermoset resins and their composites.[73,74] In contrast to bulk polymerization in which an external energy source (e.g., autoclave, oven, heated mold) is required to continuously supply heat to the resin throughout the cure cycle, FP requires minimal energy input as it is driven by the exothermic enthalpy of polymerization. In FP, a local energy stimulus is applied to the solution of monomer and initiator. Once polymerization is initiated, a propagating front is formed and advances by the exothermic heat of reaction, resulting in a self-sustained curing process.[75] Figure 1-3 shows frontal ring-opening metathesis polymerization (FROMP) of dicyclopentadiene (DCPD) monomer in a test tube. Frontal polymerization has been demonstrated in various resin systems including epoxies,[76] polyurethanes,[77] acrylates,[78] and dicyclopentadiene.[79]

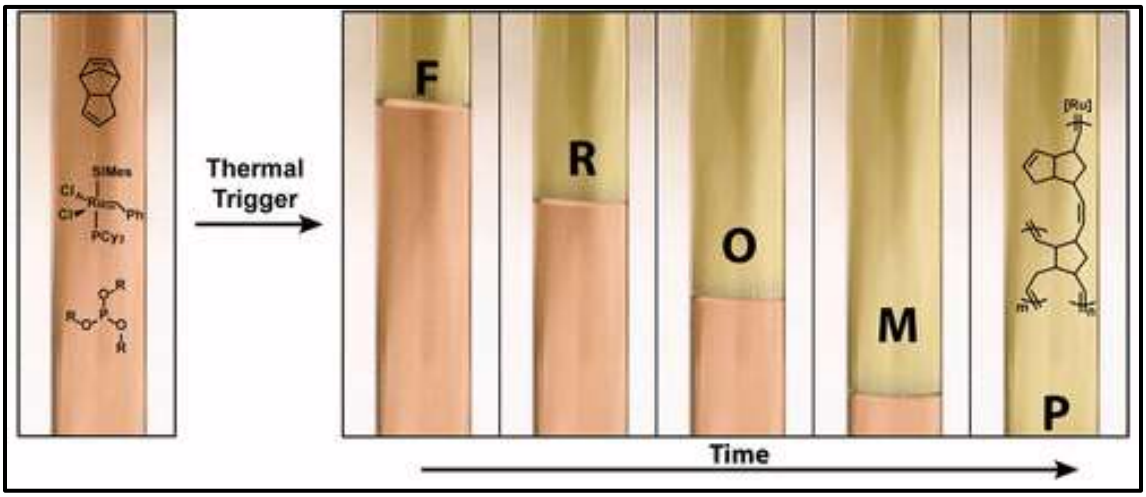

Figure 1-3. Frontal ring-opening metathesis polymerization (FROMP) of dicyclopentadiene (DCPD) resin in the presence of second-generation Grubbs' catalyst in a test tube.[74] Reprinted with permission from publisher. Copyright (2017) American Chemical Society.

While FP resin systems have been widely used for rapid manufacturing of various polymeric materials such as foams,[80] functionally graded polymers,[81] and hydrogels,[82] there are few experimental studies on the manufacturing of fiber-reinforced polymer composites via FP resin systems. The presence of a high-volume fraction of inert reinforcement in composite layup is a key issue, making frontal manufacturing of fiber-reinforced polymer composite quite challenging. Dicyclopentadiene and epoxy are two FP resin systems of importance for manufacturing FRPCs. The frontal ring-opening metathesis polymerization (FROMP) of the dicyclopentadiene resin in the presence of second-generation Grubbs' catalyst and alkyl phosphite inhibitor exhibits the high reactivity required for manufacturing FRPCs.[74] In addition, polydicyclopentadiene (pDCPD) exhibits high fracture toughness and excellent chemical resistance, making DCPD resin an attractive choice for manufacturing polymer composites used in harsh environments.[83] However, it is important to note that typical commercial fibers with epoxy type sizing are not compatible with DCPD resin due to the non-polar nature of DCPD resin.[84] Fibers with special sizing designed for non-polar resins are required for manufacturing

mechanically strong composites, which are not readily available in the market. Epoxy resins, on the other hand, have been widely used for manufacturing high-performance composites for many years. Epoxy FP systems consist of three main components including a monomer, a photo initiator, and a thermal initiator. The mechanism of curing reactions for these epoxy FP systems is radical-induced cationic frontal polymerization (RICFP).[85] In RICFP, a cation is first formed by the cleavage of a photo initiator using a UV light source. The formed cation then abstracts a proton from a monomer and forms a highly reactive super acid. Following the formation of the super acid, it reacts with a monomer, resulting in heat generation. The produced heat will subsequently cleave the thermal radical initiator producing reactive radicals which can cleave the photo initiators and form another acid. That starts the exothermic polymerization in the adjacent region. The dual-initiator configuration allows for achieving long pot life in the order of one month at 50 °C while the resin formulation is being kept in the dark.[76]

The curing characteristics of composite laminates manufactured via frontal polymerization greatly depend on how the FP is performed. The in-plane and through-thickness curing methods are two FP manufacturing strategies for curing FRPCs.[86] In the in-plane curing method, a local energy source is applied to a small area of the composite layup for a few seconds or minutes to enable the initiation and propagation of FP within the plane of the composite layup. Resistive wires and UV light have been used as an energy source for triggering FP in DCPD and epoxy matrix composites, respectively.[86,87] The in-plane FP manufacturing method was recently used to produce FRPCs panels with up to 50 vol% of carbon fibers at the laboratory scale (Figure 1-4). While this curing strategy enables several orders of magnitude of reduction in manufacturing time and energy, adoption of FP for manufacture of composite components at the industrial scale is currently facing several challenges.

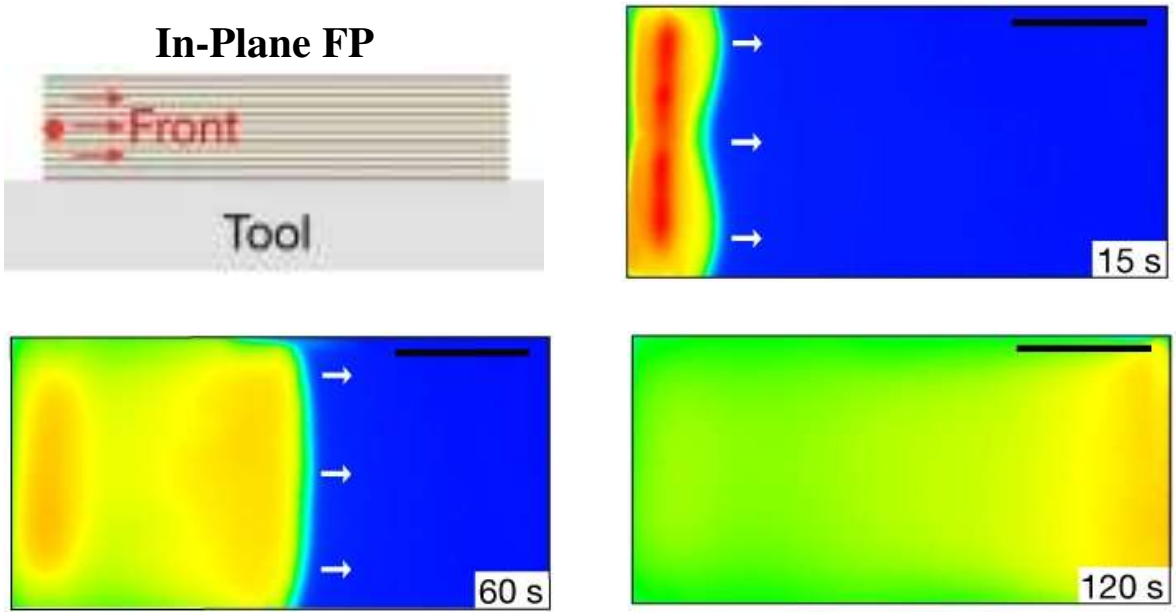

Figure 1-4. In-plane frontal curing of a carbon FRPC panel using a resistive wire as the local thermal trigger.[86] Reprinted with permission from publisher. Copyright (2018) Springer Nature.

One of the major drawbacks of in-plane FP (within the plane of reinforcements) is that the time required for curing of a part is proportional to the front travel distance. Given low front velocity of 10 cm min^{-1}, cure time for large composite structures can take up to several hours, diminishing the time saving benefit of FP for manufacturing of large composite structures. Another issue with the in-plane FP method is that thermally insulating tooling materials (e.g., polymer foam) are required to minimize heat loss to the environment and sustain front propagation. These tooling materials are not common in the composites industry due to their low durability. In addition, produced composites show a low degree of cure, ~80%, due to the reduced energy density of the resin and heat losses to the surroundings. An effective strategy for reducing cycle time in frontally cured DCPD carbon fiber panels is using multiple resistive wires for initiating FP from multiple locations to shorten front travel distance.[88] Although this strategy enables a 5-fold reduction in cure time, processing-induced defects (e.g., voids, thickness variation) were observed in the areas

where two fronts merged. Simulations showed that this issue can be mitigated by replacing thermally insulating tooling with a heated aluminum mold. Although this FP manufacturing strategy effectively reduces cure time, heated molds are required, which are costly to acquire and maintain. In addition, the short pot life of the DCPD resin system remains a major issue, limiting the adoption of the multiple-front initiation strategy at a large scale. The in-plane FP curing technique was also used to manufacture epoxy matrix composites with a fiber volume fraction of 35%. The frontally cured composite showed comparable mechanical properties to those of a panel fabricated using conventional thermal processing method.[85] One issue with FP epoxy systems in composite manufacturing is that producing laminates with a high fiber volume fraction is quite challenging due to the low reactivity of these epoxy systems. Effective approaches reported for achieving higher fiber volume fraction include tuning the resin chemistry to maximize the rate of heat release as well as utilizing thermally insulating Teflon-covered PVC foam cores as tooling to minimize the rate of heat loss through the boundaries. These techniques enable frontal curing of epoxy matrix FRPCs with a fiber volume fraction of 46 %, which is still slightly lower than the fiber volume fraction reported for DCPD matrix composites.[89]

The through-thickness FP curing method (Figure 1-5) is an alternative strategy for frontal curing FRPCs. In this curing technique, the entire surface of the composite layup is heated using a surface heater rather than local heating of a small area of the composite layup using a resistive wire or UV light.[86] This curing technique is advantageous over the in-plane curing method as the front travel distance is limited to the thickness of the composite layup, which is always in the order of a few millimeters or centimeters.

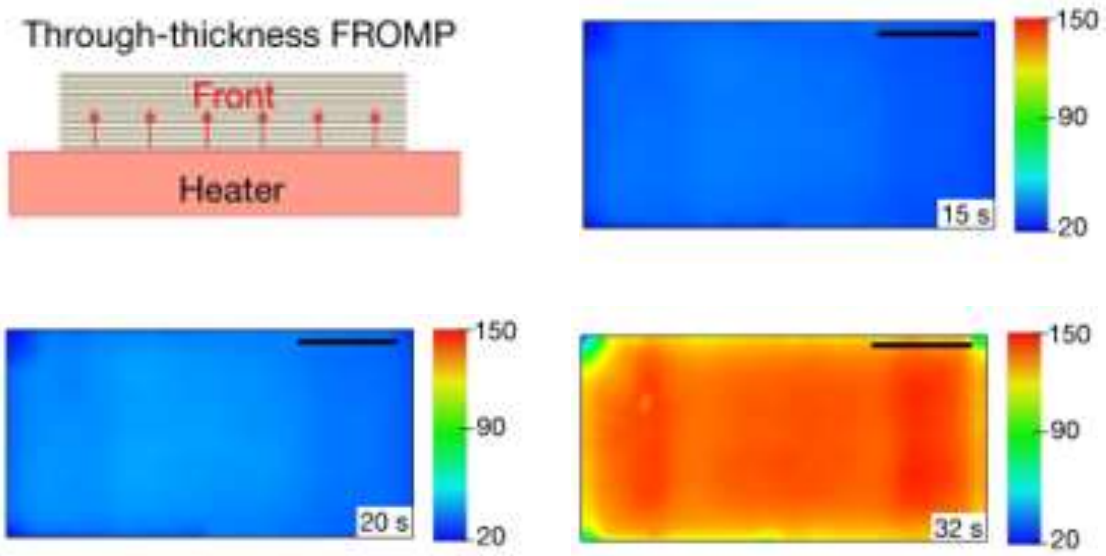

Figure 1-5. Rapid fabrication of a composite panel via the through-thickness FP manufacturing method.[86] Reprinted with permission from publisher. Copyright (2018) Nature Springer.

The through-thickness FP manufacturing method was recently used to rapidly manufacture vascularized carbon fiber-reinforced composite with circular microchannels. Indeed, the chemical energy released during frontal polymerization was used to depolymerize an embedded sacrificial template and create microchannels within the matrix. This curing strategy enabled three and four orders of magnitude reduction in the fabrication time and energy, respectively, compared to conventional curing and vascularization of similar size samples in an oven.[90] Table 1-1 summarizes the benefits and limitations of various solutions proposed for improving the manufacturability of FRPCs.

Computational studies have also been conducted to provide a better understanding of the manufacturing of FRPCs using FP resin systems. In one study, a representative volume element (RVE) model was developed to predict the effects of material property uncertainties (e.g., impurities in the monomer or catalyst) and the presence of voids in the layup on frontal curing of

DCPD matrix carbon fiber composites.[91] The results of numerical simulations revealed that both factors greatly affect the rate of polymerization, where a reduction of 25% in the rate of polymerization was predicted for a panel containing 3 vol% of voids. In another study, 2D simulations were conducted based on the reaction-diffusion model to examine the effect of the microstructure (fiber volume fraction, tow shape, and size) on the through-thickness frontal curing of unidirectional carbon fiber composites.[92] The simulation results showed that the fiber volume fraction and the tow shape affect the frontal curing of DCPD matrix carbon fiber panels, while tow size has no effect. In a follow-up study, three-dimensional finite element analysis was performed to simulate the frontal polymerization process in laminates with multiple fiber angles (e.g., cross-ply) and study the effect of reinforcement type on the frontal curing process of DCPD matrix composites.[93] This study showed that the front velocity in cross-ply laminates is 20-25 % lower than the front velocity predicted in a unidirectional laminate. In addition, the simulation results showed that the thermal conductivity of the reinforcement has a significant impact on front velocity in unidirectional composites, where a reduction of 92% in front velocity was predicted in glass fiber-reinforced composite compared to the front velocity predicted for a UD carbon fiber composite. Similarly, the degree of cure in glass fiber-reinforced composites was predicted to be 20% lower than the degree of cure predicted for a carbon fiber laminate.

Table 1-1. Comparison of the benefits and limitations of various solutions proposed for improving the manufacturability of FRPCs.

Solution	Advantages	Limitations
Infrared heating	• Energy-efficient • Controllable • Scalable	• Long cure cycle times • No multifunctionality • Difficult to manufacture geometrically complex parts
Microwave heating	• Energy-efficient • Volumetric heat generation method	• Costly microwave ovens • Special tooling materials are required. • Arc formation • No multifunctionality
Ultraviolet heating	• Fast • Energy-efficient	• Limited to thin composites • Special resin formulations are required. • Limited to glass fibers • No multifunctionality
Radio frequency heating	• Energy-efficient • High heating rate	• Costly resources are required. • No multifunctionality
Direct conductive heating	• Energy-efficient • Multifunctional composites • Low capital cost	• Long cure cycle time • Difficult to manufacture thick composites.

Fast-cure resins	• Fast • Energy-efficient	• Warpage and shape distortion • Costly ovens or autoclaves are required. • No multifunctionality
Out-of-autoclave prepregs	• No need for costly autoclaves	• Long cure cycles • Costly ovens • No multifunctionality
In-plane frontal curing	• Energy-efficient • Inexpensive	• Cure time is proportional to component size. • Thermally insulating tooling materials are required. • No multifunctionality
Through-thickness frontal curing	• Fast • Energy-efficient • Inexpensive • Scalable	• No multifunctionality • Thermally insulating tooling materials are required.

1.3 Overview of Dissertation

1.3.1 Problem Statement

Poor manufacturability of fiber-reinforced polymer composites is a major issue, limiting the widespread adoption of FRPCs in many potential applications where they outperform their metallic counterparts. In addition, the poor electrical and thermal conductivities of FRPCs lead to the conservative design of lightweight structures and the use of add-on attachments for performing non-structural functions, preventing their full weight-reduction potential. Despite extensive efforts that have been made to address the processing challenges as well as the shortcomings associated with the performance of FRPCs, there is still a need for developing alternative manufacturing techniques to enable low-cost, high throughput, and energy-efficient manufacturing of multifunctional composite components. Among various solutions proposed for improving the manufacturability of FRPCs, the through-thickness FP manufacturing method shows promise for developing the next-generation composite manufacturing technology. However, the shortcomings associated with this manufacturing technique, such as the need for using special tooling materials or heated molds, hinder the widespread adoption of this manufacturing technique at the industrial scale. In addition, the frontally cured composites lack the key non-structural functionalities essential for many applications, and still, add-on attachments are required to impart the functional properties to the composite structures.

1.3.2 Research Aims and Objectives

The aim of this dissertation is to develop a novel manufacturing technique for rapid and low-cost manufacturing of multifunctional fiber-reinforced polymer composites. This aim is achieved by exploiting the frontal polymerization concept and joule heating of nanostructured materials. A nanostructured paper or fabric is integrated into the composite layup to trigger the through-

thickness frontal polymerization. As opposed to the common FP manufacturing methods in which heat is supplied for only a few seconds, the heat is continuously supplied to the composite layup during the entire cure cycle. It is hypothesized that the uniform heating of the entire surface of the composite layup using a nanostructured heater with a uniform heat generation capability enables the initiation of frontal polymerization along the entire surface of the composite layup. Following the initiation of frontal polymerization at the surface, the front propagates through the thickness of the layup and converts liquid monomer into cured polymer. The short travel distance of the front in the through-thickness curing technique (typically a few millimeters or centimeters) allows for rapid curing of composite components, irrespective of their size, within a few minutes. In addition, short front travel distance, along with the external heat supplied to the composite layup during the entire cure cycle, mitigate the risk of front quenching once conventional thermally conductive tooling materials are used for composite manufacturing. Another benefit of continuously supplying heat to layup during frontal polymerization is that the additional heat provided by the heater contributes to the completing curing reactions and enables manufacturing of fully cured composite parts in one step. Additionally, the integrated nanostructured paper or fabric can impart new functionalities to the cured composite, eliminating the need for using the external subsystems, which add to the weight and cost.

The main research questions in this dissertation are as follows:

- How does frontal polymerization initiate in the through-thickness FP curing technique using an integrated nanostructured heater? Does FP initiate along the entire surface, or does it initiate locally? How does the front propagate in the through-thickness FP curing technique?

- How do process parameters, including tooling material and cure cycle time, affect the frontal curing of FRPCs?
- How does the position of the heater affect the curing characteristics of composite laminates?
- Can efficient resistive heaters based on LIG-aramid be fabricated as an alternative to bucky paper for composite manufacturing via the through-thickness FP method? What are the advantages and disadvantages of using LIG-based heaters for composite manufacturing?
- Can a mechanically robust nanocomposite film heater with a high electrothermal efficiency be prepared using buckypaper and dicyclopentadiene resin under mild processing conditions?

1.3.3 Scope of Research

This dissertation is focused on developing a new thermally-assisted FP manufacturing method for producing small FRPC panels at the laboratory scale, and no scale-up study is conducted. In addition, the focus of this dissertation is on developing the processing science of manufacturing FRPCs via FP methods, and no mechanical test is performed on frontally cured composites due to lack of access to fabrics sized for DCPD resin.

1.3.4 Structure of Dissertation

This dissertation consists of five chapters. Chapter 1 introduces the research topic covered in this dissertation and provides background information on fiber-reinforced polymer composites and their manufacturing challenges and performance limitations.

Chapters 2 through 4 are published as three peer-reviewed papers.[94–96] In chapter 2, a processing approach is developed for rapid and energy-efficient frontal curing of multifunctional composites using an integrated nanostructured heater (buckypaper). Electrothermal performance of the integrated heater in composite processing conditions is characterized to determine power requirement for frontal curing of a 10 cm × 10 cm composite panel. Then, various composite panels are fabricated to investigate the effect of processing parameters including cure time, position of heater in the layup, and tooling material on curing behavior of composite panels. We demonstrate that through-thickness frontal curing technique using an integrated nanostructured heater enables rapid fabrication of fully cured polymer composites on any tooling material including aluminum. In addition, produced composites exhibit excellent electrothermal and de-icing performance.

In chapter 3, a fabric heater is developed by writing laser-induced graphene on aramid fabrics using a 10.6 μm CO_2 laser and used as an alternative to buckypaper for initiation of FP in through-thickness curing technique. The lasing process parameters including input laser power, scan rate, and pulse per inch (PPI) are tuned to optimize the electrothermal performance of LIG-aramid heaters. Then, two applications are developed for the produced heater. Flexible heaters are prepared by impregnating LIG-aramid with silicone rubber and electrothermal performance of produced flexible heater is characterized under various conditions. LIG-aramid fabric heater is also used as an integrated heater for through-thickness frontal curing of FRPCs. A 10 cm × 10 cm composite panel is frontally cured within 1 min with minimal energy consumption as a proof-of-concept.

In chapter 4, a facile and rapid technique is developed based on a FP resin system for preparation of mechanically robust buckypaper-based nanocomposite film heaters. First, the rheological, wettability, and the curing characteristics of the dicyclopentadiene resin are characterized by

rheological, differential scanning calorimetry, and contact angle measurements to explore the feasibility of fabrication of pDCPD-buckypaper nanocomposite films under mild processing conditions. Then, the quality of the produced nanocomposite films is evaluated by characterizing their composition, morphology, and mechanical properties using various techniques including scanning electron microscopy, thermogravimetric analysis, and tensile testing. Then, electrodes are connected to the opposite sides of the nanocomposite films to create film heaters and determine the electrothermal performance of resulting heaters in response to various static and dynamic electrical loading conditions. Upon characterization of the electrothermal performance of film heaters, they are used to demonstrate direct conductive heating and curing of a composite panel using a commercial prepreg system.

In chapter 5, the main findings are summarized and the recommendations for the future studies are presented.

CHAPTER 2: RAPID AND ENERGY-EFFICIENT FRONTAL CURING OF MULTIFUNCTIONAL COMPOSITES USING INTEGRATED NANOSTRUCTURED HEATERS[1]

2.1 Introduction

Current technologies for the manufacture of fiber-reinforced polymer composites are energy-intensive, environmentally unfriendly, and time-consuming and require expensive equipment and resources. In addition, composites typically lack key non-structural functionalities (e.g., de-icing, and damage sensing) which are crucial to many applications such as aerospace and wind energy. Here, we present a new approach for rapid and energy-efficient manufacturing of multifunctional composites without using traditional expensive autoclaves, ovens, or heated molds used for curing composites. Our approach is predicated on embedding a thin conductive nanostructured paper in the composite layup to act as a resistive heater for triggering frontal polymerization of the matrix thermosetting resin of the composite laminate. Upon passing electric current, the nanostructured paper quickly heats up and initiates frontal polymerization, which then rapidly propagates through the thickness of the laminate, resulting in rapid curing of composites (within seconds to few minutes) irrespective of the size of the composite laminate. The integrated nanostructured paper

[1] Reprinted with permission from *ACS Appl. Mater. Interfaces* 2022, 14, 44, 50215–50224. Copyright (2022) American Chemical Society. https://pubs.acs.org/doi/abs/10.1021/acsami.2c15415

remains advantageous during the service of the composite part by imparting new functionalities to the cured composite, owing to its excellent electrical conductivity and electrothermal properties. In this work, we first study the influence of several composite processing parameters on the electrothermal properties of the nanostructured paper and determine the power required for rapid initiation of frontal polymerization. We then successfully fabricated a 10 cm × 10 cm composite panel within 1 min using only 4.49 kJ of energy, which is four orders of magnitude less than the energy consumed by traditional bulk, oven-curing technique. Detailed experiments are conducted to provide an in-depth understanding of the effect of heater position, tooling material, and input power on the frontal curing of composite laminates. The multifunctional response of produced composites is demonstrated by performing a de-icing experiment, where a $50 \times 50 \times 3$ mm^3 cube of ice is completely melted within 3 min using an input power of 77 W.

Fiber-reinforced polymer composites (FRPCs) are widely used in many industrial sectors including aerospace, wind power, defense, marine, and automotive, owing to their excellent specific stiffness and strength, chemical stability, fatigue resistance, and design flexibility.[97,98] While the excellent specific mechanical properties of composites make them an ideal material for many structural applications, their widespread adoption and full lightweighting potentials have been limited by their high cost of manufacturing, low fabrication rates, and lack of non-structural, functional properties.[4,99] Conventional manufacture of FRPCs requires high-temperature bulk polymerization of the matrix thermoset resin in an autoclave, oven, or a heated mold. This process is long (from several hours up to a day), energy-intensive with a significant carbon footprint, and requires expensive resources.[11,100] In addition, FRPCs lack key non-structural functions required for a given application. For example, in aerospace and wind energy applications, de-icing of

composite structures are typically addressed by using parasitic metal attachments, which add to the weight and cost of composite structures.[6]

The growing demand for FRPCs in various fields has motivated the development of new composite materials and manufacturing techniques that enable low cost, rapid, and energy-efficient manufacture of composite materials with improved performance. Fast curing resin formulations with cure times of less than 20 min have been used for rapid production of thermosetting polymer composites.[71] However, such resin systems have a limited pot life and produce a high amount of exothermic heat from bulk polymerization, resulting in material degradation, buildup of residual stresses, and poor dimensional stability of produced composite parts.[72,101] Radiation curing is an alternative approach for manufacturing thermoset polymer composites, where various electromagnetic waves within the electromagnetic spectrum (e.g., ultraviolet, gamma, radio frequency, infrared, and microwave) are used to provide energy for curing of composites.[12,13,102–104] Although each of these curing methods have their own distinct advantages, none of them have gained widespread acceptance in the industry due to their specific limitations. For example, UV-curing is limited to the manufacture of glass fiber-reinforced composites with a limited thickness, as the depth of penetration of radiation is very low in composites reinforced with carbon or aramid fibers.[105] Similarly, microwave heating allows for significant reduction in cure cycle time and energy input, but the large-scale application of this curing approach has been limited by the high capital cost of microwave ovens, microwave shielding effect of carbon fibers, possibility of arc formation, and altered dielectric properties of composites during the crosslinking process that affects the efficiency of microwave heating.[27,106]

Another promising method for energy-efficient and cost-effective curing of FRPCs is direct conductive heating of composite laminates via a resistive heater. In contrast to conventional

autoclave- or oven-based curing approaches, where a large fraction of the consumed energy is used to heat the gas inside an autoclave or oven to transfer the heat to the composite layup via convective heat transfer, resistive heating allows for direct heating of the composite laminate through conduction, resulting in substantial energy saving.[47] Metal meshes, carbon fibers, and various conductive nanomaterials have been used as resistive elements for conductive heating and curing of composites.[107]Nanostructured films and papers of carbon nanomaterials (e. g., buckypaper, graphene paper, and laser-induced graphene) are particularly promising for Joule heating of composites due to their excellent Joule heating properties, deformability, ease of integration into composite layups, and low thermal mass and density.[42,99,108] Another advantage of using nanostructured heaters is that they can be integrated into composite laminates and impart new functions to the host composites such as de-icing,[109] lightning strike protection,[110] and self-sensing of damage and strain.[111]

While the use of alternative heating methods can substantially improve the energy-efficiency of composite manufacturing, the manufacturing time and energy is directly affected by the cure cycle of the matrix resin. Frontal polymerization (FP), a self-propagating reaction wave driven by the exothermic heat of polymerization, is a promising curing strategy that can substantially reduce the manufacturing time and energy of polymers and FRPCs. [75,112] In FP, a local thermal stimulus is applied to a solution of monomer and initiator, which locally polymerizes the monomer and releases an exothermic heat due to the underlying chemical reaction. The heat generated by the exothermic reaction diffuses forward to advance a propagating front, resulting in a self-sustained process.[113] This curing approach can reduce the manufacturing time by up to two orders of magnitude and manufacturing energy by up to ten orders of magnitude compared to the traditional bulk curing of resins.[86]

Among various frontally polymerizable resin systems, dicyclopentadiene (DCPD) is of great interest for fabricating FRPCs due to its high front velocity and low resin viscosity combined with the good thermomechanical properties of the resulting polydicyclopentadiene (pDCPD) polymer.[79,114,115] Frontal ring opening metathesis polymerization (ROMP) of DCPD with tunable pot life has been recently shown using Grubbs' catalyst and phosphite inhibitors.[74,86,116] FP of DCPD has been recently used to produce FRPC panels with up to 50 vol% of carbon fibers by in-plane initiation and propagation (i.e., within the plane of reinforcements) of the reaction front.[86,114] However, the scalability and practical applications of the in-plane FP of DCPD is hindered by several processing issues. Self-sustaining propagation of the FP reaction in presence of a high volume fraction of reinforcements has been demonstrated using a highly thermally insulating tooling material (i.e., polymer foams) to minimize the heat loss to the substrate during polymerization and mitigate the risk of frontal quenching.[89,114] Such tooling materials however are not common in the composite industry and are challenging to form and machine. Even though the use of the thermally insulating tooling helped to maintain a self-sustaining front within the composite layup, the resulting composite panel had a low degree of cure of ~80%, due to the reduced energy density of resin and heat losses through boundaries. In addition, in the in-plane FP curing of FRPCs, as part size increases, the front travel distance and cure time increase accordingly and can take up to several hours for the fabrication of large structures such as aerospace structures and wind turbine blades. Such long cure times not only are not ideal for industrial applications but also might not be achievable due to the limited pot of FP resins. For example, the DCPD resin previously used to manufacture composite panels (10 cm × 20 cm) had a short pot life of ca. 20 min, which is not sufficient for manufacturing large composite parts.

Despite many attempts in recent years to enhance various aspects of the performance and manufacturability of composites, development of a technology that can address all these challenges remains unmet but is of immense interest to many sectors. Here, we present a novel technique for rapid and energy-efficient manufacturing of multifunctional composites by synergistic integration of an FP resin system and a conductive nanostructured paper in the processing of composites (Figure 2-1). The integrated paper provides heat by Joule heating effect to initiate frontal polymerization, which then quickly propagates through the thickness of the composite laminate. As a result, the travel distance of FP is limited to the thickness of the composite laminate, leading to a short cure time (< 5 min), irrespective of the size of the laminate. Additionally, the supplied heat by the nanostructured paper allows for full curing of the composite on any tooling material, which cannot be realized by in-plane FP propagation. The embedded conductive nanostructured paper remains advantageous during the service of the composite part and can impart various non-structural functionalities (e.g., de-icing/anti-icing, self-sensing, and lightning strike protection) to the host structure. As a result, this technique can substantially reduce the cycle time, energy, and carbon footprint of composite manufacturing while reducing the weight and design complexity of composite structures.

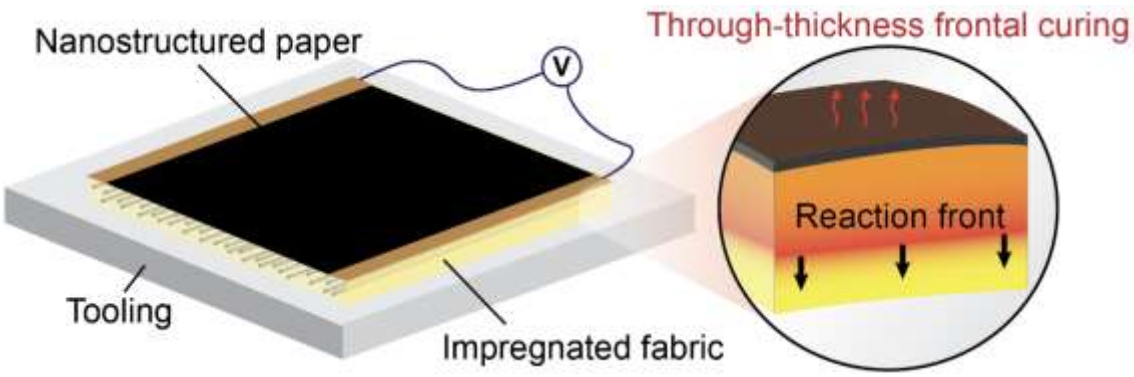

Figure 2-1. Schematic representation of the manufacturing technique. A thin, conductive nanostructured paper is integrated as the outeremost (top or bottom) ply of the composites layup. Upon passing electric current through the conductigve paper, it quickly heats up via resistive heating and initiates frontal polymerization, which then propagates through thickness to rapidly cure the available monomer. The integrated paper remains advatnagesous during the service of the composite structure by imparting various functional properteis to the composite material. In this work, de-icing capability of produced mutlifunctional composites is demonstrated.

In the present work, we demonstrate for the first time through-thickness frontal curing of multifunctional composite laminates via an integrated nanostructured heater and study the cure behavior of composite laminates under various layup conditions. We first use a systematic approach to understand the effect of various composite processing parameters (i.e., input power, vacuum condition, and infiltration of layup with resin) on the electrothermal performance of the embedded nanostructured paper and determine the power requirements for initiation and propagation of the FP reaction. The identified electrothermal conditions are then used to manufacture composite panels and explore the effect of boundary conditions including the position of the nanostructured paper (bag side or tool side) and tooling material (glass, polymer foam, and aluminum) on front properties, temperature distribution, and cure behavior of composites. Finally, the resistive heating performance of a cured composite panel in response to various input power conditions is evaluated and the results are used to demonstrate de-icing functionality of the multifunctional composite panel. The developed manufacturing technique can be used to

manufacture multifunctional composites using different fiber reinforcements, resin chemistries, and thin conductive films, papers, and printed patterns.

2.2 Experimental section

2.2.1 Characterization of nanostructured heater

In this study, we use buckypaper, which is a macroscopic assembly of carbon nanotubes, as conductive nanostructured paper to demonstrate composite manufacturing via Joule heating effect. Buckypaper (average thickness = 50 μm, areal weight = 20 g m^{-2}) was purchased from NanoTechLabs and used as received. The morphology of as-received buckypaper is imaged using a JEOL JSM-5800 field emission scanning electron microscope (FESEM) at an accelerating voltage of 3 kV without any surface coating step, due to the intrinsic electrical conductivity of buckypaper. The electrothermal performance of buckypaper is evaluated under various processing conditions using specimens with an effective heating area of 9 cm × 10 cm. Resistive heaters are prepared by attaching copper wires to the opposite ends of a buckypaper specimen using a silver-filled conductive paste (Electro-Bond 06, ConductiveX). Electrical resistance of prepared heaters is measured using a DM285 FLIR multimeter. For characterization of the electrothermal performance of heaters in the composite manufacturing process, 13 plies of fabric consisting of 12 plies of carbon fabric (Toray T300 twill weave fabric, 3,000 tow size, areal weight = 204 g m^{-2}) and one ply of glass fabric (Jushi plain weave fabric, areal weight = 100 g m^{-2}) are used as the fiber bed. One ply of buckypaper is placed on top of the fabric stack and electrically insulated from the underlying carbon fabric plies using the thin glass fabric ply. The layup is then vacuum-bagged on a glass plate based on vacuum-assisted resin transfer molding (VARTM) approach, as explained in detail in the following section. The electrothermal performance of the buckypaper heater is evaluated under various conditions by applying various voltages across the heater using a DC

power supply (9206, B&K Precision) and measuring the average temperature of the effective heating area using a FLIR T540 infrared thermal camera. To understand the effect of various process parameters on the electrothermal performance of heaters, several scenarios are considered. The resistive heating of the buckypaper heater in the as-prepared layup is first evaluated without applying vacuum and infusion of resin. Then, similar studies are performed on the composite layups under vacuum condition before and after resin infusion. The resin used in these studies is uncatalyzed (i.e., in absence of the catalyst solution) to prevent the release of exothermic heat of polymerization, which can affect the temperature measurements, and to only study the effect of resin infusion on the electrothermal response of buckypaper.

2.2.2 Fabrication of composite panels

The same layup as the one used for the electrothermal tests is used for fabricating composite panels. The FP resin system used for the manufacture of the composite panels is based on DCPD and prepared according to the procedure developed by Robertson et al.[117] Briefly, DCPD (Sigma-Aldrich) is first mixed with 5-ethylidene-2-norbornene (Sigma Aldrich) at a 95:5 weight ratio to depress its melting point. Then, 70 g of this resin solution is mixed with a catalyst solution consisting of 45 mg of 2nd generation Grubbs' catalyst (Sigma-Aldrich), 4.17 μL of tributyl phosphite (TCI America), and 2.5 mL of phenyl cyclohexane (Sigma Aldrich). Tributyl phosphite and phenyl cyclohexane function as inhibitors for tuning pot life and solvent for dissolving catalyst, respectively. Composite panels are fabricated using 10 cm × 10 cm plies of carbon and glass fabric and based on the double-bagged VARTM technique. A glass plate is used as the tooling of the composite layup unless otherwise specified. A vacuum pressure of 42.3 kPa gauge is applied to the inner bag to slowly infuse the resin into the layup while a vacuum pressure of 83.0 kPa gauge is applied to the outer bag using a separate vacuum pump to compact the fiber bed.

Following the resin infusion, a voltage is applied across the heater to initiate FP and cure the laminate by through-thickness propagation of the reaction front. A B&K 9200 software is used to measure and record voltage and current during curing process to calculate power consumption profile. Two strategies are considered and compared for placement of the buckypaper heater in the layup and initiation of the FP reaction: buckypaper ply is placed as the outermost layer of the composite laminate either on the bag side (top layer) or on the tool side (bottom layer) of the composite layup. The buckypaper ply is integrated into the composite laminate as the outermost surface layer to preserve the mechanical integrity of the laminate without interfering with the internal load-transfer mechanisms. In each strategy, the glass fabric ply electrically isolates the buckypaper ply from the 12 carbon fabric plies. The effect of tooling material on the cure behavior of composites is also studied using glass, aluminum, and polyisocyanurate foam substrates. Temperature data at the tool and bag sides of the layup during composite manufacturing are collected using two thermocouples and recorded using a LabVIEW program. Infrared thermal imaging is also used to capture the distribution and evolution of the temperature field during frontal curing.

2.2.3 Characterization of cured composites

Differential scanning calorimetry (DSC; TA Instrument DSC-2500) is used to determine the total heat of reaction of the uncured resin as well as the degree of cure of frontally cured composite panels produced under various conditions. The total enthalpy of reaction of the DCPD resin is measured by transferring and sealing ~3 mg of resin into an aluminum hermetic DSC pan, followed by heating the samples from 25 to 250 °C at a heating rate of 5 °C min^{-1}. The residual heat of reaction of cured composites is similarly measured by transferring ~25 mg of composite samples into an aluminum DSC pans and heating the material from 25 to 250 °C at a heating rate of 5 °C

min^{-1} under nitrogen atmosphere. The degree of cure is then calculated based on the adjusted exotherm peak as,

$$\alpha = 1 - \frac{\Delta H_r}{\Delta H_t} \qquad (2\text{-}1)$$

where α is the degree of cure and ΔH_r and ΔH_t respectively represent the residual heat of reaction and total enthalpy of reaction. The electrothermal response of produced composite panels is determined by applying various input voltages to the laminate and measuring the average temperature of the panel using infrared thermal imaging. This response is then used to demonstrate de-icing capability of the resulting multifunctional composites by placing a 50 mm × 50 mm × 3 mm cube of ice on the composite panel and applying a constant voltage until the ice cube is completely melted.

2.3 Results and discussion

Development of the novel rapid manufacturing of multifunctional composites requires selecting an appropriate conductive nanostructured film or paper that fulfills a stringent set of requirements. The conductive paper or film should exhibit fast and uniform heat generation capability, allow for easy integration into the composite layup, be thin, porous, lightweight, and mechanically robust, and survive composite processing conditions. Thin papers of carbon nanomaterials, such as carbon nanotube and graphene, are ideal for integration into composites and obtaining the desired functional properties. In this work, we use buckypaper as conductive nanostructured paper because of the following reasons. Buckypaper is commercially available at large scales. In contrast to

metallic counterparts, buckypaper is thin (~50 μm) and has a low density, adding minimal weight to the composite laminate. It exhibits rapid and uniform heat generation capability in undeformed and deformed states, which is crucial for frontal curing and multifunctional performance of FRPC structures. In addition, the porous microstructure of buckypaper allows impregnation with the low-viscosity DCPD resin (viscosity ~1.5 cP) during composite processing and integration into the composite laminate. Also, when embedded in composites, buckypaper can add a variety of new functions to the host structure such as de-icing/anti-icing,[42] strain and damage sensing,[118] electromagnetic interference (EMI) shielding,[119] fire retardancy,[43] and lightning strike protection.[120]

2.3.1 Electrothermal response of integrated buckypaper

Frontal curing of composites via integrated buckypaper heater requires rapidly increasing the temperature of buckypaper and its surrounding resin above the activation temperature of the resin while avoiding excessive heating and reaching high temperatures. Based on our experimental observations, FP of DCPD resin can be initiated when the resin temperature is locally raised above ~70 °C. Therefore, the electrothermal performance of buckypaper heaters should be characterized to determine the range of input power that can lead to successful triggering of FP and full curing of composites. However, the electrothermal performance of buckypaper, like any resistive heater, is highly affected by the environmental factors and boundary conditions. A systematic study is first conducted to understand and characterize the effect of various composite processing parameters on the resistive heating and electrothermal response of integrated buckypaper heaters. For all experiments, 10 cm × 10 cm buckypaper heaters (9 cm × 10 cm effective heating area between two connected electrodes) are used to eliminate the size effect and 13 plies of fabric (12

plies of carbon fabric and 1 ply of glass fabric) are used as the substrate fiber-reinforcements like the composite fabrication process.

The response of the buckypaper heater integrated in the composite layup to various input voltages at ambient pressure and dry condition (i.e., prior to applying vacuum to the layup) is shown in Figure 2-2 a. An increase in the input voltage results in an increase in the heating rate and steady-state temperature of the heater, due to the higher current that passes through the continuous network of carbon nanotubes. A steady-state temperature of ~175 °C is obtained within 30 s when an input voltage of 10 V is applied, demonstrating the excellent Joule heating performance of the buckypaper (Figure 2-2 a). In addition, the steady-state temperature of the heater increases quadratically as a function of input voltage (Figure A-2 e), indicating that the response of the heater follows Joule's law.

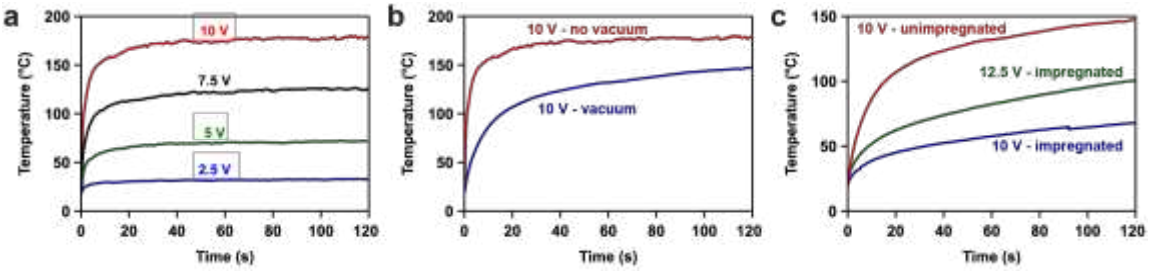

Figure 2-2. Effect of composite processing conditions on electrothermal performance of integrated buckypaper ply. (a) Joule heating response of buckypaper ply integrated into composite layup prior to applying vacuum. (b) Effect of applying vacuum on the electrothermal response of buckypaper. (c) Electrothermal response of integrated buckypaper ply upon infusion of uncatalyzed resin.

In the next step, vacuum is applied to the layup to evaluate the electrothermal response of the heater under vacuum and dry condition (i.e., prior to resin infusion) to an input voltage of 10 V and compare the result with that of the tests performed under ambient condition (Figure 2-2 b).

When vacuum is applied to the composite layup, a significant drop in the steady-state temperature and heating rate is observed, which can be explained by the following equation,[121]

$$T_{eq.} = \frac{\frac{V^2}{R} - Q_{loss}}{mC_p} + T_0 \qquad (2\text{-}2)$$

where the term V^2/R represents the amount of heat generated by Joule heating effect, m and C_p are the mass and heat capacity of the heater, respectively, Q_{loss} is the amount of heat dissipated via any mechanisms, and T_0 is the ambient temperature. Applying vacuum results in the compaction of the composite layup, which in turn leads to an enhanced and more uniform contact between the buckypaper ply and underlying fabric plies. The increased contact area facilities heat loss to the surrounding material (i.e., increased Q_{loss}), resulting in a decreased steady-state temperature.

Upon infusion of the uncatalyzed resin into the composite layup, a substantial drop in the electrothermal performance of the buckypaper heater is observed, where the steady-state temperature of the impregnated layup in response to an input voltage of 10 V decreases by ~80 °C compared with the unimpregnated condition (Figure 2-2 c). This observation can similarly be explained using eq 2-2. When buckypaper is impregnated with resin, its electrical resistance (R) increases from 1.57 Ω to 2.53 Ω, indicating a significant deterioration in the heat generation capability of the heater for a given input voltage. Impregnation with resin also increases the thermal mass (m) of the heater and facilitates heat dissipation (Q_{loss}) to the substrate via conduction. These changes in the heater properties and its surrounding environment lead to the inferior electrothermal performance of the impregnated buckypaper heater compared with unimpregnated buckypaper. Under this condition and for an applied voltage of 10 V, the steady-state temperature of the

buckypaper does not quickly reach the required activation temperature of the FP reaction. As a result, the input voltage is increased to 12.5 V to reach the target temperature of 70 °C in less than 1 min.

2.3.2 Processing of composites using integrated buckypaper heater

We manufacture carbon FRPC panels using the resin system containing the catalyst solution and the integrated buckypaper heater and investigate the effect of buckypaper position in the layup and tooling material on the temperature distribution and cure behavior of composites. Like the electrothermal characterization studies, first the buckypaper ply is placed on the bag side (top surface layer) of the composite laminate and a glass plate is used as the tool for composite manufacturing. An input voltage of 12.5 V is supplied to the integrated buckypaper ply for 1 min to initiate frontal curing. Temperature profiles at the bag (heater) and tool sides are collected and recorded using two thermocouples placed in the center of the fabric stack. Once the electric power is supplied to the integrated buckypaper, its temperature gradually increases until it reaches 73 °C at t = 39 s, after which a sudden temperature spike of ~60 °C is observed due to the initiation of FP (Figure 2-3 a). A similar temperature increase of ~63 °C is also observed at the tool side although the peak temperature is 27 °C lower than that of the heater side. This difference in the peak temperature of the two thermocouples is attributed to the lower temperature of the layup on the tool side, due to the intrinsic temperature gradient between the heater and tooling as well as the heat loss through the tooling boundaries. Interestingly, the power consumption of the buckypaper heater during the 1 min heating process is not constant and varies in response to the temperature changes in the material (Figure 2-3 b).

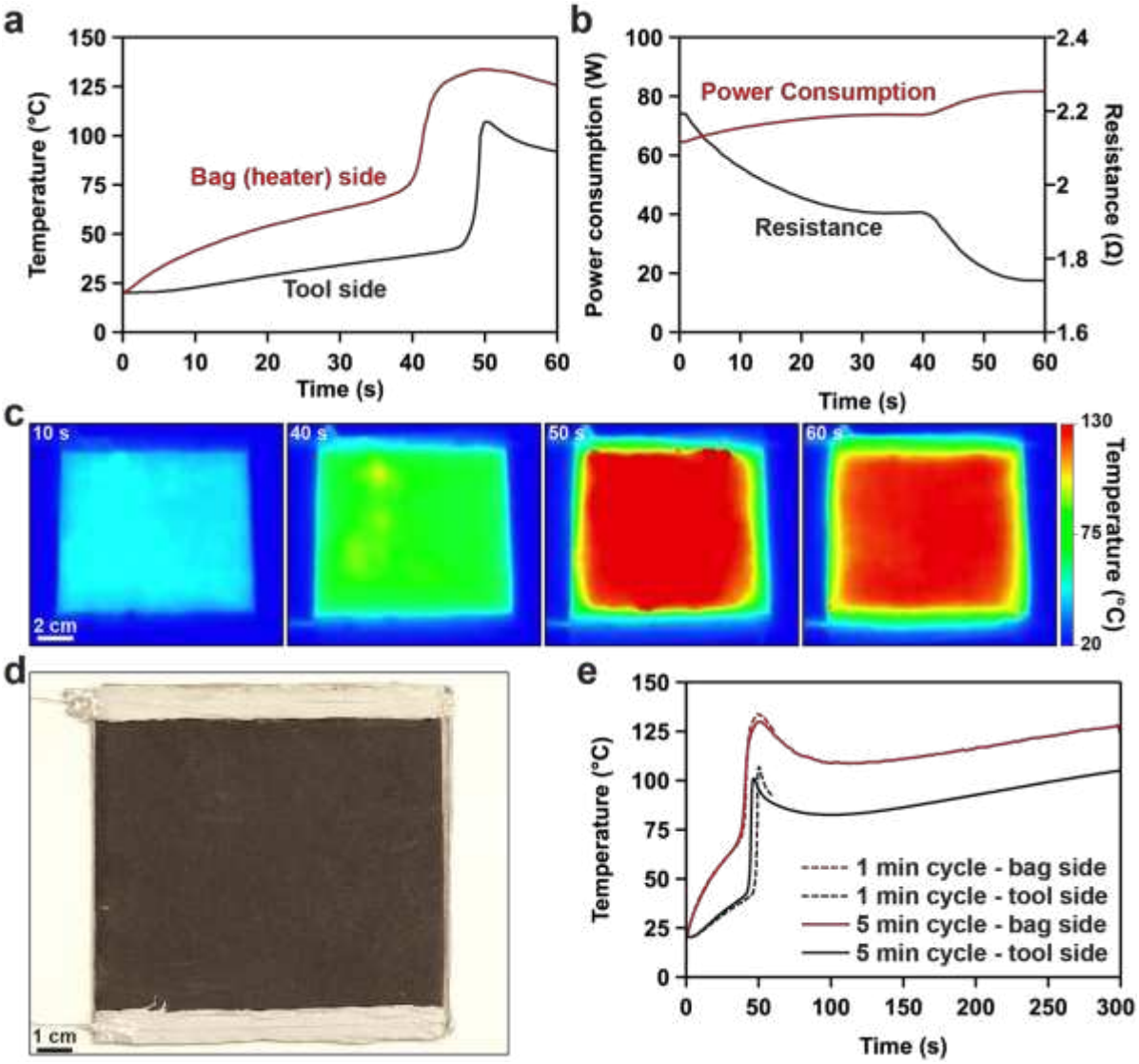

Figure 2-3. Through-thickness frontal curing of composites on a glass tool plate via a buckypaper ply integrated as the top layer of the composite laminate. (a, b) Temperature profile and power consumption of the curing process. (c) Infrared thermal images captured from the top surface of the composite layup showing the evolution of temperature during through-thickness frontal curing of the composite panel. (d) Image of the produced panel. (e) Extending the heating cycle to 5 min to understand the effect of a short post-cure step on cure behavior of composites.

Prior to the initiation of FP, the electrical resistance of buckypaper gradually decreases as the temperature is increased due to its negative temperature coefficient of resistance, leading to

increased power consumption and energy dissipation. At FP, the large temperature increase by the exothermic reaction further reduces the electrical resistance of buckypaper, resulting in considerable increase in power consumption. The total external energy consumed during this curing process is estimated to be ~4.49 kJ, which is several orders of magnitude less than the energy required in traditional autoclave- or oven-based bulk curing processes. For example, curing a composite panel with the same dimensions using an aerospace grade epoxy (assuming a 6 h cure cycle) and a small oven in our laboratory (internal volume of 0.17 m^3 and power consumption of 3 kW) requires 64.8 MJ of energy, which is four orders of magnitude larger than the energy consumed in our composite processing technique.

The spatial distribution of temperature during the curing process is monitored using infrared thermal imaging on the surface of the composite layup (Figure 2-3 c). A relatively uniform heat generation with a small spatial variation is observed throughout the layup when the power is supplied to the buckypaper heater and prior to the initiation of FP. As soon as the temperature locally exceeds the activation temperature of the frontal reaction, the front is formed and propagates in through-thickness and in-plane directions until the composite is completely cured. Based on the thermal images, frontal propagation and curing in the entire layup is finished within 60 s from the moment the electric power is supplied to the buckypaper heater. An image of the produced composite laminate is shown in Figure 2-3 d. Microscopy imaging from the cross-section of the laminate shows full integration of the buckypaper ply with minimal void formation (Figure A-4).

Given that a temperature gradient exists between the bag- and tool sides of the composite laminate during the 1 min heating and curing process, another experiment is carried out by extending the heating time to 5 min to study the role of a short post-cure step on the cure behavior of the composite laminate (Figure 2-3 e). The temperature profiles of the extended heating cycle at the bag and tool sides follow the same trend as the 1 min heating cycle during the first 60 s, indicating the reproducibility of the manufacturing process. Following the FP, the temperature first drops but then continues to increase due to the continuous supply of energy to the system. The energy consumption of the curing process using the extended heating cycle increases to 22.56 kJ, which is still several orders of magnitude less than the energy required in conventional manufacturing processes.

The degree of cure of the composite panels manufactured by both 1- and 5-min heating cycles is determined using DSC measurements. A 97% degree of cure is obtained when curing the composite laminate using the 1 min baseline heating cycle (Table 2-1), which is much higher than the 80.5% degree of cure previously reported for the in-plane frontal curing of DCPD-based composites manufactured on a highly insulating tool.[86] Post-curing the laminate based on the 5 min heating cycle increases the degree of cure only by 1.4%, indicating that the heat generated by frontal polymerization is sufficient for achieving a high degree of cure in the produced part without any post-curing step.

Table 2-1. Comparisons of cure conditions and degree of cure of FRPC panels made with different processing conditions.

Heater position	Tool material	Preheating voltage (V)	Cure voltage (V)	Cure time (min)	FP initiation time (s)	Energy consumption (kJ)	Degree of cure (%)
Top	Glass	-	12.5	1	39	4.49	97.0 ± 1.1
Top	Glass	-	12.5	5	39	22.56	98.4 ± 0.5
Bottom	Glass	-	12.5	5	97	18	95.0 ± 2
Bottom	Foam	-	12.5	5	41.5	22.62	99.3 ± 0.2
Bottom	Aluminum	-	12.5	**Frontal polymerization did not initiate**			
Bottom	Aluminum	-	17.5	5	160	46.7	87 ± 3.7
Bottom	Aluminum	10	17.5	5	43.5	56.4	94 ± 1.9

The temperature difference between the top and bottom surfaces of the composite laminate observed in Figure 2-3 a is caused by the heat loss through the glass tool plate. An alternative layup strategy is used to study the effect of heater position on temperature gradient by placing the buckypaper ply as the bottom layer of the composite laminate (Figure 2-4 a). Using this approach, the heat generated by buckypaper can simultaneously heat up the tool plate and initiate the FP, which will then propagate upward toward the top surface of the composite layup. An input voltage of 12.5 V is similarly used to generate heat in the buckypaper ply and cure the composite panel; however, a longer time is required to initiate FP, mainly due to the reduced heating rate caused by the heat loss through the tool plate. Therefore, the heating cycle is extended to 5 min to allow for the longer initiation time. Additionally, a lower peak temperature at the heater side is observed compared with the original layup strategy where buckypaper is placed as the top layer of the composite. The heat flow profile obtained from running DSC measurements on this composite panel shows minimal residual heat, where a 95% degree of cure is calculated for this curing strategy on a glass substrate (Table 2-1). While the degree of cure of the composite panel cured by placing the heater on the tool side is slightly lower than that of the panel cured by placing the

heater on the bag side due to lower temperature values, highly cured composite panels are resulted using both heater positioning approaches.

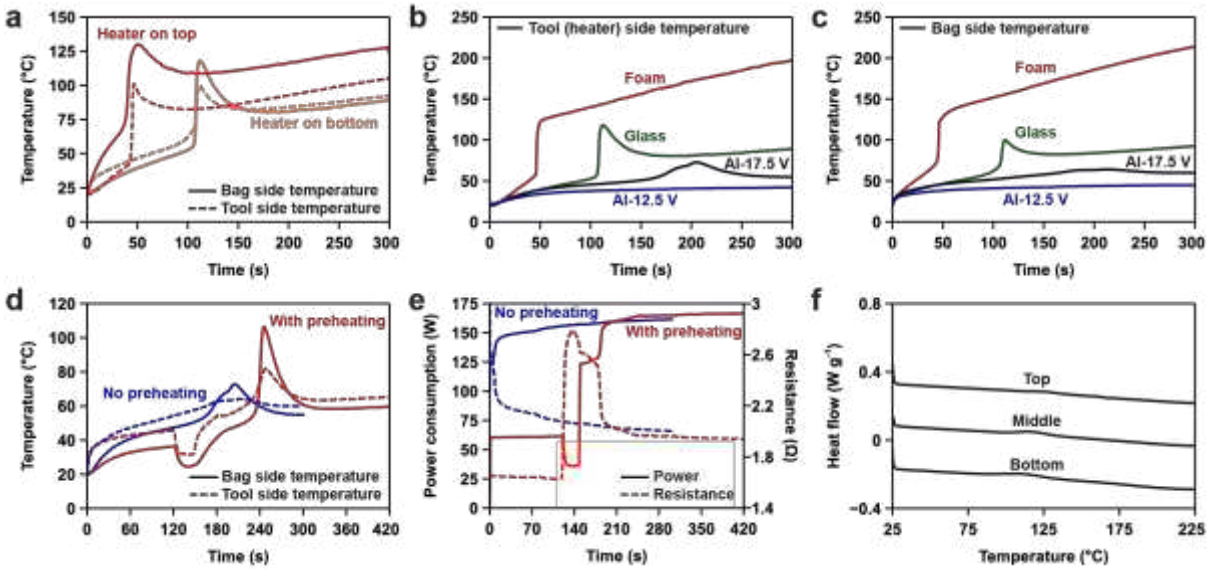

Figure 2-4. Effect of buckypaper position and tooling material on frontal curing of composites. (a) Temperature profiles of the top (bag side) and bottom (tool side) surfaces of composite layup when the buckypaper ply is placed as the top or bottom layer of the composite laminate. (b, c) Effect of tooling material on temperature profiles of the tool (b) and bag (c) sides of the layup. The buckypaper ply is placed as the bottom layer of the composite laminate. (d, e) Effect of preheating of the dry composite layup prior to resin infusion when using an aluminum tool plate on temperature profiles and power consumptions during frontal curing. (f) Heat flow curves obtained from DSC measurements on samples cut from the top, middle, and bottom sections of the composite panel manufactured on an aluminum tool plate with the preheating step. Minimal residual heat of reaction is observed in the heat flow curves, indicating the ability to produce highly cured composite panels via FP on metal tool plates.

Changing the tooling material from glass to aluminum, which is commonly used in composite industry, makes the frontal curing of composites challenging, due to the high thermal conductivity of aluminum and substantial thermal losses through tooling boundaries. The effect of tooling material including aluminum, glass, and polyisocyanurate foam on the bag- and tool-side temperature profiles of the composite layup during frontal curing using heater on the bottom side of the layup is shown in Figure 2-4 b, c. As expected, use of a highly thermally conductive tool

(aluminum) negatively affects the manufacturing process of composite, where no frontal polymerization occurs using an input voltage of 12.5 V within 5 min due to the heat sink effect of aluminum tooling. Although increasing the input voltage to 17.5 V enables frontal curing of the composite panel, temperatures are still too low for achieving a high degree of cure in the produced part. When comparing different tooling materials, the shortest FP activation time is observed for the polyisocyanurate foam (42 s), which also results in a different temperature profile due to the very low thermal conductivity of the foam, highlighting the impact of thermal properties of tooling material on front properties. As expected from temperature values recorded during curing process, the material of tool plate has a significant impact on the degree of cure of produced composite panels (Table 2-1). The composite panel fabricated on polyisocyanurate foam has a full degree of cure, whereas a low degree of cure of 87% is obtained for the panel fabricated on aluminum tool plate even though it was cured using a higher input power (i.e., voltage of 17.5 V). Additionally, the amount of energy consumed during the 5 min heating and curing process depends on the type of tooling (Table 2-1). For example, 22.62 kJ of energy is consumed when fabricating a composite part on the foam, which is 4.62 kJ higher than the energy required for producing the same part on a glass tool. This difference in energy input can be explained by the temperature dependence of the electrical resistance of the integrated nanostructured heater. The higher front temperature observed in manufacturing of composite panels on the foam substrate results in a larger reduction in the electrical resistance of the heater at the initiation of frontal reaction, leading to a higher power consumption.

We address the curing issue observed during composite manufacturing on aluminum tooling by exploiting the integrated buckypaper heater to pre-heat the composite layup and tool plate prior to resin infusion. Pre-heating the layup reduces the conductive heat loss through the tool and

accelerates the heating rate of resin and its reactivity following infusion. An input voltage of 10 V is initially applied to the dry layup for 2 min to increase the temperature of the heater to 40 °C; however, a temperature gradient ranging from 30 to 40 °C is observed across the thickness of the layup, due to the thermal lag and heat losses through tooling boundaries (Figure 2-4 d). Upon infusion of resin, a sharp drop in thermocouple temperature is observed, after which the input voltage is raised to 17.5 V to rapidly increase the layup temperature until FP is initiated. Compared to the panel fabricated at 17.5 V without the preheating step, higher peak temperatures are measured at both sides of the layup, indicating the effectiveness of preheating on increasing the reactivity of the DCPD resin. Figure 2-4 e shows the power consumption and electrical resistance curves during the manufacturing process. During the preheating stage, a constant power of ~60 W is consumed. A sharp increase in electrical resistance of the integrated buckypaper heater is observed after resin infusion, resulting in a significant drop in the heat generation capability and increased power consumption of the heater. The decreased input power along with the heat transfer from layup to resin during infusion are the main reasons for the sudden temperature drop observed in Figure 2-4 d. Increasing the input voltage from 10 V to 17.5 V to increase the layup temperature and initiation of FP both lead to a decrease in electrical resistance and a large increase in power consumption. The total electrical power consumed during this modified cure cycle is 56.4 kJ, which is 9.7 kJ higher than the total power consumed during the previous cure cycle without the preheating step.

Preheating of the dry layup increases the degree of cure of composites from 87% to 94%, demonstrating that highly cured panels can be fabricated on conventional metallic tooling. DSC measurements are also performed on small samples cut from various locations across the thickness of the laminate fabricated on the aluminum tool to understand whether the measured temperature

difference between tool and bag sides leads to spatial variation in degree of cure (Figure 2-4 f). The DSC results reveal that the degree of cure at the bottom, middle, and top sections of the cured laminate are 98.1 %, 95 %, and 93 %, respectively. This difference in the degree of cure between the top and bottom of laminate can be minimized using various approaches including increasing the preheating time or input power or extending the cure time.

2.3.3 Demonstration of multifunctional performance of composite

Another key advantage of embedding a nanostructured conductive ply in the composite layup, aside from rapid initiation of FP, is imparting new nonstructural functionalities to the cured composite part. Among potential functionalities that can be introduced by the buckypaper ply (e.g., de-icing, damage sensing, electromagnetic shielding), in this work we demonstrate the de-icing capability of produced composite laminates. The electrothermal performance of frontally cured composite panel is first characterized to determine the appropriate input voltage for conducting de-icing tests. Figure 2-5 a depicts the results of electrothermal tests performed on a representative composite panel at various input voltages. The multifunctional composite laminate exhibits an excellent Joule heating performance, where an average temperature of around 120 °C is reached within 2 min under an input voltage of 12.5 V (Figure 2-5 b). The electrothermal stability and repeatability of the panel under cyclic electric loads is also evaluated by intermittently varying the input voltage between 0 and 12.5 V during 60 s time intervals. The results of stability test reveal consistent and reproducible electrothermal performance of the multifunctional laminate under cyclic electric loading (Figure 2-5 c). The de-icing capability of the composite laminate is further demonstrated by placing a $50 \times 50 \times 3$ mm^3 cube of ice on the laminate and applying an input voltage of 12.5 V across the laminate (Figure 2-5 d). The ice cube is completely melted within 3 min, demonstrating excellent de-icing performance of the composite laminate.

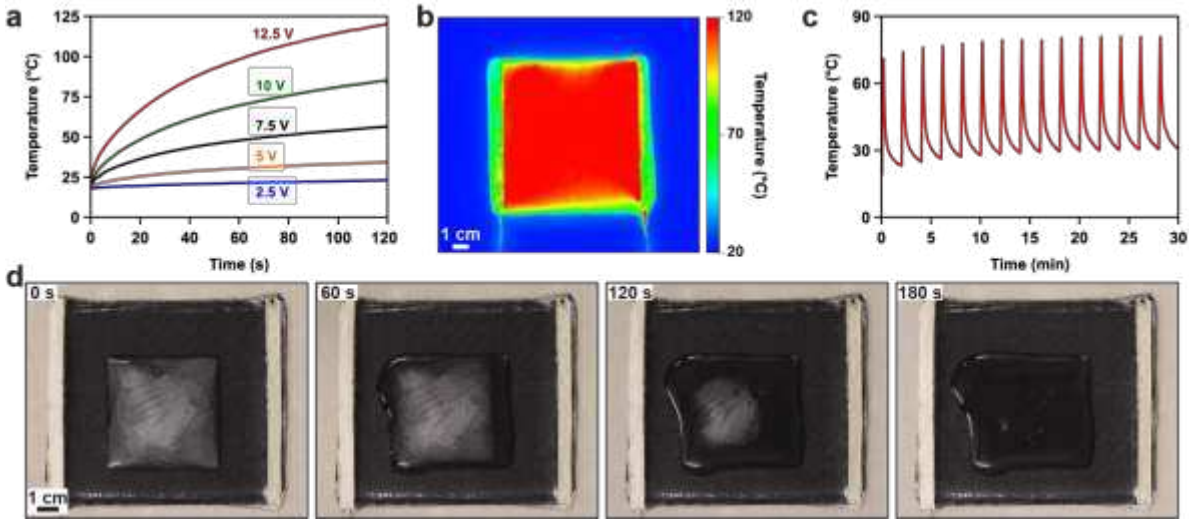

Figure 2-5. Multifunctional performance of produced composite panel. (a) Electrothermal response of the panel to various input voltages. (b) Infrared thermal image of the panel under an input voltage of 12.5 V, showing uniform heat generation within the panel. (c) Electrothermal response of the panel to a cyclic electric load. (d) Demonstration of de-icing functionality of the produced multifunctional composite panel.

2.4 Conclusions

In summary, we report a novel approach for rapid and energy-efficient manufacturing of multifunctional composites by integrating a thin, conductive nanostructured paper in the composite layup to initiate frontal polymerization of matrix DCPD resin and impart new functionalities to produced composite part. Electrothermal characterization of buckypaper heater reveals the effect of various composite processing parameters on Joule heating performance of integrated heaters and provides useful insight for supplying sufficient power to the heater for rapid initiation of frontal polymerization. Placing the buckypaper ply as the top layer of the composite layup results in faster cure times and less energy consumption compared to the case where the buckypaper is placed on the bottom of the composites layup. However, when using highly thermally conductive tooling material such as aluminum, the heater ply should be placed on the bottom of the composite layup to account for heat losses through the tooling boundary and raising the temperature above

the activation temperature of FP. Additionally, preheating of the layup with an aluminum tooling prior to resin infusion is necessary to achieve successful curing of the composite laminate with a high degree of cure. The results of DSC measurements reveal that all produced panels show a degree of cure at least 94%, which is higher than the values reported in previous works on in-plane frontal curing of fiber-reinforced composites. In addition, produced composite panels exhibit excellent de-icing performance, eliminating the need for using external sub-systems to protect composite structures from ice accumulation.

CHAPTER 3: ELECTROTHERMAL PERFORMANCE OF HEATERS BASED ON LASER-INDUCED GRAPHENE ON ARAMID FABRIC[2]

3.1 Introduction

Nanostructured heaters based on laser-induced graphene (LIG) are promising for heat generation and temperature control in a variety of applications due to their high efficiency as well as fast, facile, and highly scalable fabrication process. While recent studies have shown that LIG can be written on a wide range of precursors, the reports on LIG-based heaters are mainly limited to polyimide as the precursor material. Here, we develop and characterize nanostructured heaters by direct writing of laser-induced graphene on aramid woven fabric. The synthesis and writing of graphene on aramid fabric is conducted using a 10.6 μm CO_2 laser. The quality of laser-induced graphene and electrical properties of the heater fabric is tuned by controlling the lasing process parameters. Produced heaters exhibit good electrothermal efficiency with steady-state temperatures up to 170 °C when subjected to an input voltage of 10 V. In addition, the permeable texture of LIG-aramid fabric heaters allows for easy impregnation with thermosetting resins. We demonstrate encapsulation of fabric heaters with two different types of thermosetting resins to develop both flexible and stiff composites. A flexible heater is produced by impregnation of LIG-aramid fabric by a silicone rubber. While the flexible composite heater exhibits inferior

[2] Reprinted with permission from *ACS Omega* 2022, 7, 4, 3746–3757. Copyright (2022) American Chemical Society. https://pubs.acs.org/doi/full/10.1021/acsomega.1c06572

electrothermal performance compared to neat LIG-aramid fabric, it shows consistent electrothermal performance under various electrical and mechanical loading conditions. We also demonstrate frontal curing of a 10 cm × 10 cm composite panel using an embedded LIG-aramid heater within only 1 min with a total energy consumption of 4.13 kJ. The produced laminate shows a high degree of cure 92%, demonstrating that use of LIG-aramid heater enables rapid and energy-efficient manufacture of highly cured composite components.

Resistive heating has been widely used as a heat-generation solution in a wide variety of applications, such as de-icing of aircraft structures, composite curing, water heating, and electric home appliances, due to the high heat generation efficiency and simplicity of use.[122–124] Metal alloys (e.g., Kanthal and Nichrome) have been traditionally used as resistive elements due to their low electrical resistance and high thermomechanical stability. However, such electrothermal materials suffer from high density and rigidity, making their use in emerging technologies (e.g., flexible heaters, wearable and portable devices) impractical.[125,126] The growing demand for Joule heating materials with unique properties, such as superior electrothermal performance, high degree of deformability, and low density, motivates development of new materials and processes.[127] For example, in composite industry, use of flexible heaters can allow for energy-efficient out-of-oven manufacturing or in-the-field repair of composite parts with complex geometries.

Conductive nanomaterials are promising alternative for fabricating highly deformable and efficient resistive heaters.[128] Fabrication of a resistive heater based on nanomaterials requires forming a continuous network of conductive nanoparticles to enable flow of electrons and generating heat based on electrothermal effect. A wide range of nanomaterials, such as silver nanowires,[129] copper nanowires,[130] graphene,[131] carbon nanotubes,[132] and MXene[133] have been previously used for creating resistive heaters by generating conductive paths for the flow of electrons in various

materials systems. While nanomaterial-based resistive heaters offer great potential for fabricating highly efficient and multifunctional heaters, their widespread adoption on a commercial scale faces two major challenges. Production of such heaters typically involves multiple processing steps, including deposition and drying, which is undesirable from an economic point of view. In addition, scalability and large-scale utilization of such heaters is rather challenging and costly, making their use mainly limited to laboratory-scale research or specific applications.[134]

Laser-induced graphene (LIG) is a three-dimensional (3D) porous form of graphene that is synthesized by a rapid, facile, and scalable process and that exhibits excellent electrical and thermal conductivity, large surface area, mechanical robustness, and thermochemical stability.[135,136] The synthesis process of LIG involves lasing an appropriate precursor material with a CO_2, UV, or visible-light laser source. Upon irradiation of precursor material with a laser beam, the surface temperature locally increases via photothermal or photochemical effect, leading to direct conversion of the surface polymer layer into porous 3D graphene structures.[137] Several precursors, including polyimide, polyether sulfone, phenolic, and even wood, have been successfully converted into LIG in a single-step process.[138] Unlike conventional approaches for the synthesis of graphene and other nanomaterials, LIG synthesis process is highly scalable and inexpensive, is performed rapidly at ambient conditions, and allows for direct and concurrent patterning without any sophisticated masking or processing methods.[139] As a result, LIG has been used as an alternative to conventional conductive nanomaterials in a variety of applications such as sensing,[140] Joule heating,[141] water treatment,[142] actuators,[143] and energy storage devices.[144]

Resistive heaters based on LIG have been previously developed by directly writing graphene on polyimide films, where steady-state temperatures of more than 200 °C have been obtained under an input power of 1.4 W.[59] Such flexible heaters exhibit consistent performance after 10,000

bending cycles and are stable in high temperatures up to 225 °C. Additionally, the heaters offer better uniformity of temperature distribution compared to commercial counterparts while being less expensive. Large resistive heaters (20×20 cm^2) based on LIG have also been fabricated using porous polyimide sheets as precursor material instead of polyimide films.[60] The tailorable synthesis process of LIG has been exploited for creating heaters with multiple heating zones in one single step by changing the processing parameters during the lasing process.[60] Produced heaters were then used for out-of-oven curing of fiber-reinforced polymer composites, where ~85% reduction in manufacturing energy was obtained compared to conventional oven curing approach. In another work, composites with an integrated de-icing system based on LIG heaters were fabricated by combining extrusion-printing of polyamic acid solution on a cured composite laminate, followed by high temperature imidization and laser-induced graphene synthesis process.[145] Although creation of LIG patterns on composites involved multiple processing steps, the resulting composites showed good de-icing performance.

Development of LIG-based resistive heaters has been mainly limited to solid films of polyimide as substrate material due to ease of processing. Use of solid substrates, however, often results in shape distortion, especially as the size of the lased region increases, and prevents easy encapsulation with other polymer resins or solutions in applications where integrated or (multiyear) stacked heaters are required. Porous substrates with discontinuous distribution of polymer precursors, such as polymer fabrics or veils, allow for easy infusion of polymer resins or solutions and minimizing the shape distortion, but provide a non-uniform, textured surface for LIG synthesis. This report describes the development of resistive heaters based on LIG-aramid woven fabric as an alternative to polyimide film precursors. Aramid fabrics are less expensive substrate materials compared to polyimide films, provide porous architecture for easy infusion of solutions

and resins, and are commonly used as fiber-reinforcements in polymer composites. As a result, the LIG-aramid fabric heaters developed in the present study are compatible with most composite processing techniques and can readily be used to impart multifunctional properties to composite materials and structures.

Resistive heating of LIG-modified fabrics requires creation of a uniform and continuous network of LIG on the textured and non-uniform fabric architecture for even distribution of electric current and heat generation throughout the fabric. In comparison with solid polymer films, the spacing between individual fibers within a tow or inter-yarn spacing can affect the continuity of the LIG network and spatial uniformity of heat generation. LIG-modified aramid fabrics have been previously developed for intelligent protective clothing and composites with enhanced interlaminar mechanical properties and damage detection capability;[146–148] however, use of LIG in those applications does not necessarily require integrity, continuity, and uniformity of the LIG layer within the entire plane of the fabric. To the best of our knowledge, resistive heating of LIG network synthesized on non-uniform, architected substrates (such as fabrics) have not been studied before.

The aim of the present work is therefore to investigate the electrothermal performance of resistive heaters based on LIG-aramid fabric and understand the role of various processing parameters on the quality and performance of resulting heaters. The effect of input laser power on the quality of LIG-aramid is studied by characterizing the morphology and chemical composition of produced LIG. Detailed experiments are carried out to determine the relationship between lasing process parameters (i.e., input laser power, scan rate, and pulse per inch) and electrical properties as well as Joule heating performance of LIG-aramid fabric heaters. Fabric heaters are then used in two different applications. Highly flexible LIG heaters are prepared by impregnation of LIG-aramid

fabrics with a polydimethylsiloxane silicone rubber. While the addition of silicone rubber might adversely affect the electrothermal efficiency of heaters, it enhances their durability and reliability, which is ideal for use in applications where flexible and robust heaters are required. In addition, LIG-aramid heater is used an embedded heater for rapid initiation of frontal polymerization. A 10 cm × 10 cm carbon panel is successfully cured within only 1 min with a total energy consumption of only 4.13 kJ, which is four orders of magnitude less than energy required for producing a similar part using the conventional autoclave-based approach. Owing to the facile and scalable synthesis and writing of LIG along with the easy impregnation of substrate aramid fabric with polymeric materials, the heaters developed in this study can be used in a wide variety of applications where flexible or integrated heaters are required.

3.2 Experimental section

3.2.1 Preparation of LIG-aramid fabrics and composites

Woven aramid (Kevlar) fabric (plain weave, areal weight = 140 g m^{-2}) was purchased from ACP Composites (SKU**:** W-AR-5-PW-50-P) and used as received. LIG was synthesized on aramid fabric using a 10.6 μm CO_2 laser (ILS 12.15 platform, 75 W, Universal Laser Systems) in a raster mode. Various processing parameters (laser power, scan rate, and pulse per inch) were used to tailor and study the quality and properties of resulting LIG. For preparation of flexible composite heaters, one layer of LIG-patterned fabric (25 mm × 40 mm) was impregnated with a polydimethylsiloxane silicone rubber (SYLGARD^{TM} 184, Dow Corning) by drop-casting method and cured in oven at 70 °C for 8 hours. For preparation of silicon resin, 1 g of hardener was added to 10 g of silicone resin and thoroughly mixed. A composite panel containing an LIG surface ply is manufactured according to the procedure explained in chapter 2 using double-bagged resin infusion process. Frontal curing is performed using an input voltage of 35 V for 1 min.

3.2.2 Structural characterization of LIG

The morphology of LIG was imaged using JEOL JSM-5800 field emission scanning electron microscope (FESEM) at an accelerating voltage of 1 kV. As samples were electrically conductive, imaging was conducted without coating gold. Raman spectra were collected using a Horiba THz Raman system (26 mW, 532 nm) focused through a 10x microscope objective (Olympus) mounted on an Olympus IX73 inverted microscope. A Horiba iHR550 spectrometer was used to disperse the Raman signal on a Horiba Synapse back-illuminated CCD camera for detection. Electrical measurements were conducted using a FLIR multimeter (DM285). X-ray Photoelectron Spectroscopy (XPS) was performed using a Physical Electronics 5800 series Multi-Technique ESCA system with a monochromatic AL Kα ($h\nu$ = 1,486.6 eV) source operated at 350.0 W. An electron flood gun was used for charge neutralization. High resolution scans were collected with a pass energy of 23.5 eV and an interval of 0.1 eV/step. The instrument pressure was 5×10^{-8} torr or lower during data acquisition.

3.2.3 Characterization of electrothermal performance

Electrothermal performance of resistive heaters was evaluated using specimens with a 15 × 15 mm^2 effective heating area prepared under various processing conditions. A nickel-filled conductive paste (Pyro-Duct 598 A, Aremco) was used to attach copper electrodes to both ends of heaters. Various voltages were supplied to heaters using a DC power supply (9206, B&K Precision). The temperature at the center of heaters was measured using a T-type thermocouple and recorded by a LabView program. A FLIR T540 infrared thermal camera was also used to measure the temperature distribution and stability of heaters under static and cyclic electrical loading conditions.

3.3 Results and discussion

3.3.1 Synthesis of LIG on aramid fabric

The manufacturing process of LIG-aramid fabric is shown in Figure 3-1. Upon irradiation of aramid fabric with a CO_2 laser beam, the material is converted into porous graphene via a photothermal process. Unlike conventional nanomaterial-based Joule heating methods, which require handling and deposition of nanomaterials in multiple processing steps, synthesis and writing of graphene on aramid fabric is conducted in one simple step. In addition, highly customized and geometrically complex patterns of LIG can readily be written on aramid fabric without the need for using any masks (Figure 3-1 b).

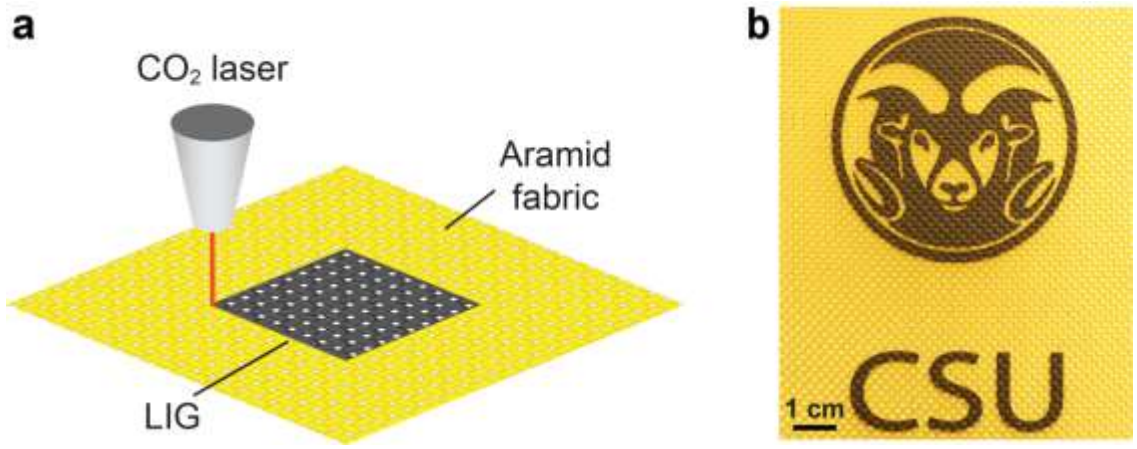

Figure 3-1. Writing laser-induced graphene (LIG) on aramid fabric. a) Schematic representation of the lasing process. b) Example of an LIG pattern created on aramid fabric.

The microstructure, composition, and morphology of LIG-aramid were studied using Raman spectroscopy, X-ray photoelectron spectroscopy (XPS), and scanning electron microscopy (SEM), respectively. Raman spectra of aramid fabric before and after laser treatment is shown in Figure

3-2. The characteristic peaks of aramid at 1,509 cm^{-1}, 1,566 cm^{-1}, 1,606 cm^{-1}, and 1,640 cm^{-1} disappeared after laser scribing, and three new bands formed at 1,337 cm^{-1}, 1,565 cm^{-1}, and 2,667 cm^{-1}. These new bands are representative of the D-band, G-band, and 2D-band of graphitic structure, respectively.[149] Specifically, the D-band is related to defects, bent sp^2 bonds, and vacancies, while the G-band is the first-order Raman band of all sp^2 hybridized carbons. The relative intensities of these three peaks are a measure of the quality of graphene. The intensity ratio of D-band to G-band (I_D/I_G) is a measure of defect level in the graphitic structure, whereas the intensity ratio of 2D-band to G-band (I_{2D}/I_G) is related to the number of graphene layers stacked in the *c*-axis. Raman spectrum of a high-quality graphene typically exhibits a low D/G band ratio and high 2D/G band ratio.[150] Although the quality of graphene produced on aramid precursor is not too high, as also previously reported for LIG-aramid,[147] the resulting LIG is still conductive enough to exhibit substantial Joule heating capability. The effect of laser input power on the quality of resulting LIG is shown in Figure 3-2 b-d. An increase in the input laser power first decreases the defect levels but then results in increased defect quantity (Figure 3-2 c). This observation can be attributed to the temperature rise during the lasing process, which is directly affected by the input laser power. When the input laser power is low, the graphitization temperature is not high enough for achieving high degree of crystallinity in the graphitic structure, resulting in high defect levels. As the input laser power increases, conversion of precursor into graphitic structures occurs at higher temperatures, leading to higher levels of order. However, thermal oxidation at high input power caused by excessively high temperatures results in the formation of high amounts of defect in the graphitic structure.[151] In addition to the influence on the level of defect, the input laser power also affects the number of layers in LIG. The values of I_{2D}/I_G ratios reveal that multilayer graphene is formed during lasing process (Figure 3-2 d).

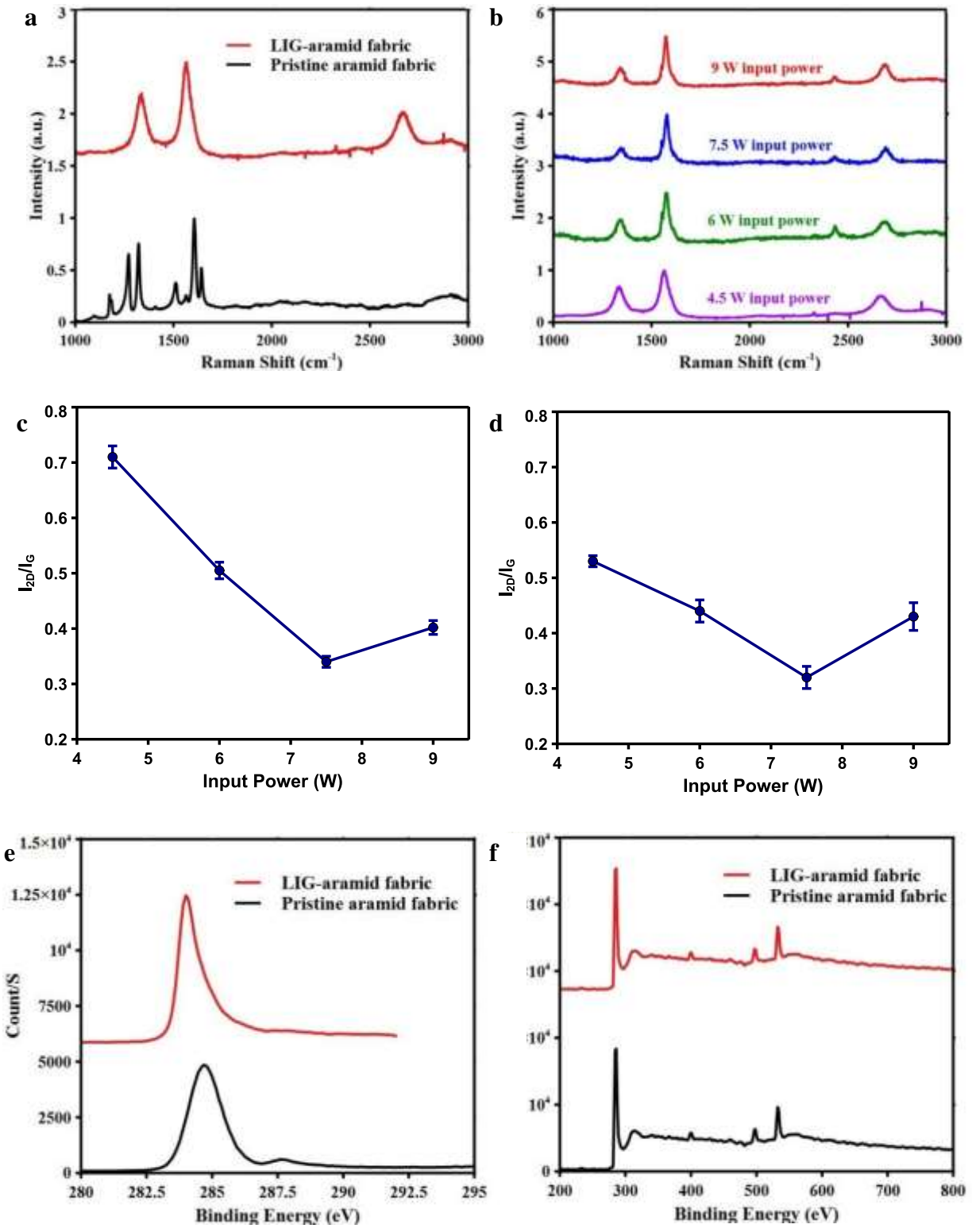

Figure 3-2. Characterization of the microstructure and composition of LIG-aramid. a) Raman spectra of aramid fabric before and after laser treatment under input laser power of 4.5 W, PPI of 800, and scan rate of 90 mm s^{-1}. b) Effect of laser input power on the Raman spectra of LIG. c, d) Variation of D/G and 2D/G peak intensity ratios as a function of input laser power, respectively. e) High-resolution XPS carbon spectra before and after laser ablation. f) XPS general survey before and after laser treatment (input laser power = 9 W, PPI = 800, and scan rate = 90 mm s^{-1}).

The surface compositions of untreated and treated fabrics were characterized using XPS measurements (Figure 3-2 e, f). A comparison of the survey spectra before and after laser scribing reveals a reduction in the atomic percentages of nitrogen and oxygen elements. This reduction in concentrations of oxygen and nitrogen elements is also confirmed by the high-resolution carbon spectra of LIG (Figure 3-2 f). In addition, the asymmetric peak of the LIG-aramid fabric at low binding energies is another evidence for the formation of graphitic structures (Figure 3-2 e).

The morphological changes of aramid fabric after laser treatment were determined using SEM imaging. While untreated aramid fibers exhibit a very smooth surface (Figure 3-3 a), the treated fibers show a relatively rough and porous surface structure (Figure 3-3 b, c). The higher magnification micrograph in Figure 3-3 c shows the sheet-like porous structure of the scribed fibers, caused by the release of gaseous products during the lasing process due to the photothermal breakage of chemical bonds, such as C-N and C=O.[111]

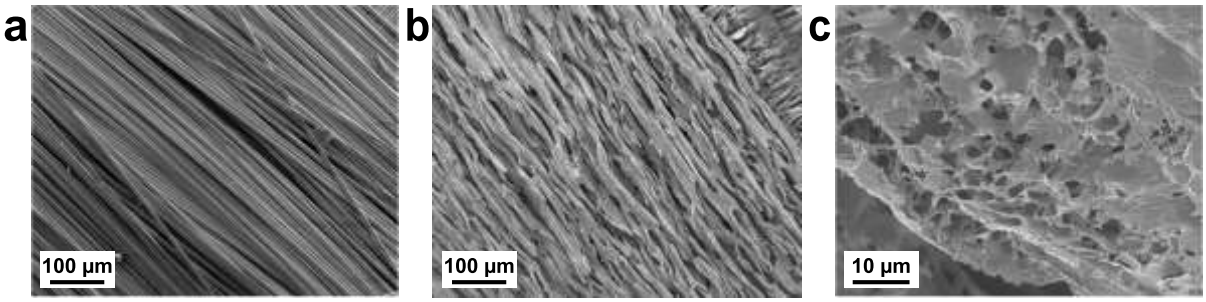

Figure 3-3. Morphological characterization of aramid fabric before and after laser treatment using SEM imaging (input power = 9 W, PPI = 800, and scan rate = 90 mm s^{-1}). a) Pristine aramid fabric. b, c) LIG-aramid fabric at two magnifications.

3.3.2 Electrothermal characterization of LIG-aramid fabric

Developing efficient resistive heaters based on LIG-aramid requires thorough understanding of the effect of processing parameters on the electrothermal performance of modified fabrics. Three key processing parameters, which can directly affect the quality and performance of heaters, are input laser power, laser scan rate, and pulse per inch (PPI). The effects of these three lasing process parameters on electrical and electrothermal performance of LIG-aramid heaters are shown in Figure 3-4. As laser power increases from 4.1 W to 6.1 W, the electrical resistance of modified fabrics decreases from 422 Ω to 42 Ω (Figure 3-4 a). Further increase in laser power results in steady drop in the electrical resistance such that a sheet resistance of 19 Ω is achieved at an input laser power of 8.9 W. Incomplete conversion of aramid precursor to graphene along with the relatively low quality of graphene is responsible for the relatively high electrical resistance of LIGs at low input laser powers. With an increase in laser power, a thicker layer of aramid is converted into graphene and the defect level in graphitic structure is decreased, leading to lower measured resistance. The electrothermal performance of nanostructured heaters produced by various input laser powers was determined by applying a constant voltage of 10 V across specimens and measuring their time-dependent temperature profiles (Figure 3-4 b). As the driving voltage is applied, the temperature of resistive heaters rapidly increases until a steady-state temperature is reached. Additionally, higher steady-state temperatures are observed for heaters produced by higher input laser powers, indicating the significance of graphene quality and electrical conductivity on the electrothermal performance of LIG-based heaters.

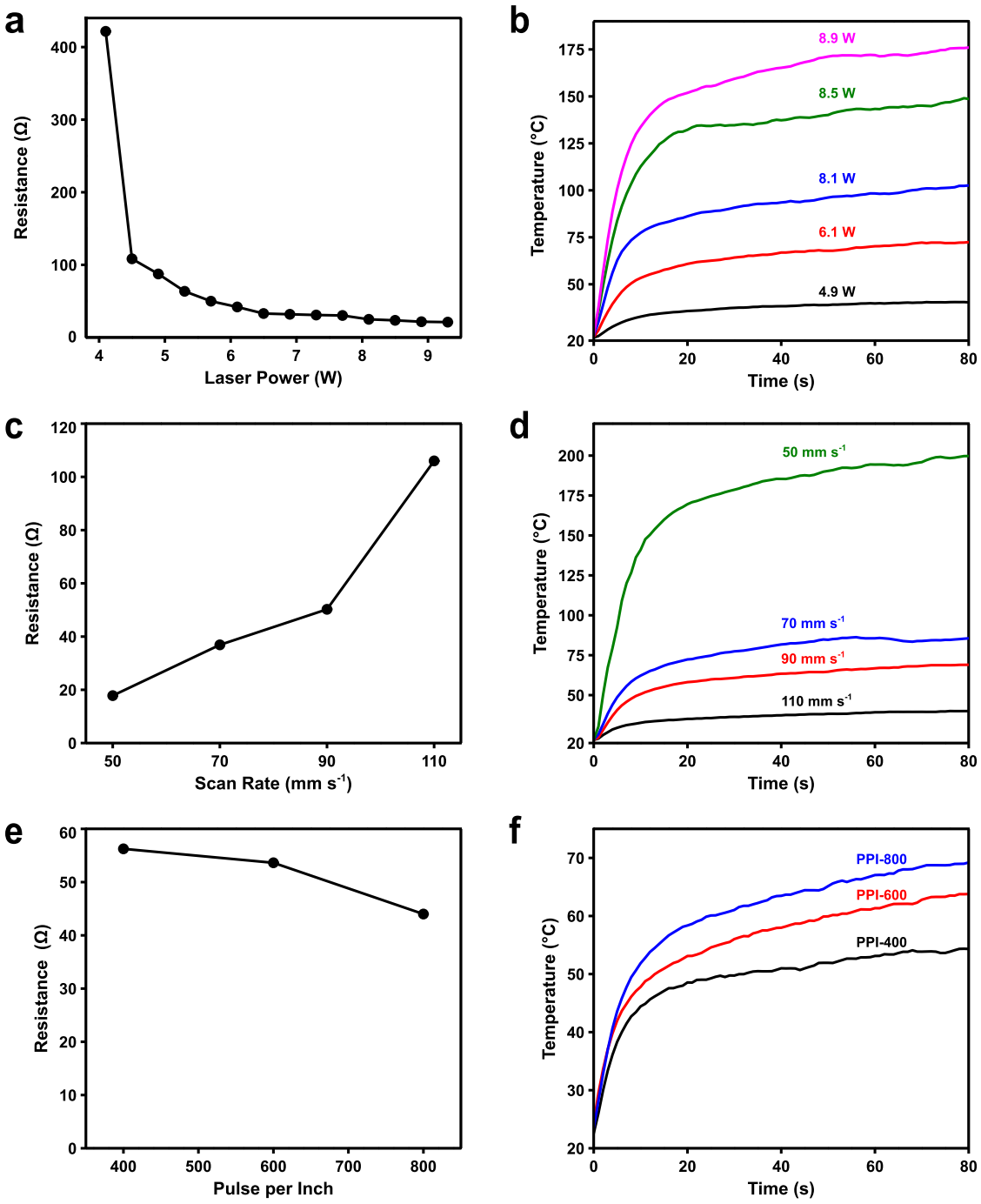

Figure 3-4. Effect of lasing processing parameters on electrical properties and time-dependent electrothermal performance of LIG-aramid fabrics. a, b) Electrical resistance and electrothermal response of LIG samples prepared by various input laser powers at a fixed scan rate of 90 mm s^{-1} and PPI of 800, respectively. c, d) Electrical resistance and electrothermal response of LIG samples prepared by various scan rates at a fixed input laser power of 6.1 W and PPI of 800, respectively. e, f) Electrical resistance and electrothermal response of LIG samples prepared by various PPI values at a fixed laser input power of 6.1 W and scan rate of 90 mm s^{-1}.

This improvement in electrothermal performance can be explained by the inverse relationship between the generated heat (Q) and heater resistance (R) for a given input voltage,[152]

$$Q = \frac{V^2}{R} \tag{3-1}$$

As the resistance of heaters decreases, more electric current can pass through the heater when subjected to a constant input voltage, leading to a higher frequency of collision between electrons and increased heat generation because of energy loss. As shown in Figure 3-4 c, heater resistance increases with an increase in the scan rate. The electrothermal performance of heaters improves at lower lasing speeds, where steady-state temperatures of up to 200 °C can be obtained using the lasing speed of 50 mm s^{-1} (Figure 3-4 d).

PPI is a processing parameter that is used to control the number of laser pulses per linear inch of engraving. The electrical resistance of LIG-aramid decreases from 56 Ω to 42 Ω as PPI varies from 400 to 600 (Figure 3-4 e). With an increase in the PPI, a relatively more uniform layer of graphene is created on the aramid precursor, leading to a slight reduction in the electrical resistance of LIG-aramid fabric. This reduction in electrical resistance is associated with a 15 °C increase in steady-state temperature of heaters during the electrothermal tests under an input voltage of 10 V (Figure 3-4 f).

We performed additional experiments to understand the electrothermal response of heaters to various applied voltages. For these experiments, the temperature profile of a heater produced under input laser power of 8.9 W, PPI of 800, and scan rate of 90 mm s^{-1} was determined by varying the value of voltage applied across the heater (Figure 3-5 a). The steady-state temperatures of the heater increased quadratically as a function of the applied voltage (Figure 3-5 b), verifying that the

response of the resistive heater follows Joule's law. The consumed power density for reaching a temperature of 170 °C from room temperature is 1.5 W cm^{-2} (Figure 3-5 c), which is equivalent to a heating performance of 100 °C cm^2 W^{-1}. While this heating performance is slightly lower than that of LIG heaters produced using PI films as a precursor (131 °C cm^2 W^{-1}),[59] it is sufficiently high to meet the heating requirements of a wide range of applications.

A larger heater (effective heating area = 49 cm^2) was also produced under the same processing condition (i.e., input power = 8.9 W, scan rate = 90 mm s^{-1}, and PPI = 800) to demonstrate the scalability of the manufacturing process and resistive heating performance of produced heaters (Figure 3-5 d). The thermal infrared image of the heater shows an even distribution of temperature (average temperature = 170 °C) with 10 °C variation throughout the heater in response to a power density of 1.3 W cm^{-2} (Figure 3-5 e). In addition, similar temperature profiles were measured along the two midlines of the sample (Figure 3-5 f); however, a more uniform temperature distribution was observed along the lasing direction compared to transverse direction. This directional difference in temperature distribution is attributed to the more controlled and uniform creation of graphene along the lasing direction compared to the transverse direction.

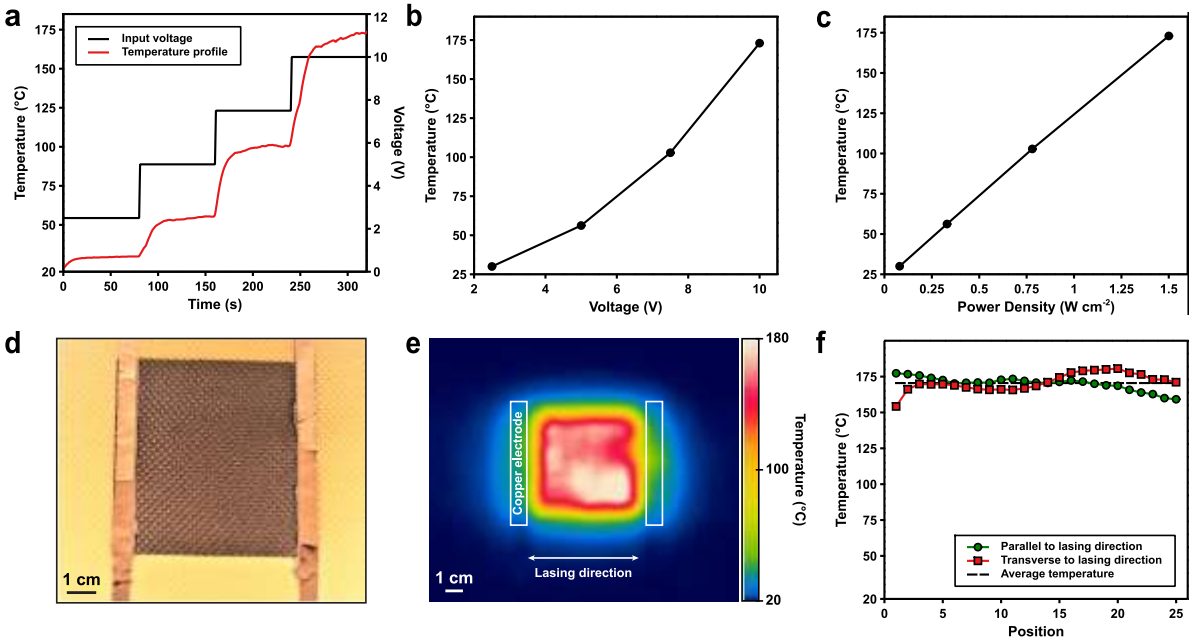

Figure 3-5. Electrothermal performance of LIG-aramid fabric heaters under various input voltages. a) Temperature profile of an LIG-aramid heater (input power = 8.9 W, PPI = 800, and scan rate = 90 mm s^{-1}) in response to an increasing input voltage load. b) Steady-state temperature of the heater in (a) as a function of input voltage. c) Relationship between steady-state temperature of the heater in (a) and power density. d, e) Digital and thermal infrared images of a large LIG-aramid heater (effective heating area = 35 cm^2), respectively. f) Temperature distribution along the midlines of the sample shown in (d, e). The midline directions are parallel and transverse to the lasing direction.

3.3.3 Silicone-encapsulated LIG-aramid fabric

While LIG-modified films and fabrics exhibit excellent electrothermal performance, they are prone to mechanical damage during handling and service due to the brittle structure of LIG layers. Loss of the conductive LIG layers can consequently result in increased resistance and degradation of the performance of LIG heaters. We improve the mechanical robustness of LIG-aramid fabrics by encapsulating them with silicone rubber and protecting the LIG structure against mechanical damage and scratches. Although silicone rubber is an intrinsically insulating polymer, we observed no significant change in the electrical resistance of LIG after encapsulation with silicone. We hypothesize that the resistance of LIG does not vary when encapsulated by silicone due to two competing effects. The presence of the electrically insulating rubber is typically expected to

increase the overall resistance of the LIG structure after filling the porous spacing within graphene layers. However, deformation of LIG structure due to cure shrinkage of silicone can lead to compaction of the LIG network and therefore a reduction in resistance. As a result, no significant change in the resistance of LIG-modified fabric was observed upon the encapsulation process. However, the electrothermal performance of LIG fabric remarkably decreased upon encapsulation by silicone rubber (Figure 3-6 a). For example, the steady-state temperature of the composite heater is ~100 °C under an applied voltage of 10 V whereas the equilibrium temperature of the unencapsulated fabric heater is ~170 °C under the same condition (Figure 3-6 b). The difference in the equilibrium temperature ($T_{eq.}$) of encapsulated and unencapsulated heaters can be explained by equation 2-2. Since the resistance of the heater remains unchanged after adding silicone rubber, the amount of heat generated via Joule heating effect remains constant. However, the thermal mass of the heater increases when adding silicone encapsulant, resulting in reduced equilibrium temperature of the composite heater. In addition, presence of silicone rubber can facilitate heat dissipation to substrate via conduction heat transfer. As a result, both higher thermal mass of the composite heater and increased heat loss to surrounding are responsible for the observed inferior performance of the composite heater compared with as-prepared LIG-aramid fabric heaters. Similarly, the composite heater requires higher input electric power for reaching a given steady-state temperature compared to the LIG-aramid fabric without silicone rubber (Figure 3-6 c).

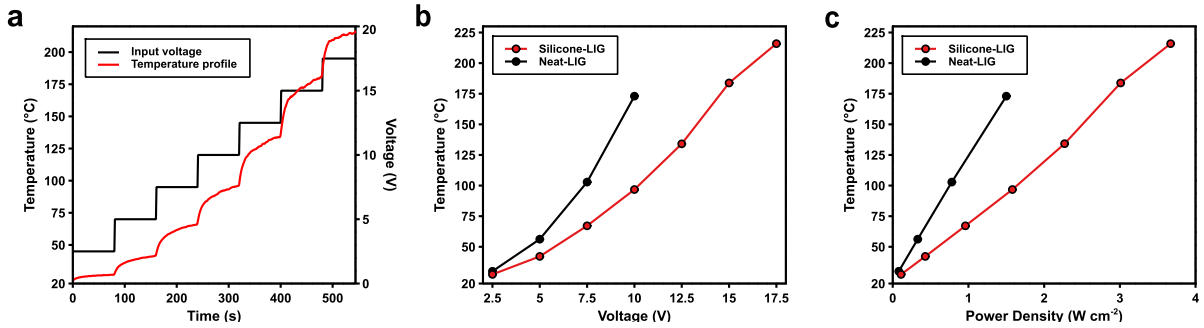

Figure 3-6. Electrothermal response of a flexible silicone-encapsulated LIG-aramid fabric. a) Temperature profile of the encapsulated heater in response to an increasing input voltage load. b, c) Steady-state temperature of both encapsulated and unencapsulated heaters as a function of applied voltage and power density, respectively.

The electrothermal stability of composite heaters were determined using both electrical static and cyclic loads to evaluate the time-dependent and dynamic response of heaters to applied power (Figure 3-7 a, b). For static electrothermal tests, a constant voltage of 10 V was applied on the heater while monitoring its average temperature over time (Figure 3-7 a). In dynamic electrothermal tests, the applied voltage was intermittently varied between 0 and 10 V during 30 s time intervals (Figure 3-7 b). The steady-state temperature of the composite resistive heater did not significantly change even after one hour of continuously applying electric power. Similarly, the results of cyclic electrothermal stability test reveal that the performance of the heater is consistent under electrical cyclic loading conditions, further verifying the reliability and reproducibility of produced composite heaters. In addition, the encapsulated LIG heater could preserve its heat generation capability when deformed from original flat shape to a bent geometry (Figure 3-7 c, d). However, a small difference (~5 °C) between steady-state temperatures of deformed and undeformed heaters was observed, which is due to slight increase in resistance of heater under bending deformation.

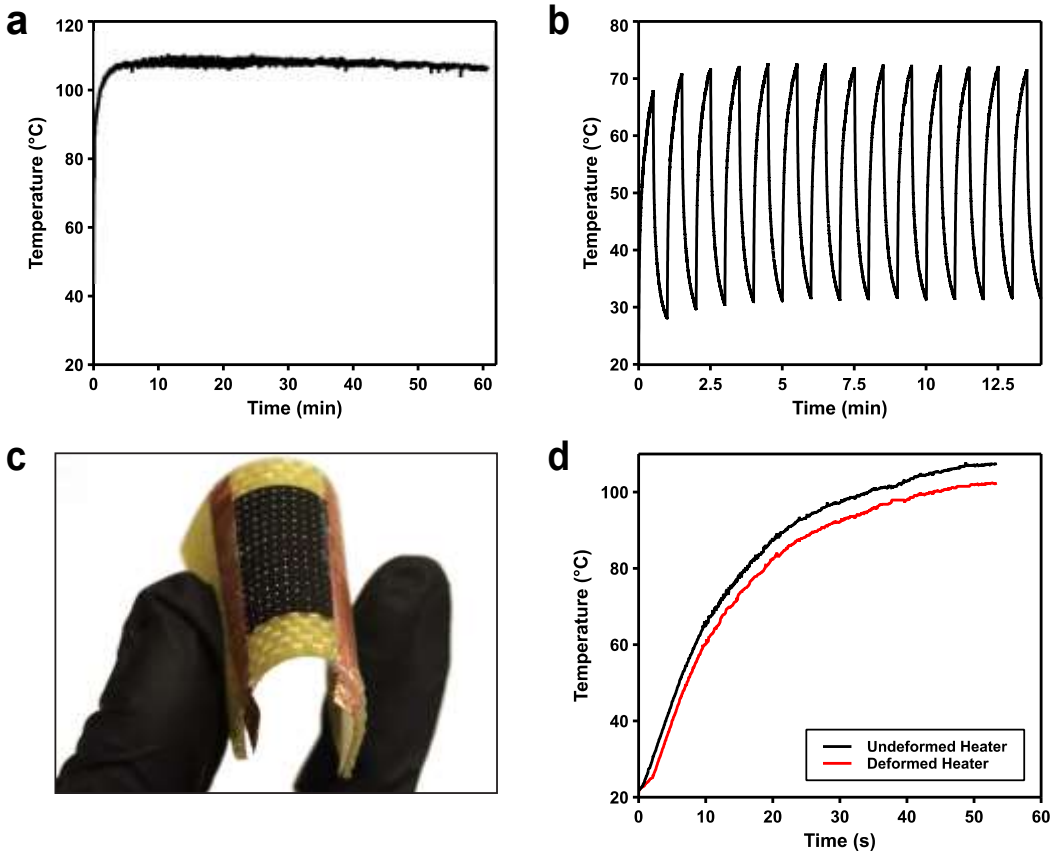

Figure 3-7. Electrothermal performance of silicone-encapsulated LIG-aramid fabric under various electrical and mechanical loading conditions. a) Long-term stability test at a constant input voltage of 10 V. b) Cyclic stability test by varying the applied voltage between 0 and 10 V within 30 s time intervals. c) Digital image of the bent encapsulated LIG-aramid fabric. d) Time-dependent temperature profile of the heater in bent (radius of curvature ~7 mm) and flat configurations.

3.3.4 Frontal curing of FRPCs using an integrated LIG-aramid heater[3]

Another application of LIG-aramid heater is embedding it in the composite layup for initiation of frontal polymerization. LIG-aramid fabric possesses superior mechanical and handling properties compared to buckypaper, while showing excellent electrothermal performance. A 10 cm × 10 cm LIG-aramid heater is prepared (8 W, 90 mm s^{-1}, 800 PPI) using a CO_2 laser according to the procedure explained in previous section. Detailed experiments were conducted similar to those

[3] This section was not included in the paper published in ACS Omega.

performed on buckypaper to determine power requirement for rapid initiation of FP. Figure 3-8 a shows temperature data collected at the center of the top surface of layup during the curing process of a carbon composite panel on a glass plate using an input voltage of 35 V. Upon supplying power into the layup, temperature slowly increases until it reaches the activation temperature of frontal polymerization. Then, a drastic rise of 66 °C in temperature is observed, indicating the initiation of FP. While a similar trend is observed for electrical resistance and power consumption profiles as those observed for curing of composite panel using an integrated BP heater (Figure 2-3 b), the extent of reduction in electrical resistance is much less compared to that observed for BP, leading to only a slight increase in power consumption upon initiation of FP. Although we did not directly measure the temperature dependency of electrical resistance of LIG-aramid heater, this observation shows that the temperature coefficient of resistance of LIG-aramid is very small compared to BP. The energy consumed during 1 min curing process is only 4.13 kJ, which is comparable to energy input required for producing the same part using an embedded buckypaper heater.

The spatial temperature distribution during the curing process is monitored using infrared thermal imaging on the surface of the composite layup. Compared to the panel produced using BP (Figure 2-3 c), heat generation is less uniform prior to initiation of FP due to inferior thermal and electrical properties of LIG combined with the fabric structure of LIG heater. Front polymerization is initiated slightly earlier (at 25 s), probably because of the larger temperature gradient that exists, leading to formation of a local hot spot. Once the front is initiated, it propagates in both through-thickness and in-plane directions (Figure 3-8 c). The total energy consumption during 1 min cure cycle is only 4.13 kJ, which is comparable to the energy required for curing a similar part using buckypaper heater. DSC measurements are also performed on samples cut from top and bottom

sections of the produced panel to determine the degree of cure. DSC results reveal that a degree of cure ca. 92 % is obtained for both sides of laminate, which is slightly lower than the degree of cure reported for panel cured using an embedded buckypaper heater. However, the degree of cure is still high enough to ensure excellent thermo-mechanical properties of the produced laminate.

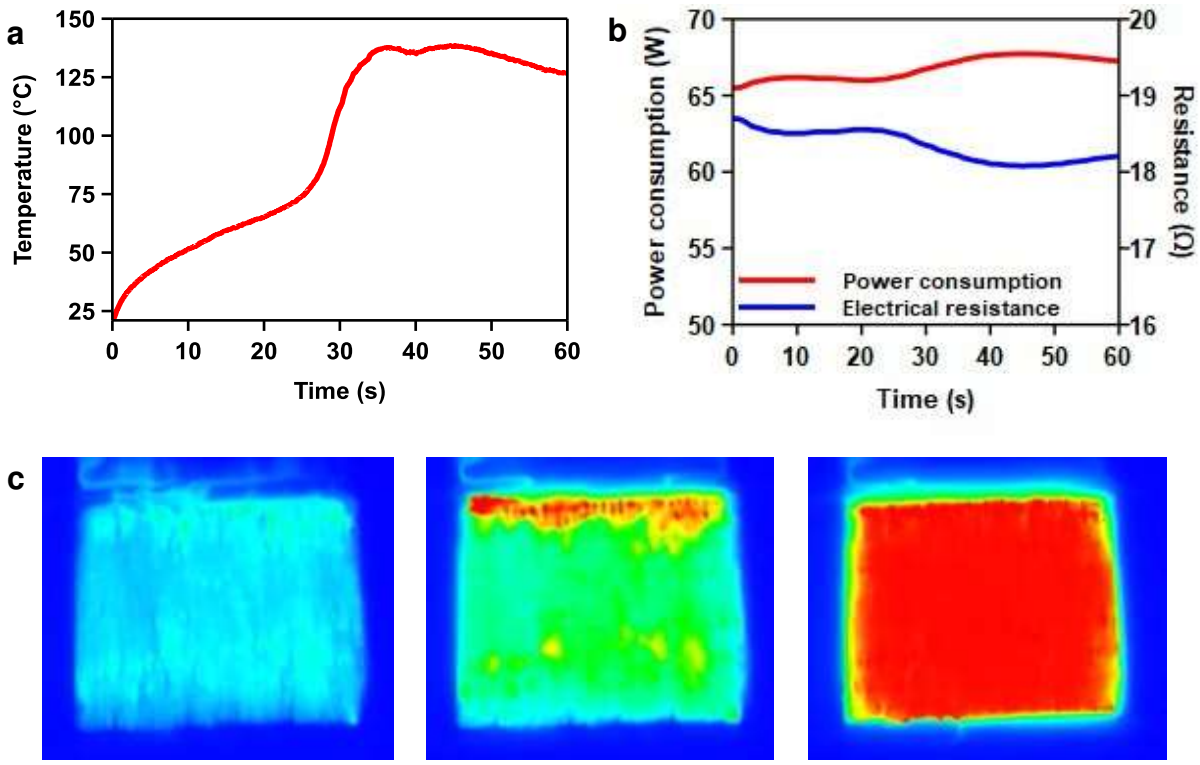

Figure 3-8. Through-thickness frontal curing of a 10 cm × 10 cm carbon composite panel using an integrated LIG-aramid heater. (a) Temperature data collected at top surface during the curing process. (b) Electrical resistance and power consumption profiles measured and recorded during 1 min heating cycle. (c) Infrared Imaging of the frontal curing process of a composite panel using an integrated LIG-aramid heater.

3.4 Conclusions

We have demonstrated that aramid fabric can be successfully used as an inexpensive precursor for fabricating LIG-based resistive heaters with a high electrothermal efficiency. The quality and performance of fabric heaters were directly affected by the key processing parameters, namely input laser power, scan rate, and pulse per inch of engraving. The electrothermal response of the produced LIG heaters followed Joule's law, where a linear correlation was obtained between the steady-state temperature of heaters and the square of the input voltage. The fabric structure of LIG-heaters allowed for facile impregnation with polymer resins for development of integrated heaters and multifunctional composites. Two applications were developed for produced LIG-aramid heaters. Highly flexible and stable heaters were prepared by impregnation of LIG-modified aramid fabric with a silicone rubber. In addition, LIG-aramid was embedded in composite layup as an alternative to BP for rapid initiation of FP. A 10 cm × 10 cm carbon panel was successfully cured within 1 min using a total energy consumption of 4.13 kJ, which is comparable to the time and energy required for curing the same part using an integrated buckypaper heater.

CHAPTER 4: RAPID AND FACILE PREPARATION OF NANOCOMPOSITE FILM HEATERS FOR COMPOSITE MANUFACTURING[4]

4.1 Introduction

Nanocomposite film heaters are promising for out-of-oven (OoO) and energy-efficient curing of fiber-reinforced polymer composites. However, the current techniques for manufacturing nanocomposite film heaters are intensive in terms of time and energy and require expensive resources. In this work, we present a facile and rapid approach for preparation of nanocomposite film heaters with excellent heat generation properties based on a frontally polymerizable resin system. This approach enables rapid fabrication of nanocomposite films within a few minutes and without the need for using expensive equipment, making it suitable for mass production of nanocomposite film heaters. Various characterization techniques are used to determine the morphology, composition, and mechanical properties of nanocomposite films. The electrothermal performance of nanocomposite film heaters are then evaluated under various conditions. Nanostructured heaters exhibit excellent Joule heating properties, where temperatures as high as ~132 °C can be reached within only 2 min using a low input power density of ~2 W cm^{-2}. Finally, a nanocomposite film heater is used for OoO curing of a small composite panel with minimal energy consumption. Using this approach, 0.1 MJ of energy is consumed during the four-hour cure

[4] Reprinted from Frontiers in Materials 2023, 10, 124. Copyright (2023) Frontiers. https://www.frontiersin.org/articles/10.3389/fmats.2023.1166986/full.

cycle of a commercial prepreg system, which would otherwise require at least 40.5 MJ of energy to cure using a convection oven.

Fiber-reinforced polymer composites (FRPCs) exhibit excellent specific mechanical properties, chemical stability, and fatigue resistance, making them an ideal material for designing lightweight and durable structures in a variety of industries including aerospace, wind energy, defense, construction, and marine.[2,3] However, the widespread use of FRPCs in various applications is limited by their underlying challenging manufacturing processes. The traditional technology for manufacture of polymer composites involves elevated-temperature curing of the matrix thermoset resin for several hours (up to 24 h) in an autoclave or oven. This process is highly intensive in terms of time, energy, carbon footprint, and resources. In addition, the production rate and size of components are limited by the internal dimensions and availability of ovens and autoclaves.[5]

Composite layups are typically heated in an autoclave or oven via convection, which is highly inefficient in terms of energy consumption, as a significant amount of energy is required to heat up a large volume of gas inside the equipment.[7] Developing alternative heating methods that enable fast and efficient heating of a composite layup has been the focus of extensive research over the past decade. One of the alternative heating approaches is using electromagnetic waves (e.g., infrared, microwave, and ultraviolet) for supplying the energy required for composite curing.[10,106] Although each of these radiation curing methods offers distinct advantages, they are challenging to use at an industrial scale due to their specific limitations. For example, the high cost of microwave ovens, use of special tooling materials, and microwave shielding effect of carbon fibers are key issues that limit the widespread adoption of microwave heating technique for composite processing.[27] Direct conductive heating is a promising heating method, which can substantially reduce the energy demand of curing process while eliminating the need for expensive autoclaves

or ovens. In this curing approach, heat is directly supplied to the composite layup via conduction, either from a heated mold or direct resistive heating of a conductive material.[47] The latter approach is advantageous as the acquisition and maintenance of heated tools are costly. In direct resistive heating approach, the heat required for curing of the matrix thermoset resin is supplied by passing electric current through a conductor, in which the electric energy is converted into heat via Joule's effect. A wide range of conductive materials including carbon fiber, metal meshes, and nanocomposite films have been used as a resistive element for direct heating of composite layups. Nanocomposite films in particular show a great promise for curing polymer composites in part because of their excellent electrothermal conversion efficiency, low thermal mass, and deformability. Additionally, nanocomposite films can be integrated into a composite layup and remain advantageous in service conditions by imparting new functionalities (e.g., de-icing, damage sensing) to the host composite structure.[119,123]

Adoption of direct conductive curing technique using nanocomposite film heaters requires developing new approaches for scalable, rapid, and inexpensive preparation of nanocomposite films with excellent electrothermal properties. There are two main approaches for preparation of nanocomposite film heaters. In the more traditional approach, conductive nanoparticles (e.g., carbon nanotubes, graphene) are added to the polymer matrix of composites via solvent-based or direct mechanical mixing techniques to enhance the electrical conductivity of the matrix polymer for heat generation via Joule's effect. While these approaches are useful for bulk preparation of polymer nanocomposites, they suffer from the challenging processing steps, safety hazards, and limited amount of nanoparticles that can be added to polymers.[153,154] For example, in preparation of carbon nanotube-modified polymers, often less than 1 wt.% of nanotubes can be added to polymers, as increasing the nanotube content substantially increases the resin viscosity and makes

the processing conditions quite challenging.[155] Additionally, it is extremely difficult to evenly disperse all nanotubes, resulting in agglomeration of nanoparticles in the polymer matrix and degradation of the mechanical properties of produced nanocomposites compared to the pristine polymer.[156,157] An alternative approach for preparation of polymer nanocomposite heaters with a high content of nanoparticles is creation of papers of nanoparticles followed by impregnation of the produced nanostructured papers by the polymer resin.[158] Buckypaper, which is a macroscopic assembly of carbon nanotubes, is one of such papers that has been produced at large scales and allows for creating polymer nanocomposites with a high concentration of nanoparticles (up to 30 vol.%) while enabling easier and safer handling of nanoparticles compared to bulk processing methods.[159] The high concentration of nanotubes in buckypaper results in a high electrical conductivity in produced nanocomposites, which is crucial for obtaining the desired electrothermal performance via Joule heating effect; therefore, produced heaters deliver superior electrothermal properties compared to nanocomposite heaters produced using bulk mixing approaches. The preparation process of nanocomposite films typically involves infiltration of the nanoparticle network with a thermosetting resin (e.g., epoxy) under vacuum and often at elevated temperatures to reduce the resin viscosity and facilitate the impregnation of the highly dense, porous network of nanotubes.[160] Following the infiltration step, the material is cured in an oven according to the cure cycle of the thermosetting resin, which can typically take several hours to obtain a fully crosslinked polymer network. These processing steps make the manufacturing process of nanocomposite heaters slow and arduous.

Recently, frontal polymerization (FP) has emerged as an energy-efficient and rapid approach for curing of thermoset resins and their composites.[116] In FP, a monomer solution containing a latent catalyst is heated locally to activate the latent catalyst and initiate an exothermic polymerization

reaction. The released heat is used to activate more catalyst and polymerize more resin. As a result, a self-propagating reaction wave is formed that propagates through the monomer solution until all available monomers are converted to polymer.[75] FP has been demonstrated for a wide range of resin systems including cyclic olefins, epoxies, and acrylates. Dicyclopentadiene (DCPD), a member of the cyclic olefin family, is one of the FP resin systems, which is of great interest due to its excellent front properties, long and tunable pot life, very low viscosity of ~1.5×10^{-3} Pa s, and excellent thermo-mechanical properties of resulting polydicyclopentadiene (pDCPD) polymer.[74,79]

The aim of this study is to introduce a facile approach for rapid and energy-efficient fabrication of thermoset-based nanocomposite film heaters at room temperature without using any vacuum conditions or ovens. To achieve this goal, we use a low-viscosity resin (η ~1.5×10^{-3} Pa s) based on dicyclopentadiene (DCPD) that can readily impregnate buckypaper networks at room temperature and ambient pressure. Following the rapid impregnation, the DCPD-based resin is cured via through-thickness frontal polymerization. In this work, we first evaluate the quality of the produced nanocomposite films by characterizing their composition, morphology, and mechanical properties using various techniques including scanning electron microscopy, thermogravimetric analysis, and tensile testing. Then, electrodes are connected to the opposite sides of the nanocomposite films to create film heaters and determine the electrothermal performance of resulting heaters in response to various static and dynamic electrical loading conditions. Upon characterization of the electrothermal performance of film heaters, they are used to demonstrate direct conductive heating and curing of a composite panel using a commercial prepreg system.

4.2 Experimental section

4.2.1 Materials

Dicyclopentadiene (DCPD), 5-ethylidene-2-norbornene (ENB), and second-generation Grubbs' catalyst (GC2) were purchased from Sigma Aldrich. DCPD is solid at room temperature; therefore a 95:5 wt.% solution of DCPD:ENB was prepared to depress the melting point of the resin solution. The DCPD/ENB solution will be referred to as DCPD resin hereafter in this article. Phenylcyclohexane (PCH) and tributyl phosphite (TBP) were obtained from TCI America. PCH is used to facilitate the dissolution of the GC2 catalyst in the resin solution, whereas TPB is used as an inhibitor to control the reactivity and pot life of the resin system. In a typical experiment, 3.21 mg of GC2 was measured and dissolved in 1 mL of PCH. An appropriate amount of TBP (1 molar equivalent with respect to GC2) was added to the GC2/PCH solution via a volumetric syringe. This solution was then added to 5 mL of DCPD and thoroughly mixed. Buckypaper with an average thickness of 60 μm was prepared in-house using multiwalled carbon nanotubes (Nanocyl NC7000) and based on the vacuum filtration technique. A silver-filled conductive paste (ConductiveX) was used for attaching copper electrodes to buckypaper films. A unidirectional carbon fiber prepreg (AX-6201XL, Axiom) was used for fabrication of composite panels.

4.2.2 Preparation and characterization of nanocomposite films

Differential scanning calorimetry (DSC) measurements were carried out on uncured DCPD resin as well as pDCPD films cured at various temperatures to determine an appropriate cure cycle for preparation of nanocomposites. For measurement of the total heat of reaction of the uncured resin, ~3 mg of resin was transferred into an aluminum hermetic DSC pan and sealed. DSC measurements were performed from 25 to 250 °C at a heating rate of 5 °C min^{-1}. The residual heat of reaction of cured pDCPD films was similarly measured by transferring 5 mg of cured resin into

a DSC pan, followed by heating from 25 to 250 °C at a heating rate of 5 °C min^{-1}. Degree of cure was calculated as $\alpha = 1 - H_r/H_t$, where α is the degree of cure and H_t and H_r are the total heat of reaction of the liquid resin and the residual heat of reaction of the cured films, respectively. A Discovery HR-2 Rheometer (TA Instrument) with a 40 mm flat geometry and a gap of 500 μm was used to determine the rheological properties of the DCPD resin containing 1 molar equivalent of inhibitor with respect to Grubbs' catalyst. Time-sweep measurements were performed at 23 °C with a frequency of 1 Hz. The wettability of pristine buckypaper by the DCPD resin was characterized by measuring the static contact angle at room temperature using a goniometer (Rame-Hart Instrument). A droplet of the DCPD resin was placed on the surface of a buckypaper specimen, and the contact angle was immediately measured. Five measurements were carried out and the average value is reported.

Nanocomposite films were prepared by droplet casting of resin onto the surface of buckypaper (Figure 4-1). Upon dropping a few droplets of resin, the resin was observed to quickly saturate the nanotube network, after which the excess resin was removed using a lint-free wipe. Through-thickness frontal polymerization was initiated by heating the DCPD-impregnated buckypaper using a laboratory-scale hot plate at ~140 °C. Since the thickness of the film is low (~100-200 μm), the propagation of the FP reaction through the thickness of the film was not noticeable and the overall cure process, from initiation to full cure, was completed within a few minutes. In other words, the resin was used here as a cure-on-demand resin system rather than as a self-propagating FP resin system. Thermogravimetric analysis (TGA) was used to determine the resin and nanotube contents in the nanocomposite films. Calculation of resin or nanotube content requires performing TGA experiments on neat polymer, pristine buckypaper, and nanocomposite film. TGA measurements were carried out from 25 to 600 °C at a heating rate of 10 °C min^{-1} under nitrogen

environment. A 30-min hold was also added to the temperature profile at 470 °C to obtain an accurate weight measurement of the residue from each specimen at this processing temperature. Two measurements were performed on each material. The resin content in the nanocomposite is calculated as,[161]

$$w_{\mathrm{R}} = \frac{(m_{\mathrm{F}} - m_{\mathrm{C}} + w_{\mathrm{I}}(1 - m_{\mathrm{F}}))}{(m_{\mathrm{F}} - m_{\mathrm{R}})} \tag{4-1}$$

$$1 = w_{\mathrm{R}} + w_{\mathrm{F}} + w_{\mathrm{I}} \tag{4-2}$$

w_{R} and w_{F} are weight fraction of resin and carbon nanotube in the nanocomposite film, m_{R}, m_{F}, and m_{C} are residual mass of neat resin, pristine buckypaper, and nanocomposite film measured at 470 °C, respectively. The concentration of solid (i.e., metal) impurities in pristine buckypaper (w_{I}) was determined by performing an additional TGA measurement on pristine buckypaper specimens from 25 to 1000 °C at a heating rate of 10 °C min^{-1} under air environment. The impurity content of the pristine buckypaper was calculated to be 9.5%. Scanning electron microscopy (SEM) was performed using a JEOL JSM-5800 field emission scanning electron microscope to observe the morphology of buckypaper films after impregnation. The cross-section of the nanocomposite film was sputter-coated with a 10 nm thick layer of gold and imaged at an accelerating voltage of 15 kV. Tensile tests were performed on rectangular specimens (2 × 30 mm^2) to determine the mechanical properties of pristine buckypaper and nanocomposite films. All tests were performed at a displacement rate of 1 mm min^{-1}. Electrothermal performance of nanocomposite films were characterized using specimens with an effective heating area of 10 × 20 mm^2. Copper electrodes were attached to both ends of the nanocomposite films using a silver-filled conductive paste. A

vacuum pressure of 81.3 kPa was applied to the heaters by vacuum-bagging them on a glass substrate to simulate boundary conditions that heaters undergo during the composite manufacturing process. Various voltages were supplied to the heater films using a direct current (DC) power supply (9206, B&K Precision). The voltage and current data during electrothermal tests were recorded to determine the power consumption. The temperature at the center of the heater was measured using a K-type thermocouple and recorded by a LabView program.

4.2.3 Composite fabrication

For fabrication of composite panels, a nanocomposite heater with an effective heating area of 30 × 30 mm^2 was used. Eight plies of a unidirectional prepreg (40 × 30 mm^2) were cured using the nanocomposite heater placed on top of the layup and separated from prepreg plies using a release film. The input power to the heater was gradually increased to ~8.9 W within 45 min to increase the temperature of the heater to 82 °C at a heating rate of 1.3 °C min^{-1} and then the input power was held unchanged for 3 h to simulate the cure cycle recommended by the prepreg manufacturer (3 h at 82°C). Two K-type thermocouples were used to measure the temperature profiles at the bottom and top of the layup during the curing process. An infrared thermal camera (FLIR T540) was also used to monitor the spatial distribution of temperature during the cure cycle. A control composite panel was also prepared using the same layup strategy but with curing the layup in an oven at 82 °C for 3 h. The degree of cure of the composite panels produced using direct conductive heating and oven curing approaches were determined using DSC measurements. The residual heat of reaction of the cured composites was measured by transferring 15 mg of the cured composites into a DSC pan, followed by heating from 25 to 250 °C at a heating rate of 5 °C min^{-1}. The total heat of reaction of the uncured prepreg was measured by performing DSC measurements on 5 mg specimens of the uncured prepreg using the same experimental procedure.

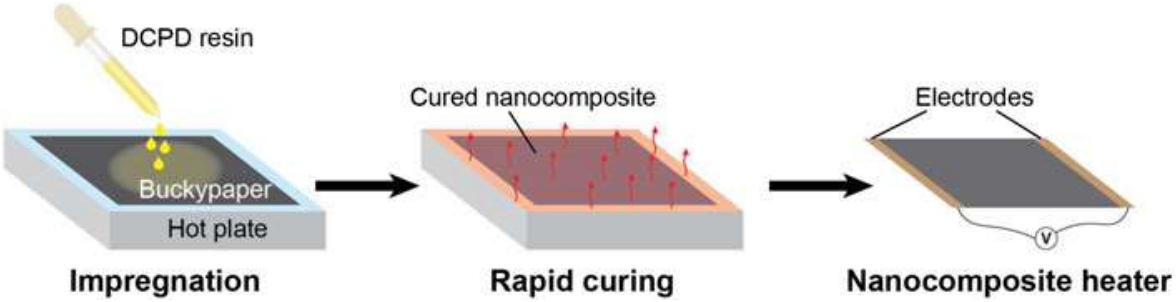

Figure 4-1. Schematic representation of the fabrication process of the nanocomposite film heater. A sample of buckypaper is first impregnated by the DCPD resin using droplet casting approach, followed by rapid curing via frontal polymerization. Nanocomposite film heaters are then prepared by connecting two copper electrodes to the two opposite sides of the produced films.

4.3 Results and discussion

4.3.1 Characterization of DCPD resin

Facile fabrication of buckypaper-based nanocomposites with a high density of nanotubes and low void content requires using a resin system that has a low initial viscosity and long pot life at room temperature while being rapidly curable at elevated temperatures and also having good compatibility with buckypaper for easy impregnation. DCPD meets such requirements and is a promising resin for facile preparation of polymer nanocomposite films; therefore, we studied processing of buckypaper impregnated with the DCPD cure-on-demand resin system to explore the feasibility of fabrication of pDCPD-buckypaper nanocomposite films under mild processing conditions compared with traditional approaches used for epoxy resins. The results of room-temperature rheological measurements on the DCPD resin show that the initial viscosity of the resin remained unchanged for approximately two hours, after which it slowly increased and reached a value of 750 Pa s after five hours (Figure 4-2 a); however, no gelation was observed within five hours of the measurement (Figure 4-2 b). As opposed to conventional epoxy resins, which have a high initial viscosity and short pot life, the low initial viscosity along with the long pot life of the DCPD resin enable facile impregnation of buckypaper at room temperature and

ambient pressure without the need for adding any solvents, which is highly desirable from the processing point of view. In addition, while the DCPD resin is stable for a few hours at room temperature, it rapidly cures at elevated temperatures and yields a fully cured solid polymer within a few minutes. Figure 4-2 c shows the results of DSC measurements on an uncured DCPD resin sample as well as a sample cured at 100 °C for 5 min. The tall and sharp exothermic peak observed in the thermal profile of the uncured resin sample, which indicates the range of cure temperature, clearly disappeared in the thermal profile of the cured sample. As a result, a high degree of cure (~93%) could be achieved by curing the resin for only 5 min. Contact angle measurements were also carried out to evaluate the wettability of buckypaper by the DCPD resin (Figure 4-2 d). While an initial contact angle of 17.3 ± 0.8° was formed between the DCPD resin and buckypaper, the resin completely infused into the porous structure of buckypaper within a few seconds, demonstrating the excellent compatibility of the resin and carbon nanotube network.

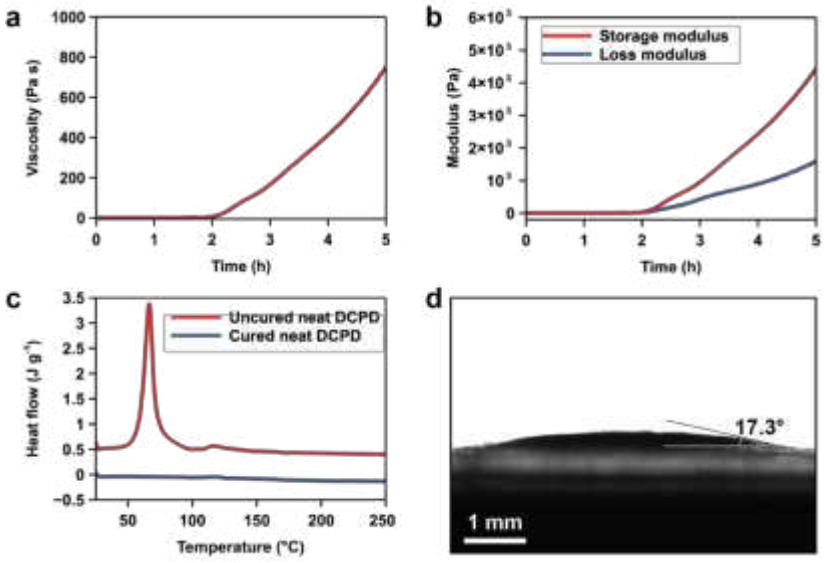

Figure 4-2. Characterization of DCPD resin system. (a, b) Time-sweep viscosity and modulus profiles of an uncured DCPD resin containing 1 molar equivalent of inhibitor with respect to Grubbs' catalyst at 23 °C. (c) Thermal profile of an uncured resin sample and a pDCPD film sample cured at 100 °C for 5 min. (d) Contact angle measurement for a droplet of DCPD resin on the buckypaper substrate.

4.3.2 Characterization of nanocomposite films

The appropriate cure temperature for preparation of nanocomposite films was determined by heating the neat DCPD resin samples for 5 min at various temperatures (100, 120, and 140 °C) and measuring the degree of cure of the resulting pDCPD films using DSC experiments. The degree-of-cure data obtained from DSC measurements are presented in Table 4-1. An increase in the cure temperature from 100 to 140 °C increased the degree of cure of pDCPD films from 93.8% to 99.4%, indicating that fully cured pDCPD films can be prepared by heating the material for 5 min at 140 °C.

DSC measurements were also conducted on a nanocomposite film sample cured according to the developed cure cycle (i.e., heating for 5 min at 140 °C) to determine the degree of cure of polymer in the nanocomposite film. A high degree of cure of ~98.2% was obtained for the cured nanocomposite film, further verifying that highly cured nanocomposite films can be prepared using the developed cure cycle.

Table 4-1. The degree of cure of various samples measured using DSC experiments.

Material	Cure temperature (°C)	Cure time (min)	Degree of cure (%)
pDCPD film	100	5	93.8 ± 1.2
pDCPD film	120	5	99.1 ± 0.3
pDCPD film	140	5	99.4 ± 0.1
Nanocomposite film	140	5	98.2 ± 0.4
Oven-cured FRPC panel	82	180	96.3 ± 0.1
Heater-cured FRPC panel	82	180	91.3 ± 0.05

The microstructure of the cured nanocomposite samples was examined by performing SEM imaging on the cross-section of cured nanocomposite films. Figures 3a, b show the SEM micrographs of the nanocomposite sample at two different magnifications. The low-magnification image (Figure 4-3 a) indicates that a thin (~10 μm) layer of neat resin is formed on the film surface, caused by the incomplete removal of the excess surface resin during the drop casting process. The average thickness of nanocomposite films is ~77 μm, caused by the swelling of the nanotube network by the impregnated resin as well as the formation of the surface resin layer. The image captured at the higher magnification (Figure 4-3 b) demonstrates the high quality of impregnation and low volume fraction of pores in the produced nanocomposite film, which are necessary for producing films with good mechanical performance. Nanotube content is one of the key factors that affect the mechanical and electrothermal properties of nanocomposite films. TGA measurements were performed to determine the carbon nanotube content in cured nanocomposite films (Figure 4-3 c). The residual masses of constituents and nanocomposite at 470 °C were used to determine the carbon nanotube content in produced nanocomposites using Equations 1 and 2. A carbon nanotube content of ~12.6 wt.% was calculated, which is high enough to ensure excellent heat generation capability in nanocomposite films. Compared to the pristine buckypaper, which is mechanically weak and fragile, the nanocomposite films are mechanically robust and can withstand various forms of deformation including twisting and bending. Tensile tests were performed on pristine buckypaper and nanocomposite film specimens to compare the mechanical properties of the buckypaper before and after impregnation and encapsulation by the polymer resin (Figure 4-3 d). In pristine buckypaper, carbon nanotubes in the porous network are held together only via van der Waals forces and physical entanglement resulting in poor tensile properties. Impregnation of the porous structure of buckypaper with the matrix polymer enhances the

mechanical robustness of the paper, where its tensile strength is increased 22-fold from 1.4 MPa to 31.3 MPa and its tensile modulus is increased 5-fold from 0.150 to 0.708 GPa.

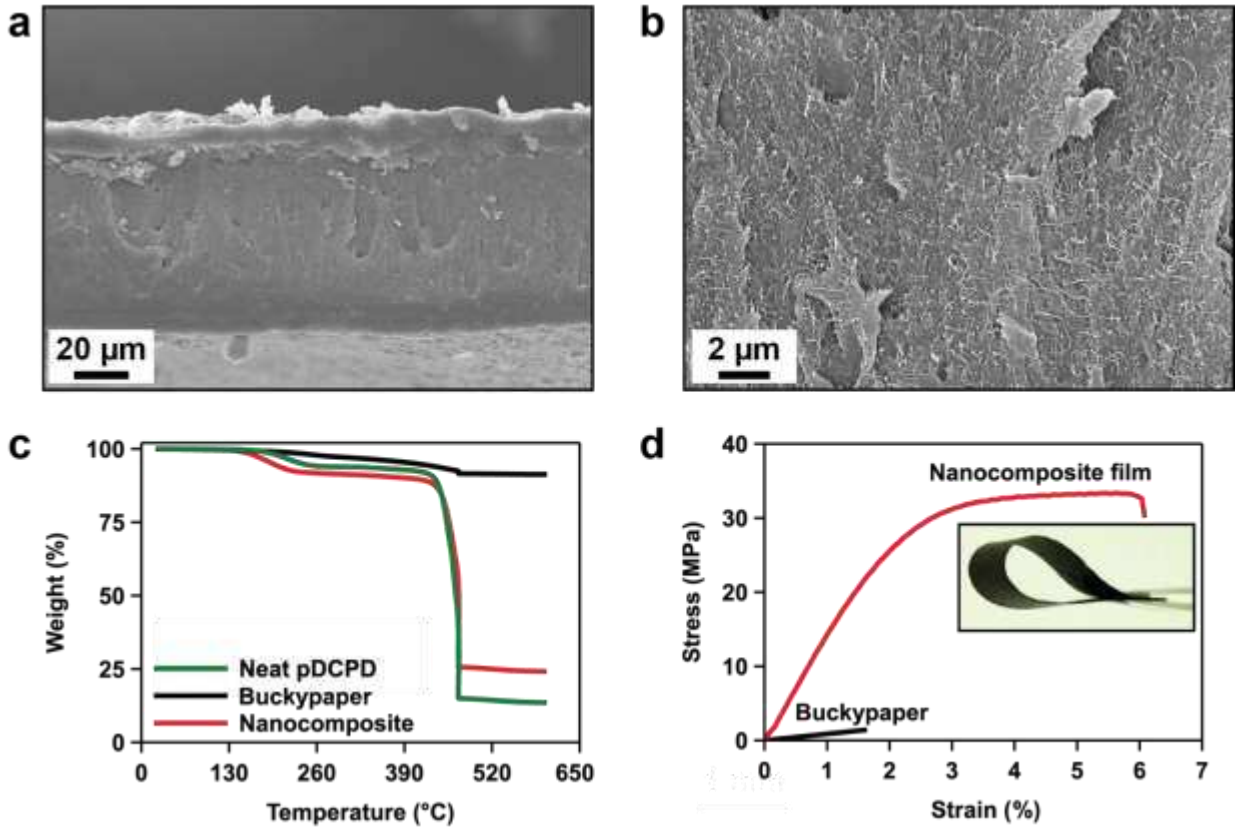

Figure 4-3. Characterization of polymer nanocomposite films. (a, b) Scanning electron microscopy (SEM) micrographs from the cross-section of a nanocomposite film. (c) TGA profiles of pristine buckypaper, neat cured pDCPD film, and nanocomposite film. (d) Tensile stress-strain curves of pristine buckypaper and nanocomposite films. The inset shows a nanocomposite film bent using a tweezer.

Use of the produced nanocomposite film heaters for successful conductive curing of FRPCs first requires characterizing the Joule heating performance of the nanocomposite films. We performed electrothermal tests on nanocomposite film specimens by applying various voltages across the specimens and measuring their time-dependent temperature profiles (Figure 4-4 a). An increase in

the applied input voltage results in an increase in the heating rate as well as the steady-state temperature of film heaters. The nanocomposite film heaters demonstrate an excellent electrothermal performance, where a temperature of ~132 °C can be reached in 2 min using a low input voltage of 11 V (equivalent power consumption of 6.16 W). The measured linear relationship between the input power density and steady-state temperature also demonstrates that the heat generation in the nanocomposite heaters follows Joule's law (Figure 4-4 b). Another important requirement for using nanocomposite films as a heater for curing FRPCs is the stability and reproducibility of their electrothermal properties, as they must survive long and repeated cure cycles for composite manufacturing. The electrothermal stability of nanocomposite heaters were evaluated by applying both static and dynamic electric loads on the heater films and measuring their temperature response. Figure 4-4 c shows the temperature response of a heater to an input voltage of 9 V when continuously applied for 1 h. After the initial transient stage, temperature remains almost unchanged, demonstrating the stable and reliable electrothermal performance of the nanocomposite heater. The response of the heater to a cyclic electric load was also measured to evaluate the reproducibility of heat generation by produced film heaters; the results of the cyclic electrothermal stability tests reveal that the temperature profile of the heater follows a similar pattern for a given electric loading condition, indicating the good reproducibility of the observed electrothermal properties in the nanocomposite films (Figure 4-4 d).

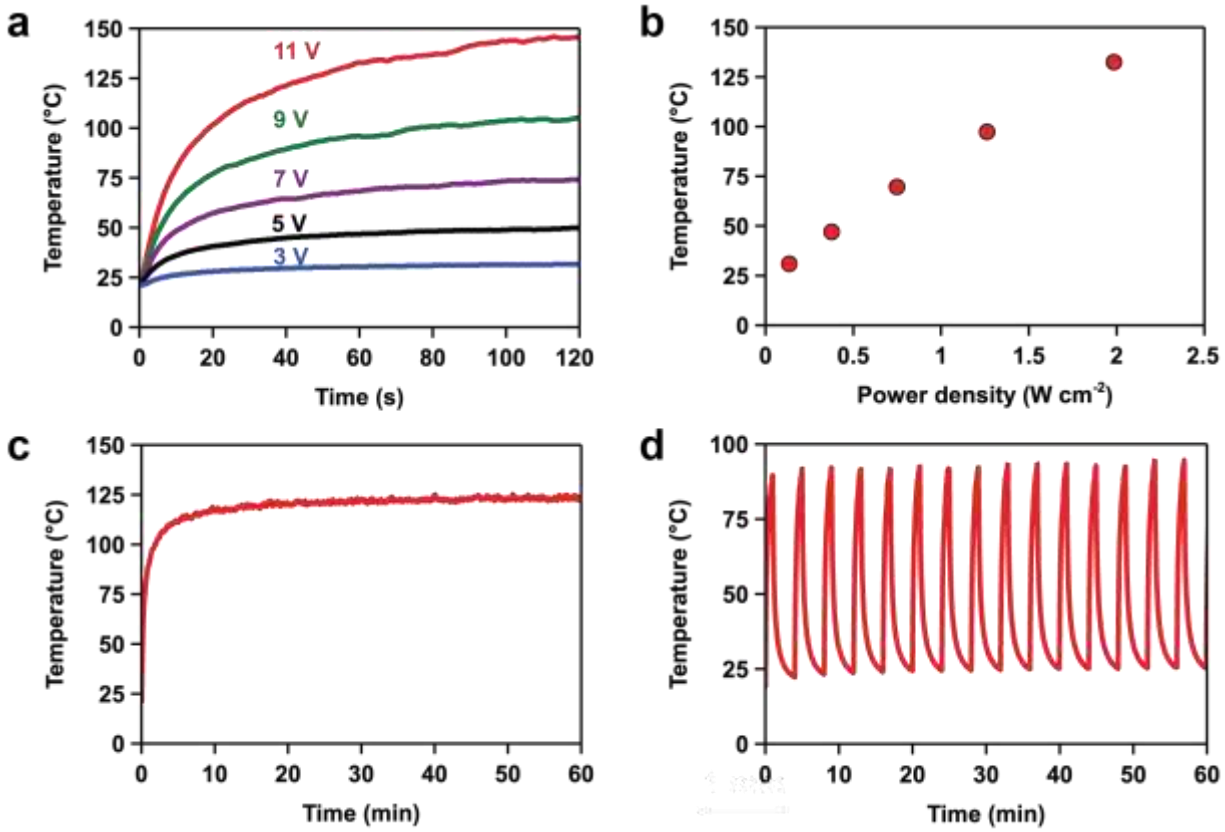

Figure 4-4. Evaluation of the electrothermal performance of produced nanocomposite films. (a) Temperature profiles of a nanocomposite film heater in response to various input voltages. (b) Relationship between input power density and steady-state temperature. (c) Static electrothermal stability test at a constant input voltage of 9 V. (d) Cyclic stability test by varying the input voltage between 0 and 9 V.

4.3.3 Composite fabrication

Following the successful demonstration of the Joule heating performance of the produced buckypaper-DCPD nanocomposite films, we used the films as a heat source for direct conductive heating and curing of carbon FRPC laminates. Composite layups were prepared by stacking eight small (4×3 cm^2) plies of an out-of-autoclave carbon fiber prepreg on a glass tool and placing the film heater (effective heating area of 3×3 cm^2) on top of the prepreg stack. A thin layer of a release film was used under the film heater to separate it from the prepreg stack for easy removal and reuse of the heater following the curing process. The layup was then vacuum bagged, and then

the cure process was initiated by supplying power to the film heater to generate heat according to the recommended cure cycle. Figure 4-5 a shows temperature profiles measured using two thermocouples placed in the center of the composite layup at the top and bottom surfaces of the laminate during the applied cure cycle. The input power to the film heater was gradually increased until the temperature at the top (heater side) of the laminate reached the cure temperature of the prepreg (i.e., 82 °C), after which the power was maintained unchanged for 3 h. A steady-state temperature of ~76 °C was measured at the bottom of the layup, which is slightly lower than the required cure temperature, caused by heat losses through tooling boundaries; however, the temperature distribution across the laminate is sufficient for proper curing of the composite laminate. Infrared thermal imaging was also used to monitor the spatial distribution of temperature throughout the top surface of the layup during the curing process. A uniform heat generation and temperature distribution was observed in the composite layup (Figure 4-5 b), indicating the effectiveness of the nanocomposite film heater for uniform heating and curing of the composite laminate. The energy consumption of this direct conductive curing approach was calculated from the power consumption profile recorded during the applied cure cycle (Figure 4-5 c). Using this approach, only 0.1 MJ of energy was required to successfully cure the composite laminate, whereas curing the same composite panel using a small convection oven in our laboratory (internal volume of 0.17 m^3) is estimated to require 40.5 MJ of energy. The degree of cure of the composite laminate cured by the nanocomposite film heater was determined using DSC measurements. As a control, the degree of cure of a similar composite panel cured using the traditional, bulk oven curing approach was also measured. The degree of cure of the composite panels made using the heater and oven curing approaches was 91.3% and 96.3%, respectively (Table 4-1). The slightly lower degree of cure obtained in conductive curing approach is attributed to the observed temperature

gradient across the thickness of the layup. This issue can potentially be mitigated by modifying the cure cycle by increasing the dwell temperature and/or the cure time or alternatively by placing the heater on the bottom (tool side) of the composite layup.

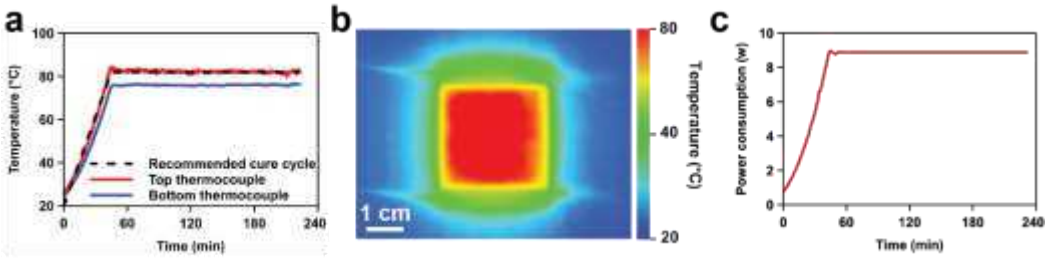

Figure 4-5. Direct conductive curing of a FRPC panel using a nanocomposite film heater. (a) Temperature profiles measured at the bottom and top of the composite layup during the cure cycle. (b) Thermal infrared image of the nanocomposite film heater during composite manufacturing. (c) Power consumption profile recorded during the cure cycle.

4.4 Conclusions

In this work, we used a frontally curable thermoset resin with a low initial resin viscosity to fabricate buckypaper-based polymer nanocomposites. The low viscosity of the resin system allows for quick impregnation of the carbon nanotube network at room temperature and ambient pressure. Following the impregnation step, complete curing of the matrix resin was achieved in a few minutes via through-thickness heating of the material. Produced nanocomposite films are mechanically robust and exhibit excellent electrical conductivity and electrothermal performance, which are ideal for using the films as a heater for curing of fiber-reinforced polymer composites. Finally, a nanocomposite film heater was used to cure a carbon fiber composite panel using a low energy consumption of 0.1 MJ, which is 350 times less than the energy required for producing a similar panel using the conventional oven curing approach.

CHAPTER 5: CONCLUSIONS AND FUTURE WORKS

This Chapter will conclude the study by summarizing the key research findings and discussing the values and contributions of this study to the composite community.

5.1 Conclusions

The aim of this dissertation was to develop a new technique for rapid and low-cost manufacturing of multifunctional fiber-reinforced polymer composites by exploiting the frontal polymerization concept and joule heating of nanostructured materials. It was demonstrated that the through-thickness FP manufacturing method using an integrated bucky paper heater allows for the rapid manufacturing of fully cured composite laminates using the conventional tooling materials utilized in the composite industry. However, the curing characteristics of the composite are greatly affected by the thermal properties of the tooling material, where preheating the composite layup and the tool is essential for achieving a high degree of cure when thermally conductive tooling materials such as aluminum are used. Another important finding from this study was that the heater position also affects the frontal curing of FRPCs, where a shorter cycle time and a higher degree of cure are achieved when the heater is placed on the vacuum bag side of the composite layup due to the less heat loss happening through the boundaries. The thermal infrared imaging of the curing process of the produced composite panels rejected our hypothesis that uniform heating of the entire surface of the composite layup using a nanostructured heater (e.g., buckypaper) with a uniform heat generation capability leads to the initiation of FP along the entire surface of the composite layup. In practice, FP initiates from multiple spots and then propagates in both in-plane and through-thickness directions of the composite layup.

This study has shown that efficient resistive heaters based on LIG-aramid fabric can be created when the LIG-aramid fabric is prepared using the optimum process parameters. Two applications were developed for the LIG-aramid fabric heaters. First, silicone-encapsulated LIG-aramid flexible heaters were created and subjected to electrothermal tests under various conditions. The results of the electrothermal tests revealed that although adding an electrically insulating rubber adversely affects the electrothermal efficiency of the LIG-aramid heaters, it significantly enhances the durability and reliability of LIG-aramid heaters. Next, LIG-aramid fabric was successfully used as an integrated heater for the manufacture of FRPCs via the through-thickness FP method. An important finding from comparing the curing characteristics of the two composite panels fabricated via the through-thickness FP method using a buckypaper heater and an LIG-aramid fabric heater was that the characteristics of the heater, such as heat generation uniformity, thermal conductivity, and temperature coefficient of resistance, affect the curing characteristics of the composite panels. The panel fabricated using the buckypaper heater exhibited more uniform front propagation and slightly higher front temperature and degree of cure compared to the panel cured using the LIG-aramid heater.

This study also showed that mechanically robust nanocomposite film heaters can be prepared in ambient conditions at high rate using a FP resin system. The produced heaters show good electrothermal properties and can be used for out-of-oven curing FRPCs.

In this dissertation, a new FP manufacturing strategy was developed that enables rapid and energy-efficient manufacturing multifunctional composites using the conventional tooling materials utilized in the composite industry. The findings from this study extend our understanding of the processing science of FP resin systems for the manufacture of FRPCs and provide valuable insight into the influence of various process parameters on the curing characteristics of frontally cured

composites. Another important contribution of this study is providing researchers with extensive experimental data to validate and enhance the accuracy of their models.

Table 5-1. The main research questions and their answers.

Question	Findings
How does frontal polymerization initiate in through-thickness FP manufacturing method using an integrated nanostructured heater?	• Front initiates from multiple spots and then propagates in both in-plane and through-thickness directions.
How does the process parameters affect the curing characteristics of composite layup?	• Shorter cure cycle time, more uniform temperature distribution, and higher degree of cure are achieved when heater is placed on the vacuum bag side of composite layup. • Thermal conductivity of tooling material greatly affects the curing characteristics of composite panels. • Preheating of dry composite layup is essential to manufacture fully cured composite parts when an aluminum tool is used.

Can efficient heaters based on LIG-aramid fabric be prepared and used for composite manufacturing using the through-thickness FP manufacturing method?	• Efficient fabric heaters can be prepared when process parameters are tuned. • the higher laser power and pulse per inch improve the electrothermal performance of LIG-aramid heater while lower laser scan speed enhances the Joule heating properties of LIG-aramid fabric heaters. • Although LIG-aramid heaters are inferior to buckypaper heaters in terms of heat generation uniformity, no significant difference was observed between panels produced in terms of time to front initiation and degree of cure.
Can frontally polymerizable resin systems be used for enhancing the mechanical properties of buckypaper?	• Frontal ring-opening metathesis polymerization of dicyclopentadiene resin allows for rapid preparation of nanocomposite films using mild processing conditions without the need for using costly ovens. • A 22-fold increase in tensile strength is achieved compared to pristine buckypaper. • Nanocomposite film heaters show excellent heat generation properties and can be used for out-of-oven composite manufacturing.

5.2 Future work

The scope of this study was limited to developing the processing science of manufacturing small composite panels at the laboratory scale via the through-thickness FP manufacturing method, and the mechanical performance of the produced laminates was not characterized. However, adopting the manufacturing technique developed in this dissertation at a larger scale requires conducting more research to address the limitations associated with the current study. The following areas of research are recommended for future work based on the limitations of this study.

5.2.1 Scalable manufacturing of FRPCs

Adopting the through-thickness FP manufacturing technique to produce large composite structures at the industrial scale requires conducting follow-up research to address the challenges associated with scaling up the technique. The main challenge for manufacturing large composite components is the uniform heating of the entire surface of the composite layup. While small resistive heating devices can be easily fabricated and used to initiate the FP, fabricating large resistive heaters is challenging. Numerical simulations are typically required to optimize the electrode design. COMSOL software is recommended for this purpose owing to its powerful Multiphysics module. Alternatively, the infrared radiation heating technique can initiate frontal polymerization in large composite components, due to its efficiency, scalability, and low cost. Fabricating large composite components using the direct conductive and infrared heating techniques and studying the impact of the heating method on the cure characteristics and performance of composite panels is recommended for future work.

5.2.2 Improving the interfacial strength of DCPD matrix composites

The poor mechanical properties of the frontally cured DCPD matrix composites are a significant issue, limiting the widespread adoption of the through-thickness FP manufacturing method to

produce reliable and durable composite structures. The poor mechanical properties of DCPD matrix composites originate from the weak interfacial bonds formed between the DCPD resin and the reinforcement. This occurs due to the chemical incompatibility between the resin and the sizing of the fiber which causes a poor bond between the matrix and reinforcement. Two strategies can be adopted to improve the strength of bonds between the DCPD resin and the reinforcement. One approach is modifying the chemical composition of the DCPD resin system by adding another component (e.g., epoxy resin, coupling agent) to enhance the polarity of the resin and improve the chemical compatibility of the DCPD resin with conventional fabrics sized for polar resins. Although modifying the chemical composition of DCPD resin through adding another component can increase the compatibility between DCPD resin and commercial fabrics and enable manufacturing of strong composite components, it may alter the processing characteristics as well as thermal and mechanical performance of cured resin, which is not desirable. For instance, addition of polar components such as epoxy can negatively affect the fracture toughness of DCPD resin, which is undesirable in applications where high impact properties is of great importance. Alternatively, non-polar sizing agents can be formulated and applied to unsized fabrics to create fabrics which are compatible with non-polar resin systems such as DCPD. As opposed to the former approach, this approach ensures maintaining excellent processing and mechanical characteristics of DCPD resin while enabling forming a robust bond between resin and fabric. Evaluating the effectiveness of these two strategies to manufacture mechanically robust FRPCs is one area of research recommended for future work.

5.2.3 Residual stresses measurement

One of the main concerns regarding the thorough-thickness FP manufacturing technique to produce FRPCs is the lack of data on the nature and the level of residual stresses developed during

the curing process. The nature of the curing mechanism in FP manufacturing methods causes a highly complex and non-uniform temperature field to be formed in the composite layup. Forming a highly non-uniform temperature field can build up a high level of residual stresses in the cured composites. The shape distortion and warpage or degradation of the mechanical performance of frontally cured composites are negative consequences of the residual stresses developed during the curing cycle. One direction for future work is conducting a comparative study to measure the residual stresses built up in composite panels cured using various techniques, including 1) the through-thickness FP manufacturing method, 2) the in-plane FP manufacturing method, and 3) the conventional oven curing method. The comparative study can be conducted by either measuring the level of residual stresses or by measuring the extent of shape distortion caused by the residual stresses. The latter approach is preferred as the sample preparation is easier and the accuracy of the measurement is higher. L-shaped composite parts can be fabricated using various curing techniques and the magnitude of spring-in in the produced L-shaped parts can be measured.

Bibliography

(1) Chen, X.; Cheng, S.; Wen, K.; Wang, C.; Zhang, J.; Zhang, H.; Ma, H.; Wu, L.; Li, T.; Li, B.; Shao, J. In-Situ Damage Self-Monitoring of Fiber-Reinforced Composite by Integrating Self-Powered ZnO Nanowires Decorated Carbon Fabric. *Composites Part B: Engineering* **2023**, *248*, 110368.

(2) Hua, X.; Higuchi, R.; Yokozeki, T. Enhancement of Tensile Strength of Tapered Laminates by Utilizing Thin-Ply Composites. *Composites Part B: Engineering* **2023**, *248*, 110372.

(3) Moorthy, V.; Marappan, K. Identification of Delamination Severity in a Tapered FRP Composite Plate. *Composite Structures* **2022**, *299*, 116054.

(4) Lee, J.; Ni, X.; Daso, F.; Xiao, X.; King, D.; Gómez, J. S.; Varela, T. B.; Kessler, S. S.; Wardle, B. L. Advanced Carbon Fiber Composite Out-of-Autoclave Laminate Manufacture via Nanostructured out-of-Oven Conductive Curing. *Composites Science and Technology* **2018**, *166*, 150–159.

(5) Xu, X.; Zhang, Y.; Jiang, J.; Wang, H.; Zhao, X.; Li, Q.; Lu, W. In-Situ Curing of Glass Fiber Reinforced Polymer Composites via Resistive Heating of Carbon Nanotube Films. *Composites Science and Technology* **2017**, *149*, 20–27.

(6) Gagné, M.; Therriault, D. Lightning Strike Protection of Composites. *Progress in Aerospace Sciences* **2014**, *64*, 1–16.

(7) Bohne, T.; Frerich, T.; Jendrny, J.; Jürgens, J.-P.; Ploshikhin, V. Simulation and Validation of Air Flow and Heat Transfer in an Autoclave Process for Definition of Thermal Boundary

Conditions during Curing of Composite Parts. *Journal of Composite Materials* **2018**, *52* (12), 1677–1687.

(8) Boey, F. Y. C.; Lee, T. H. Electromagnetic Radiation Curing of an Epoxy/Fibre Glass Reinforced Composite. *International Journal of Radiation Applications and Instrumentation. Part C. Radiation Physics and Chemistry* **1991**, *38* (4), 419–423.

(9) Liu, S.; Li, Y.; Xiao, S.; Wu, T. Self-Resistive Electrical Heating for Rapid Repairing of Carbon Fiber Reinforced Composite Parts. *Journal of Reinforced Plastics and Composites* **2019**, *38* (11), 495–505.

(10) Sarmah, A.; Desai, S. K.; Tezel, G. B.; Vashisth, A.; Mustafa, M. M.; Arole, K.; Crowley, A. G.; Green, M. J. Rapid Manufacturing via Selective Radio-Frequency Heating and Curing of Thermosetting Resins. *Advanced Engineering Materials* **2022**, *24* (7), 2101351.

(11) Abliz, D.; Duan, Y.; Steuernagel, L.; Xie, L.; Li, D.; Ziegmann, G. Curing Methods for Advanced Polymer Composites - A Review. *Polymers and Polymer Composites*. 2013;21(6):341-348.

(12) Kumar, P. K.; Raghavendra, N. V.; Sridhara, B. K. Optimization of Infrared Radiation Cure Process Parameters for Glass Fiber Reinforced Polymer Composites. *Materials & Design* **2011**, *32* (3), 1129–1137.

(13) Przybytniak, G.; Nowicki, A.; Mirkowski, K.; Stobiński, L. Gamma-Rays Initiated Cationic Polymerization of Epoxy Resins and Their Carbon Nanotubes Composites. *Radiation Physics and Chemistry* **2016**, *121*, 16–22.

(14) Klikovits, N.; Liska, R.; D'Anna, A.; Sangermano, M. Successful UV-Induced RICFP of Epoxy-Composites. *Macro Chemistry & Physics* **2017**, *218* (18), 1700313.

(15) Odom, M. G. B.; Sweeney, C. B.; Parviz, D.; Sill, L. P.; Saed, M. A.; Green, M. J. Rapid Curing and Additive Manufacturing of Thermoset Systems Using Scanning Microwave Heating of Carbon Nanotube/Epoxy Composites. *Carbon* **2017**, *120*, 447–453.

(16) Le Maoult, Y.; Schmidt, F. Infrared Radiation Applied to Polymer Processes. In *Heat Transfer in Polymer Composite Materials*; Boyard, N., Ed.; Wiley, 2016; pp 385–423.

(17) Chern, B.-C.; Moon, T. J.; Howell, J. R. On-Line Processing of Unidirectional Fiber Composites Using Radiative Heating: I. Model. *Journal of Composite Materials* **2002**, *36* (16), 1905–1934.

(18) Kumar, P. K.; Raghavendra, N. V.; Sridhara, B. K. Effect of Infrared Cure Parameters on the Mechanical Properties of Polymer Composite Laminates. *Journal of Composite Materials* **2012**, *46* (5), 549–556.

(19) Danezis, A.; Williams, D.; Edwards, M.; Skordos, A. A. Heat Transfer Modelling of Flashlamp Heating for Automated Tape Placement of Thermoplastic Composites. *Composites Part A: Applied Science and Manufacturing* **2021**, *145*, 106381.

(20) Alpay, Y.; Uygur, I.; Kilincel, M. On the Optimum Process Parameters of Infrared Curing of Carbon Fiber-Reinforced Plastics. *Polymers and Polymer Composites* **2020**, *28* (6), 433–439.

(21) Zhilyaev, I.; Brauner, C.; Queloz, S.; Jordi, H.; Lüscher, R.; Conti, S.; Conway, R. Controlled Curing of Thermoset Composite Components Using Infrared Radiation and Mathematical Modelling. *Composite Structures* **2021**, *259*, 113224.

(22) Chern, B.-C.; Moon, T. J.; Howell, J. R. On-Line Processing of Unidirectional Fiber Composites Using Radiative Heating: II. Radiative Properties, Experimental Validation and Process Parameter Selection. *Journal of Composite Materials* **2002**, *36* (16), 1935–1965.

(23) Mo, Q.; Huang, Y.; Ma, L.; Lai, W.; Zheng, Y.; Li, Y.; Xu, M.; Huang, Z. Study on Microwave Curing of Unsaturated Polyester Resin and Its Composites Containing Calcium Carbonate. *Polymers* **2022**, *14* (13), 2598.

(24) Ariff, Z. M.; Afolabi, L. O.; Salmazo, L. O.; Rodriguez-Perez, M. A. Effectiveness of Microwave Processing Approach and Green Blowing Agents Usage in Foaming Natural Rubber. *Journal of Materials Research and Technology* **2020**, *9* (5), 9929–9940.

(25) Naik, T. P.; Singh, I.; Sharma, A. K. Processing of Polymer Matrix Composites Using Microwave Energy: A Review. *Composites Part A: Applied Science and Manufacturing* **2022**, *156*, 106870.

(26) Rani, M.; Carlone, P.; Zafar, S. Analysis of Mechanical Performance and Energy Consumption of Microwave Cured GFRP Composites: A Low-Energy Footprint Manufacturing Process. *CIRP Journal of Manufacturing Science and Technology* **2023**, *42*, 36–46.

(27) Nuhiji, B.; Swait, T.; Bower, M. P.; Green, J. E.; Day, R. J.; Scaife, R. J. Tooling Materials Compatible with Carbon Fibre Composites in a Microwave Environment. *Composites Part B: Engineering* **2019**, *163*, 769–778.

(28) Mgbemena, C. O.; Li, D.; Lin, M.-F.; Liddel, P. D.; Katnam, K. B.; Thakur, V. K.; Nezhad, H. Y. Accelerated Microwave Curing of Fibre-Reinforced Thermoset Polymer Composites for Structural Applications: A Review of Scientific Challenges. *Composites Part A: Applied Science and Manufacturing* **2018**, *115*, 88–103.

(29) Nightingale, C.; Day, R. J. Flexural and Interlaminar Shear Strength Properties of Carbon Fibre/Epoxy Composites Cured Thermally and with Microwave Radiation. *Composites Part A: Applied Science and Manufacturing* **2002**, *33* (7), 1021–1030.

(30) Papargyris, D. A.; Day, R. J.; Nesbitt, A.; Bakavos, D. Comparison of the Mechanical and Physical Properties of a Carbon Fibre Epoxy Composite Manufactured by Resin Transfer Moulding Using Conventional and Microwave Heating. *Composites Science and Technology* **2008**, *68* (7–8), 1854–1861.

(31) G. Pérez-de-Eulate, N.; Iztueta, A. A.; Gondra, K.; Vallejo, F. J. Influence of the Fibre Content, Exposure Time, and Compaction Pressure on the Mechanical Properties of Ultraviolet-Cured Composites. *Journal of Composite Science* **2020**, *4* (1), 30.

(32) Zhou, C.; Chen, W.; Wang, L.; Zhang, G. Influence of Glass Fiber on Mechanical Properties of UV-Cured Lining Materials. *J. Phys.: Conf. Ser.* **2023**, *2539* (1), 012009.

(33) Vashisth, A.; Healey, R. E.; Pospisil, M. J.; Oh, J. H.; Green, M. J. Continuous Processing of Pre-Pregs Using Radio Frequency Heating. *Composites Science and Technology* **2020**, *195*, 108211.

(34) Sarmah, A.; Morales, M. A.; Srivastava, A.; Upama, S.; Nandi, A.; Henry, T. C.; Green, M. J.; Vashisth, A. Interfacial Carbon Fiber–Matrix Interactions in Thermosetting Composites Volumetrically Cured by Electromagnetic Fields. *Composites Part A: Applied Science and Manufacturing* **2023**, *164*, 107276.

(35) Weiland, J. S.; Hartmann, M. P.; Hinterhölzl, R. M. Cure Simulation with Resistively in Situ Heated CFRP Molds: Implementation and Validation. *Composites Part A: Applied Science and Manufacturing* **2016**, *80*, 171–181.

(36) Kontaxis, L. C.; Chontzoglou, I. E.; Papanicolaou, G. C. Efficient Use of Carbon Fibers as Heating Elements for Curing of Epoxy Matrix Composites. *Molecules* **2021**, *26* (16), 5095.

(37) Wei, D.; Gu, Y.; Zhu, H.; Li, M.; Wang, S. Influence of Electrical Heating Metal Mesh and Power Density on Resistance Welding of Carbon Fiber/PEEK Composite. *Polymers* **2022**, *14* (13), 2563.

(38) Villegas, I. F.; Bersee, H. E. Characterisation of a Metal Mesh Heating Element for Closed-Loop Resistance Welding of Thermoplastic Composites. *Journal of Thermoplastic Composite Materials* **2015**, *28* (1), 46–65.

(39) Collinson, M. G.; Swait, T. J.; Bower, M. P.; Nuhiji, B.; Hayes, S. A. Development and Implementation of Direct Electric Cure of Plain Weave CFRP Composites for Aerospace. *Composites Part A: Applied Science and Manufacturing* **2023**, *172*, 107615.

(40) Anusak, N.; Virtanen, J.; Kangas, V.; Promarak, V.; Yotprayoonsak, P. Enhanced Joule Heating Performance of Flexible Transparent Conductive Double-Walled Carbon Nanotube Films on Sparked Ag Nanoparticles. *Thin Solid Films* **2022**, *750*, 139201.

(41) Kostaras, C.; Pavlou, C.; Koutroumanis, N.; Paterakis, G.; Trakakis, G.; Galiotis, C.; Dassios, K. Rapid Resistive Heating in Graphene/Carbon Nanotube Hybrid Films for De-Icing Applications. *ACS Applied Nano Materials* **2023**, *6* (7), 5155–5167.

(42) Chu, H.; Zhang, Z.; Liu, Y.; Leng, J. Self-Heating Fiber Reinforced Polymer Composite Using Meso/Macropore Carbon Nanotube Paper and Its Application in Deicing. *Carbon* **2014**, *66*, 154–163.

(43) Fu, X.; Zhang, C.; Liu, T.; Liang, R.; Wang, B. Carbon Nanotube Buckypaper to Improve Fire Retardancy of High-Temperature/High-Performance Polymer Composites. *Nanotechnology* **2010**, *21* (23), 235701.

(44) Wang, X.; Lin, L.; Lu, S.; Zhang, L.; Li, B.; Zhang, D.; Luo, Y. Evaluation of Embedded Buckypaper Sensors in Composite Overwrappedped Pressure Vessels for Progressive Damage Monitoring. *Composite Structures* **2022**, *284*, 115223.

(45) Rashid, Md. H.-O.; Triani, G.; Scales, N.; In Het Panhuis, M.; Nghiem, L. D.; Ralph, S. F. Nanofiltration Applications of Tough MWNT Buckypaper Membranes Containing Biopolymers. *Journal of Membrane Science* **2017**, *529*, 23–34.

(46) Luo, J.; Lu, H.; Zhang, Q.; Yao, Y.; Chen, M.; Li, Q. Flexible Carbon Nanotube/Polyurethane Electrothermal Films. *Carbon* **2016**, *110*, 343–349.

(47) Lee, J.; Stein, I. Y.; Kessler, S. S.; Wardle, B. L. Aligned Carbon Nanotube Film Enables Thermally Induced State Transformations in Layered Polymeric Materials. *ACS Applied Materials & Interfaces* **2015**, *7* (16), 8900–8905.

(48) Rojas, J. A.; Ribeiro, B.; Rezende, M. C. Curing of Glass Fiber/Epoxy Resin Composites Using Multiwalled Carbon Nanotubes Buckypaper as a Resistive Element. *Journal of Manufacturing Science and Engineering* **2021**, *143* (4), 041007.

(49) Yao, X.; Hawkins, S. C.; Falzon, B. G. An Advanced Anti-Icing/de-Icing System Utilizing Highly Aligned Carbon Nanotube Webs. *Carbon* **2018**, *136*, 130–138.

(50) Nguyen, N.; Hao, A.; Park, J. G.; Liang, R. In Situ Curing and Out-of-Autoclave of Interply Carbon Fiber/Carbon Nanotube Buckypaper Hybrid Composites Using Electrical Current. *Advanced Engineering Materials* **2016**, *18* (11), 1906–1912.

(51) Avinash, K.; Patolsky, F. Laser-Induced Graphene Structures: From Synthesis and Applications to Future Prospects. *Materials Today* **2023**, S1369702123003383.

(52) Stanford, M. G.; Zhang, C.; Fowlkes, J. D.; Hoffman, A.; Ivanov, I. N.; Rack, P. D.; Tour, J. M. High-Resolution Laser-Induced Graphene. Flexible Electronics beyond the Visible Limit. *ACS Applied Materials & Interfaces* **2020**, *12* (9), 10902–10907.

(53) Ye, R.; James, D. K.; Tour, J. M. Laser-Induced Graphene: From Discovery to Translation. *Advanced Materials* **2019**, *31* (1), 1803621.

(54) Yang, F.; Yu, C.; Zhang, L.; Zhang, Y.; Wei, B.; Liu, J.; Zhang, Y. High-Performance Electrothermal Film Based on Laser-Induced Graphene. *Advanced Engineering Materials* **2022**, *24* (11), 2200368.

(55) Wang, H.; Zhao, Z.; Liu, P.; Guo, X. A Soft and Stretchable Electronics Using Laser-Induced Graphene on Polyimide/PDMS Composite Substrate. *npj Flex Electron* **2022**, *6* (1), 26.

(56) Tang, L.; Zhou, J.; Zhang, D.; Sheng, B. Laser-Induced Graphene Electrodes on Poly(Ether–Ether–Ketone)/PDMS Composite Films for Flexible Strain and Humidity Sensors. *ACS Applied Nano Materials* **2023**, *6* (19), 17802–17813.

(57) Steinke, K.; Groo, L.; Sodano, H. A. Laser Induced Graphene for In-Situ Ballistic Impact Damage and Delamination Detection in Aramid Fiber Reinforced Composites. *Composites Science and Technology* **2021**, *202*, 108551.

(58) Ye, R.; Chyan, Y.; Zhang, J.; Li, Y.; Han, X.; Kittrell, C.; Tour, J. M. Laser-Induced Graphene Formation on Wood. *Advanced Materials* **2017**, *29* (37), 1702211.

(59) Bobinger, M. R.; Romero, F. J.; Salinas-Castillo, A.; Becherer, M.; Lugli, P.; Morales, D. P.; Rodríguez, N.; Rivadeneyra, A. Flexible and Robust Laser-Induced Graphene Heaters Photothermally Scribed on Bare Polyimide Substrates. *Carbon* **2019**, *144*, 116–126.

(60) Chen, J.; Wang, Y.; Liu, F.; Luo, S. Laser-Induced Graphene Paper Heaters with Multimodally Patternable Electrothermal Performance for Low-Energy Manufacturing of Composites. *ACS Applied Materials & Interfaces* **2020**, *12* (20), 23284–23297.

(61) Jiang, Y.; Zhao, W.; Yu, W.; Yu, Z.; Xiao, X.; Zhou, W.; Liu, X. Free-Standing Laser-Induced Graphene Heaters for Efficient Curing and Repairing of Composites. *Journal of Material Science* **2023**, *58* (6), 2604–2618.

(62) Al-Hartomy, O. A.; Al-Salamy, F.; Al-Ghamdi, A. A.; Al-Ghamdi, A. A.; Abdel Daiem, A. M.; El-Tantawy, F. New Resistive Switching and Self-Regulating Heating in Foliated Graphite/Nickel Polyvinyl Chloride Nanocomposites. *Journal of Nanomaterials* **2011**, *2011*, 1–10.

(63) Setnescu, R.; Lungulescu, E.-M.; Marinescu, V. E. Polymer Composites with Self-Regulating Temperature Behavior: Properties and Characterization. *Materials* **2022**, *16* (1), 157.

(64) Liu, Y.; Van Vliet, T.; Tao, Y.; Busfield, J. J. C.; Peijs, T.; Bilotti, E.; Zhang, H. Sustainable and Self-Regulating out-of-Oven Manufacturing of FRPs with Integrated Multifunctional Capabilities. *Composites Science and Technology* **2020**, *190*, 108032.

(65) Wang, Y.; Yao, X.; Thorn, T. D. S.; Huo, S.; Porwal, H.; Newton, M.; Liu, Y.; Papageorgiou, D.; Bilotti, E.; Zhang, H. Energy Efficient Out-of-Oven Manufacturing of Natural Fibre Composites with Integrated Sensing Capabilities and Improved Water Barrier Properties. *Composites Science and Technology* **2023**, *239*, 110062.

(66) Karalis, G.; Tzounis, L.; Dimos, E.; Mytafides, C. K.; Liebscher, M.; Karydis-Messinis, A.; Zafeiropoulos, N. E.; Paipetis, A. S. Printed Single-Wall Carbon Nanotube-Based Joule Heating Devices Integrated as Functional Laminae in Advanced Composites. *ACS Applied Materials & Interfaces* **2021**, *13* (33), 39880–39893.

(67) Tu, R.; Liu, T.; Steinke, K.; Nasser, J.; Sodano, H. A. Laser Induced Graphene-Based out-of-Autoclave Curing of Fiberglass Reinforced Polymer Matrix Composites. *Composites Science and Technology* **2022**, *226*, 109529.

(68) Torres, J. J.; Simmons, M.; Sket, F.; González, C. An Analysis of Void Formation Mechanisms in Out-of-Autoclave Prepregs by Means of X-Ray Computed Tomography. *Composites Part A: Applied Science and Manufacturing* **2019**, *117*, 230–242.

(69) Centea, T.; Grunenfelder, L. K.; Nutt, S. R. A Review of Out-of-Autoclave Prepregs – Material Properties, Process Phenomena, and Manufacturing Considerations. *Composites Part A: Applied Science and Manufacturing* **2015**, *70*, 132–154.

(70) Gong, M.; Zhang, D.; Zhang, J.; Chen, X. Effects of Lay-up Types of Out-of-Autoclave Prepregs on Preparation Quality of L-Shape Composite Laminates. *Journal of Wuhan University-Technology and Material Science Edition* **2021**, *36* (5), 629–635.

(71) Hübner, F.; Meuchelböck, J.; Wolff-Fabris, F.; Mühlbach, M.; Altstädt, V.; Ruckdäschel, H. Fast Curing Unidirectional Carbon Epoxy Prepregs Based on a Semi-Latent Hardener: The

Influence of Ambient Aging on the Prepregs Tg_0, Processing Behavior and Thus Derived Interlaminar Performance of the Composite. *Composites Science and Technology* **2021**, *216*, 109047.

(72) Groh, F.; Kappel, E.; Hühne, C.; Brymerski, W. Investigation of Fast Curing Epoxy Resins Regarding Process Induced Distortions of Fibre Reinforced Composites. *Composite Structures* **2019**, *207*, 923–934.

(73) Goli, E.; Peterson, S. R.; Geubelle, P. H. Instabilities Driven by Frontal Polymerization in Thermosetting Polymers and Composites. *Composites Part B: Engineering* **2020**, *199*, 108306.

(74) Robertson, I. D.; Dean, L. M.; Rudebusch, G. E.; Sottos, N. R.; White, S. R.; Moore, J. S. Alkyl Phosphite Inhibitors for Frontal Ring-Opening Metathesis Polymerization Greatly Increase Pot Life. *ACS Macro Letter* **2017**, *6* (6), 609–612.

(75) Li, Q.; Shen, H.-X.; Liu, C.; Wang, C.-F.; Zhu, L.; Chen, S. Advances in Frontal Polymerization Strategy: From Fundamentals to Applications. *Progress in Polymer Science* **2022**, *127*, 101514.

(76) Bomze, D.; Knaack, P.; Liska, R. Successful Radical Induced Cationic Frontal Polymerization of Epoxy-Based Monomers by C–C Labile Compounds. *Polymer Chemistry* **2015**, *6* (47), 8161–8167.

(77) Chen, S.; Tian, Y.; Chen, L.; Hu, T. Epoxy Resin/Polyurethane Hybrid Networks Synthesized by Frontal Polymerization. *Chemistry of Materials* **2006**, *18* (8), 2159–2163.

(78) Bynum, S.; Tullier, M.; Morejon-Garcia, C.; Guidry, J.; Runnoe, E.; Pojman, J. A. The Effect of Acrylate Functionality on Frontal Polymerization Velocity and Temperature. *Journal of Polymer Science Part A: Polymer Chemistry* **2019**, *57* (9), 982–988.

(79) Ruiu, A.; Sanna, D.; Alzari, V.; Nuvoli, D.; Mariani, A. Advances in the Frontal Ring Opening Metathesis Polymerization of Dicyclopentadiene. *Journal of Polymer Science Part A: Polymer Chemistry* **2014**, *52* (19), 2776–2780.

(80) Valette, V.; Lecamp, L.; Astruc, J.; Burel, F.; Kebir, N. Elaboration of Epoxy Foam by Radical Induced Cationic Frontal Polymerization (RICFP): A Proof of Concept. *Journal of Photochemistry and Photobiology A: Chemistry* **2023**, *442*, 114811.

(81) Nuvoli, D.; Alzari, V.; Pojman, J. A.; Sanna, V.; Ruiu, A.; Sanna, D.; Malucelli, G.; Mariani, A. Synthesis and Characterization of Functionally Gradient Materials Obtained by Frontal Polymerization. *ACS Applied Materials & Interfaces* **2015**, *7* (6), 3600–3606.

(82) Li, Q.; Liu, J.-D.; Liu, S.-S.; Wang, C.-F.; Chen, S. Frontal Polymerization-Oriented Self-Healing Hydrogels and Applications toward Temperature-Triggered Actuators. *Industrial & Engineering Chemistry Research* **2019**, *58* (9), 3885–3892.

(83) Hayne, D. J.; Singleton, M. A.; Patterson, B. A.; Athulya Wickramasingha, Y.; Sietins, J. M.; Knorr, D. B.; Stojcevski, F.; Henderson, L. C. Assessing the Properties of Poly(Dicyclopentadiene) Reinforced with Discontinuous Carbon Fibers. *Composites Part A: Applied Science and Manufacturing* **2022**, *155*, 106839.

(84) Vallons, K. A. M.; Drozdzak, R.; Charret, M.; Lomov, S. V.; Verpoest, I. Assessment of the Mechanical Behaviour of Glass Fibre Composites with a Tough Polydicyclopentadiene (PDCPD) Matrix. *Composites Part A: Applied Science and Manufacturing* **2015**, *78*, 191–200.

(85) Tran, A. D.; Koch, T.; Knaack, P.; Liska, R. Radical Induced Cationic Frontal Polymerization for Preparation of Epoxy Composites. *Composites Part A: Applied Science and Manufacturing* **2020**, *132*, 105855.

(86) Robertson, I. D.; Yourdkhani, M.; Centellas, P. J.; Aw, J. E.; Ivanoff, D. G.; Goli, E.; Lloyd, E. M.; Dean, L. M.; Sottos, N. R.; Geubelle, P. H.; Moore, J. S.; White, S. R. Rapid Energy-Efficient Manufacturing of Polymers and Composites via Frontal Polymerization. *Nature* **2018**, *557* (7704), 223–227.

(87) Zhou, J.; Jia, S.; Fu, W.; Liu, Z.; Tan, Z. Fast Curing of Thick Components of Epoxy via Modified UV-Triggered Frontal Polymerization Propagating Horizontally. *Materials Letters* **2016**, *176*, 228–231.

(88) Centellas, P. J.; Yourdkhani, M.; Vyas, S.; Koohbor, B.; Geubelle, P. H.; Sottos, N. R. Rapid Multiple-Front Polymerization of Fiber-Reinforced Polymer Composites. *Composites Part A: Applied Science and Manufacturing* **2022**, *158*, 106931.

(89) Staal, J.; Smit, E.; Caglar, B.; Michaud, V. Thermal Management in Radical Induced Cationic Frontal Polymerisation for Optimised Processing of Fibre Reinforced Polymers. *Composites Science and Technology* **2023**, *237*, 110009.

(90) Garg, M.; Aw, J. E.; Zhang, X.; Centellas, P. J.; Dean, L. M.; Lloyd, E. M.; Robertson, I. D.; Liu, Y.; Yourdkhani, M.; Moore, J. S.; Geubelle, P. H.; Sottos, N. R. Rapid Synchronized Fabrication of Vascularized Thermosets and Composites. *Nature Communication* **2021**, *12* (1), 2836.

(91) Sharifi, A. M.; Kwon, D.-J.; Shah, S. Z. H.; Lee, J. Modeling of Frontal Polymerization of Carbon Fiber and Dicyclopentadiene Woven Composites with Stochastic Material Uncertainty. *Composite Structures* **2023**, *326*, 117582.

(92) Wang, Y. Modeling the Through-thickness Frontal Polymerization of Unidirectional Carbon Fiber Thermoset Composites: Effect of Microstructures. *Journal of Applied Polymer Sci*ence **2022**, *139* (31), e52735.

(93) Tarafdar, A.; Jia, C.; Hu, W.; Hosein, I. D.; Fu, K. (Kelvin); Wang, Y. Three-Dimensional Modeling of Frontal Polymerization for Rapid, Efficient, and Uniform Thermoset Composites Manufacturing. *Composites Part B: Engineering* **2023**, *266*, 111029.

(94) Naseri, I.; Ziaee, M.; Nilsson, Z. N.; Lustig, D. R.; Yourdkhani, M. Electrothermal Performance of Heaters Based on Laser-Induced Graphene on Aramid Fabric. *ACS Omega* **2022**, *7* (4), 3746–3757.

(95) Naseri, I.; Yourdkhani, M. Rapid and Energy-Efficient Frontal Curing of Multifunctional Composites Using Integrated Nanostructured Heaters. *ACS Applied Materials & Interfaces* **2022**, *14* (44), 50215–50224.

(96) Naseri, I.; Ashrafi, B.; Jakubinek, M.; Martinez-Rubi, Y.; Yourdkhani, M. Rapid and Facile Preparation of Nanocomposite Film Heaters for Composite Manufacturing. *Front. Mater.* **2023**, *10*, 1166986.

(97) Ning, N.; Wang, M.; Zhou, G.; Qiu, Y.; Wei, Y. Effect of Polymer Nanoparticle Morphology on Fracture Toughness Enhancement of Carbon Fiber Reinforced Epoxy Composites. *Composites Part B: Engineering* **2022**, *234*, 109749.

(98) Zhang, Z.; Liu, R.; Li, W.; Liu, Y.; Pei, Z.; Qiu, J.; Wang, S. Frontal Polymerization-Assisted 3D Printing of Short Carbon Fibers/Dicyclopentadiene Composites. *Journal of Manufacturing Processes* **2021**, *71*, 753–762.

(99) Tu, R.; Liu, T.; Steinke, K.; Nasser, J.; Sodano, H. A. Laser Induced Graphene-Based out-of-Autoclave Curing of Fiberglass Reinforced Polymer Matrix Composites. *Composites Science and Technology* **2022**, *226*, 109529.

(100) J. Timmis, A.; Hodzic, A.; Koh, L.; Bonner, M.; Soutis, C.; W. Schäfer, A.; Dray, L. Environmental Impact Assessment of Aviation Emission Reduction through the Implementation of Composite Materials. *The International Journal of Life Cycle Assessment 20*, 233–243.

(101) Agius, S. L.; Joosten, M.; Trippit, B.; Wang, C. H.; Hilditch, T. Rapidly Cured Epoxy/Anhydride Composites: Effect of Residual Stress on Laminate Shear Strength. *Composites Part A: Applied Science and Manufacturing* **2016**, *90*, 125–136.

(102) Li, N.; Li, Y.; Jelonnek, J.; Link, G.; Gao, J. A New Process Control Method for Microwave Curing of Carbon Fibre Reinforced Composites in Aerospace Applications. *Composites Part B: Engineering* **2017**, *122*, 61–70.

(103) Abliz, D.; Duan, Y.; Zhao, X.; Li, D. Low-Energy Electron Beam Cured Tape Placement for out-of-Autoclave Fabrication of Advanced Polymer Composites. *Composites Part A: Applied Science and Manufacturing* **2014**, *65*, 73–82.

(104) Abulizi, D.; Duan, Y.; Li, D.; Lu, B. A New Method for Glass-Fiber Reinforced Composites Manufacturing: Automated Fiber Placement with in-Situ UV Curing. In *2011 IEEE International Symposium on Assembly and Manufacturing (ISAM)*; IEEE: Tampere, Finland, 2011; pp 1–4.

(105) Endruweit, A.; Ruijter, W.; Johnson, M. S.; Long, A. C. Transmission of Ultraviolet Light through Reinforcement Fabrics and Its Effect on Ultraviolet Curing of Composite Laminates. *Polymer Composites* **2008**, *29* (7), 818–829.

(106) Li, Y.; Li, N.; Zhou, J.; Cheng, Q. Microwave Curing of Multidirectional Carbon Fiber Reinforced Polymer Composites. *Composite Structures* **2019**, *212*, 83–93.

(107) Zhang, B.; Li, Y.; Liu, S.; Shen, Y.; Hao, X. Layered Self-resistance Electric Heating to Cure Thick Carbon Fiber Reinforced Epoxy Laminates. *Polymer Composites* **2021**, *42* (5), 2469–2483.

(108) Karim, N.; Zhang, M.; Afroj, S.; Koncherry, V.; Potluri, P.; S. Novoselov, K. Graphene-Based Surface Heater for de-Icing Applications. *RSC Advances* **2018**, *8*, 16815.

(109) Liu, F.; Wang, G.; Ding, X.; Luo, S. Multifunctional Laser-Induced Graphene Enabled Polymeric Composites. *Composites Communications* **2021**, *25*, 100714.

(110) Xia, Q.; Zhang, Z.; Liu, Y.; Leng, J. Buckypaper and Its Composites for Aeronautic Applications. *Composites Part B: Engineering* **2020**, *199*, 108231.

(111) Groo, L.; Nasser, J.; Inman, D.; Sodano, H. Laser Induced Graphene for in Situ Damage Sensing in Aramid Fiber Reinforced Composites. *Composites Science and Technology* **2021**, *201*, 108541.

(112) Pojman, J. A. Cure-on-Demand Composites by Frontal Polymerization. In *Encyclopedia of Materials: Plastics and Polymers*; Elsevier, 2022; pp 85–100.

(113) Pojman, J. A. Frontal Polymerization. In *Polymer Science: A Comprehensive Reference*; Elsevier, 2012; pp 957–980.

(114) Goli, E.; Parikh, N. A.; Yourdkhani, M.; Hibbard, N. G.; Moore, J. S.; Sottos, N. R.; Geubelle, P. H. Frontal Polymerization of Unidirectional Carbon-Fiber-Reinforced Composites. *Composites Part A: Applied Science and Manufacturing* **2020**, *130*, 105689.

(115) Mariani, A.; Fiori, S.; Chekanov, Y.; Pojman, J. A. Frontal Ring-Opening Metathesis Polymerization of Dicyclopentadiene. *Macromolecules* **2001**, *34* (19), 6539–6541.

(116) Ziaee, M.; Johnson, J. W.; Yourdkhani, M. 3D Printing of Short-Carbon-Fiber-Reinforced Thermoset Polymer Composites via Frontal Polymerization. *ACS Applied Materials & Interfaces* **2022**, *14* (14), 16694–16702.

(117) Robertson, I. D.; Yourdkhani, M.; Centellas, P. J.; Aw, J. E.; Ivanoff, D. G.; Goli, E.; Lloyd, E. M.; Dean, L. M.; Sottos, N. R.; Geubelle, P. H.; Moore, J. S.; White, S. R. Rapid Energy-Efficient Manufacturing of Polymers and Composites via Frontal Polymerization. *Nature* **2018**, *557* (7704), 223–227.

(118) Wang, X.; Li, B.; Zhang, D.; Lu, J.; Lin, L.; Lu, S.; Ma, C.; Zhang, L.; Ma, K.; Jiang, X.; Yang, B. Strain Monitoring Using Carbon Nanotube Buckypaper Sensor on Composite Repaired Structure. *Applied Physics A* **2021**, *127* (12), 935.

(119) Ribeiro, B.; Gomes, N. A. S.; Rezende, M. C. Lightweight Multi-Walled Carbon Nanotube Buckypaper/Glass Fiber–Epoxy Composites for Strong Electromagnetic Interference Shielding and Efficient Microwave Absorption. *Journal of Material Science: Mater Electron* **2021**, *32* (11), 14494–14508.

(120) Han, J.; Zhang, H.; Chen, M.; Wang, D.; Liu, Q.; Wu, Q.; Zhang, Z. The Combination of Carbon Nanotube Buckypaper and Insulating Adhesive for Lightning Strike Protection of the Carbon Fiber/Epoxy Laminates. *Carbon* **2015**, *94*, 101–113.

(121) Yao, S.; Cui, J.; Cui, Z.; Zhu, Y. Soft Electrothermal Actuators Using Silver Nanowire Heaters. *Nanoscale* **2017**, *9* (11), 3797–3805.

(122) Jeong, Y. G.; Jeon, G. W. Microstructure and Performance of Multiwalled Carbon Nanotube/ *m* -Aramid Composite Films as Electric Heating Elements. *ACS Applied Materials & Interfaces* **2013**, *5* (14), 6527–6534.

(123) Tarfaoui, M.; El Moumen, A.; Boehle, M.; Shah, O.; Lafdi, K. Self-Heating and Deicing Epoxy/Glass Fiber Based Carbon Nanotubes Buckypaper Composite. *Journal of Material Sci*ence **2019**, *54* (2), 1351–1362.

(124) Wang, T.; Zheng, Y.; Raji, A.-R. O.; Li, Y.; Sikkema, W. K. A.; Tour, J. M. Passive Anti-Icing and Active Deicing Films. *ACS Applied Materials & Interfaces* **2016**, *8* (22), 14169–14173.

(125) Zhan, Y.; Li, Y.; Meng, Y.; Xie, Q.; Lavorgna, M. Electric Heating Behavior of Reduced Oxide Graphene/Carbon Nanotube/Natural Rubber Composites with Macro-Porous Structure and Segregated Filler Network. *Polymers* **2020**, *12* (10), 2411.

(126) Wu, Z. P.; Wang, J. N. Preparation of Large-Area Double-Walled Carbon Nanotube Films and Application as Film Heater. *Physica E: Low-dimensional Systems and Nanostructures* **2009**, *42* (1), 77–81.

(127) Li, Y.; Zhang, Z.; Li, X.; Zhang, J.; Lou, H.; Shi, X.; Cheng, X.; Peng, H. A Smart, Stretchable Resistive Heater Textile. *Journal of Material Chemistry C* **2017**, *5* (1), 41–46.

(128) Hong, S.; Lee, H.; Lee, J.; Kwon, J.; Han, S.; Suh, Y. D.; Cho, H.; Shin, J.; Yeo, J.; Ko, S. H. Highly Stretchable and Transparent Metal Nanowire Heater for Wearable Electronics Applications. *Advanced Materials* **2015**, *27* (32), 4744–4751.

(129) Park, J.; Han, D.; Choi, S.; Kim, Y.; Kwak, J. Flexible Transparent Film Heaters Using a Ternary Composite of Silver Nanowire, Conducting Polymer, and Conductive Oxide. *RSC Advances* **2019**, *9* (10), 5731–5737.

(130) Cheng, Y.; Zhang, H.; Wang, R.; Wang, X.; Zhai, H.; Wang, T.; Jin, Q.; Sun, J. Highly Stretchable and Conductive Copper Nanowire Based Fibers with Hierarchical Structure for Wearable Heaters. *ACS Applied Materials & Interfaces* **2016**, *8* (48), 32925–32933.

(131) Lin, S.-Y.; Zhang, T.-Y.; Lu, Q.; Wang, D.-Y.; Yang, Y.; Wu, X.-M.; Ren, T.-L. High-Performance Graphene-Based Flexible Heater for Wearable Applications. *RSC Advances* **2017**, *7* (43), 27001–27006.

(132) Kim, D.; Zhu, L.; Jeong, D.-J.; Chun, K.; Bang, Y.-Y.; Kim, S.-R.; Kim, J.-H.; Oh, S.-K. Transparent Flexible Heater Based on Hybrid of Carbon Nanotubes and Silver Nanowires. *Carbon* **2013**, *63*, 530–536.

(133) Park, T. H.; Yu, S.; Koo, M.; Kim, H.; Kim, E. H.; Park, J.-E.; Ok, B.; Kim, B.; Noh, S. H.; Park, C.; Kim, E.; Koo, C. M.; Park, C. Shape-Adaptable 2D Titanium Carbide (MXene) Heater. *ACS Nano* **2019**, *13* (6), 6835–6844.

(134) Wang, Y.; Wang, Y.; Zhang, P.; Liu, F.; Luo, S. Laser-Induced Freestanding Graphene Papers: A New Route of Scalable Fabrication with Tunable Morphologies and Properties for Multifunctional Devices and Structures. *Small* **2018**, *14* (36), 1802350.

(135) Kong, D.; Kang, M.; Kim, K. Y.; Jang, J.; Cho, J.; In, J. B.; Lee, H. Hierarchically Structured Laser-Induced Graphene for Enhanced Boiling on Flexible Substrates. *ACS Applied Materials & Interfaces* **2020**, *12* (33), 37784–37792.

(136) Park, H.; Kim, M.; Kim, B. G.; Kim, Y. H. Electronic Functionality Encoded Laser-Induced Graphene for Paper Electronics. *ACS Applied Nano Materials* **2020**, *3* (7), 6899–6904.

(137) Beckham, J. L.; Li, J. T.; Stanford, M. G.; Chen, W.; McHugh, E. A.; Advincula, P. A.; Wyss, K. M.; Chyan, Y.; Boldman, W. L.; Rack, P. D.; Tour, J. M. High-Resolution Laser-Induced Graphene from Photoresist. *ACS Nano* **2021**, *15* (5), 8976–8983.

(138) Chyan, Y.; Ye, R.; Li, Y.; Singh, S. P.; Arnusch, C. J.; Tour, J. M. Laser-Induced Graphene by Multiple Lasing: Toward Electronics on Cloth, Paper, and Food. *ACS Nano* **2018**, *12* (3), 2176–2183.

(139) Dallinger, A.; Keller, K.; Fitzek, H.; Greco, F. Stretchable and Skin-Conformable Conductors Based on Polyurethane/Laser-Induced Graphene. *ACS Appliede Materials & Interfaces* **2020**, *12* (17), 19855–19865.

(140) Kulyk, B.; Silva, B. F. R.; Carvalho, A. F.; Silvestre, S.; Fernandes, A. J. S.; Martins, R.; Fortunato, E.; Costa, F. M. Laser-Induced Graphene from Paper for Mechanical Sensing. *ACS Applied Materials & Interfaces* **2021**, *13* (8), 10210–10221.

(141) Huang, Y.; Tao, L.-Q.; Yu, J.; Zheng, K.; Wang, G.; Chen, X. Improved Performance of Flexible Graphene Heater Based on Repeated Laser Writing. *IEEE Electron Device Letters* **2020**, *41* (3), 501–504.

(142) Thamaraiselvan, C.; Thakur, A. K.; Gupta, A.; Arnusch, C. J. Electrochemical Removal of Organic and Inorganic Pollutants Using Robust Laser-Induced Graphene Membranes. *ACS Applied Materials & Interfaces* **2021**, *13* (1), 1452–1462.

(143) Xu, Y.; Fei, Q.; Page, M.; Zhao, G.; Ling, Y.; Chen, D.; Yan, Z. Laser-Induced Graphene for Bioelectronics and Soft Actuators. *Nano Research* **2021**.

(144) Zhang, C.; Peng, Z.; Huang, C.; Zhang, B.; Xing, C.; Chen, H.; Cheng, H.; Wang, J.; Tang, S. High-Energy All-in-One Stretchable Micro-Supercapacitor Arrays Based on 3D Laser-Induced Graphene Foams Decorated with Mesoporous ZnP Nanosheets for Self-Powered Stretchable Systems. *Nano Energy* **2021**, *81*, 105609.

(145) Liu, F.; Wang, G.; Ding, X.; Luo, S. Multifunctional Laser-Induced Graphene Enabled Polymeric Composites. *Composites Communications* **2021**, *25*, 100714.

(146) Wang, H.; Wang, H.; Wang, Y.; Su, X.; Wang, C.; Zhang, M.; Jian, M.; Xia, K.; Liang, X.; Lu, H.; Li, S.; Zhang, Y. Laser Writing of Janus Graphene/Kevlar Textile for Intelligent Protective Clothing. *ACS Nano* **2020**, *14* (3), 3219–3226.

(147) Nasser, J.; Groo, L.; Zhang, L.; Sodano, H. Laser Induced Graphene Fibers for Multifunctional Aramid Fiber Reinforced Composite. *Carbon* **2020**, *158*, 146–156.

(148) Steinke, K.; Groo, L.; Sodano, H. A. Laser Induced Graphene for In-Situ Ballistic Impact Damage and Delamination Detection in Aramid Fiber Reinforced Composites. *Composites Science and Technology* **2021**, *202*, 108551.

(149) Lamberti, A.; Perrucci, F.; Caprioli, M.; Serrapede, M.; Fontana, M.; Bianco, S.; Ferrero, S.; Tresso, E. New Insights on Laser-Induced Graphene Electrodes for Flexible Supercapacitors: Tunable Morphology and Physical Properties. *Nanotechnology* **2017**, *28* (17), 174002.

(150) Mahmood, F.; Zhang, C.; Xie, Y.; Stalla, D.; Lin, J.; Wan, C. Transforming Lignin into Porous Graphene *via* Direct Laser Writing for Solid-State Supercapacitors. *RSC Advances* **2019**, *9* (39), 22713–22720.

(151) d'Amora, M.; Lamberti, A.; Fontana, M.; Giordani, S. Toxicity Assessment of Laser-Induced Graphene by Zebrafish during Development. *Journal of Physics of Materials* **2020**, *3* (3), 034008.

(152) Gueye, M. N.; Carella, A.; Demadrille, R.; Simonato, J.-P. All-Polymeric Flexible Transparent Heaters. *ACS Applied Materials & Interfaces* **2017**, *9* (32), 27250–27256.

(153) Chakraborty, A. K.; Plyhm, T.; Barbezat, M.; Necola, A.; Terrasi, G. P. Carbon Nanotube (CNT)–Epoxy Nanocomposites: A Systematic Investigation of CNT Dispersion. *J Nanoparticle Research* **2011**, *13* (12), 6493–6506.

(154) Wan Dalina, W. A. D.; Mariatti, M.; Tan, S. H. Multi-Walled Carbon Nanotubes Buckypaper/Epoxy Composites: Effect of Loading and Pressure on Tensile and Electrical Properties. *Polymer Bulletin* **2019**, *76* (6), 2801–2817.

(155) Ma, P.-C.; Siddiqui, N. A.; Marom, G.; Kim, J.-K. Dispersion and Functionalization of Carbon Nanotubes for Polymer-Based Nanocomposites: A Review. *Composites Part A: Applied Science and Manufacturing* **2010**, *41* (10), 1345–1367.

(156) Isaza M, C. A.; Herrera Ramírez, J.; Ledezma Sillas, J.; Meza, J. Dispersion and Alignment Quantification of Carbon Nanotubes in a Polyvinyl Alcohol Matrix. *Journal of Composite Materials* **2018**, *52* (12), 1617–1626.

(157) Zeinedini, A.; Shokrieh, M. M.; Ebrahimi, A. The Effect of Agglomeration on the Fracture Toughness of CNTs-Reinforced Nanocomposites. *Theoretical and Applied Fracture Mechanics* **2018**, *94*, 84–94.

(158) Khan, F.; Kausar, A.; Siddiq, M. A Review on Properties and Fabrication Techniques of Polymer/Carbon Nanotube Composites and Polymer Intercalated Buckypapers. *Polymer-Plastics Technology and Engineering* **2015**, *54* (14), 1524–1539.

(159) Lopes, P. E.; Van Hattum, F.; Pereira, C. M. C.; Nóvoa, P. J. R. O.; Forero, S.; Hepp, F.; Pambaguian, L. High CNT Content Composites with CNT Buckypaper and Epoxy Resin Matrix: Impregnation Behaviour Composite Production and Characterization. *Composite Structures* **2010**, *92* (6), 1291–1298.

(160) Ribeiro, B.; Botelho, E. C.; Costa, M. L.; Bandeira, C. F. Carbon Nanotube Buckypaper Reinforced Polymer Composites: A Review. *Polímeros* **2017**, *27* (3), 247–255.

(161) Ashrafi, B.; Guan, J.; Mirjalili, V.; Hubert, P.; Simard, B.; Johnston, A. Correlation between Young's Modulus and Impregnation Quality of Epoxy-Impregnated SWCNT Buckypaper. *Composites Part A: Applied Science and Manufacturing* **2010**, *41* (9), 1184–1191.

APPENDIX A: SUPPLEMENTARY DATA FOR CHAPTER TWO

A.1 Preparation of buckypaper heaters

Heat generation in buckypaper via the electrothermal effect requires forming a robust bond between the buckypaper and the copper electrode. Various factors, including the type of copper electrode and conductive paste, affect the quality of the bonding between the buckypaper and the copper electrode. Copper tape and wire are two electrode types used when preparing nanostructured resistive heating devices. An adhesive-backed copper tape was used first to create a buckypaper heater. However, the electrical resistance measurement revealed that the adhesive layer lacks sufficient electrical conductivity required to create a conductive path between the buckypaper and the copper tape, leading to a poor Joule heating effect in the buckypaper. Next, a copper wire (gauge 28) was used as an electrode to prepare the resistive heaters. Using copper wire as an electrode when creating resistive heaters requires a conductive adhesive paste to attach the wire to the resistive element. Two types of conductive adhesive paste based on nickel particles (Pyro-Duct 598 A, Aremco) and silver-coated ceramic flakes (Electro-bond 06, ConductiveX) were tested when attaching the copper wire to the buckypaper. The adhesive containing the silver-coated flakes was compatible with the buckypaper due to its ability to easily wet the buckypaper material and form a uniform layer on top. In contrast, the nickel-filled adhesive showed poor compatibility with the buckypaper, as it was difficult to apply a uniform layer of paste on top. As a result, the Electro-bond 06 was selected to create the buckypaper heaters. The manufacturer

recommends two separate cure cycles that can be used to ensure full curing of the Electro-bond 06 adhesive. The conductive paste can be either cured at room temperature or at elevated temperatures. Two heaters were prepared using the conductive paste and one was cured at 25 °C for 24 hours and the other at 65 °C for 3 hours to determine the suitable cure cycle. Curing the conductive paste at 65 °C caused the buckypaper to wrinkle due to the mismatch between the coefficient of thermal expansion of the buckypaper and the conductive paste. The formation of wrinkles might cause cracking in the buckypaper, therefore the room temperature cure was selected as the suitable cure cycle.

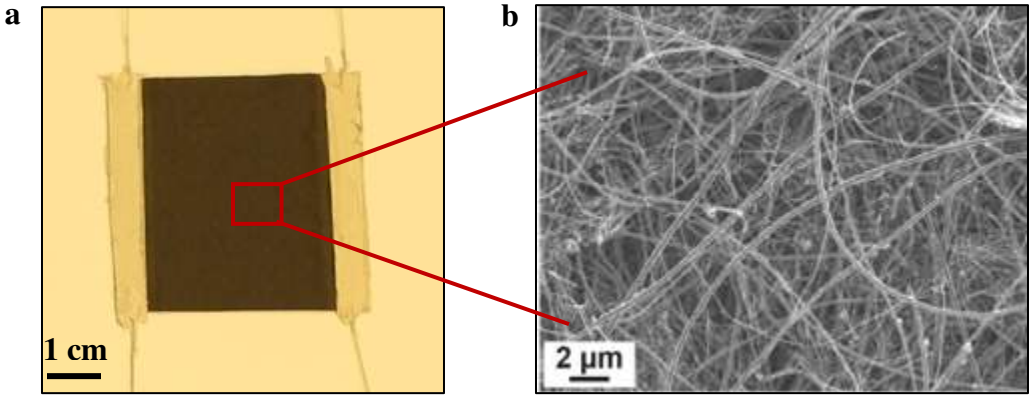

Figure A-1. (a) Digital image of a buckypaper heater. (b) The microstructure of the buckypaper was imaged using a scanning electron microscope (SEM).

A.2 Characterization of buckypaper heater

Thermogravimetric analysis (TGA) is widely used in the polymer industry for evaluating the thermal stability of polymeric materials. In this technique, the mass of a polymer is monitored as a function of temperature as the specimen is subjected to a controlled temperature program in a controlled atmosphere. In this work, TGA measurements were performed on a pristine buckypaper sample to determine the thermal stability of the buckypaper that was used for creating the resistive

heaters. The TGA measurement was performed from room temperature to 600 °C at a heating rate of 10 °C min^{-1} in an atmosphere of air. According to the TGA thermogram in Figure A-2 a, only a minor weight loss of ~ 0.8% occurs when the material reaches 200 °C. This indicates the thermal stability of the buckypaper used in this study as the heating source for initiating frontal polymerization.

Joule's law states that the efficiency of heat generation in a resistive element via the electrothermal effect is determined by the electrical resistance of the resistive element. Temperature is one of the factors that affects the electrical resistance of buckypaper. The electrical resistance of a buckypaper heater was measured at various temperatures to understand how the temperature rise during the frontal curing of a composite would affect the heat generation properties of the buckypaper heater. Figure A-2 b shows the electrical resistance as a function of temperature. The electrical resistance of the buckypaper heater drops as the temperature increases, resulting in an improvement in the heat generation capabilities of the buckypaper heater. Indeed, the negative coefficient of thermal expansion of buckypaper causes a reduction of interparticle distances at elevated temperatures, leading to a drop in the electrical resistance of the heater.

In the next step, several heaters of varying heating areas were prepared (Figure A-2 c), and the power required to achieve a target average temperature of 150 °C was determined for each heater. The relationship between the effective heating area and power requirement is shown in Figure A-2 d. A linear relationship exists between the effective heating area and the power required to achieve a specific temperature, which is desirable as it allows for predicting the power requirements to achieve a target temperature when larger heaters are required. In addition, the data presented in Figure A-2 e demonstrates that the buckypaper heater follows Joule's law, as a linear relationship can be observed between the square of input voltage and the steady-state temperature.

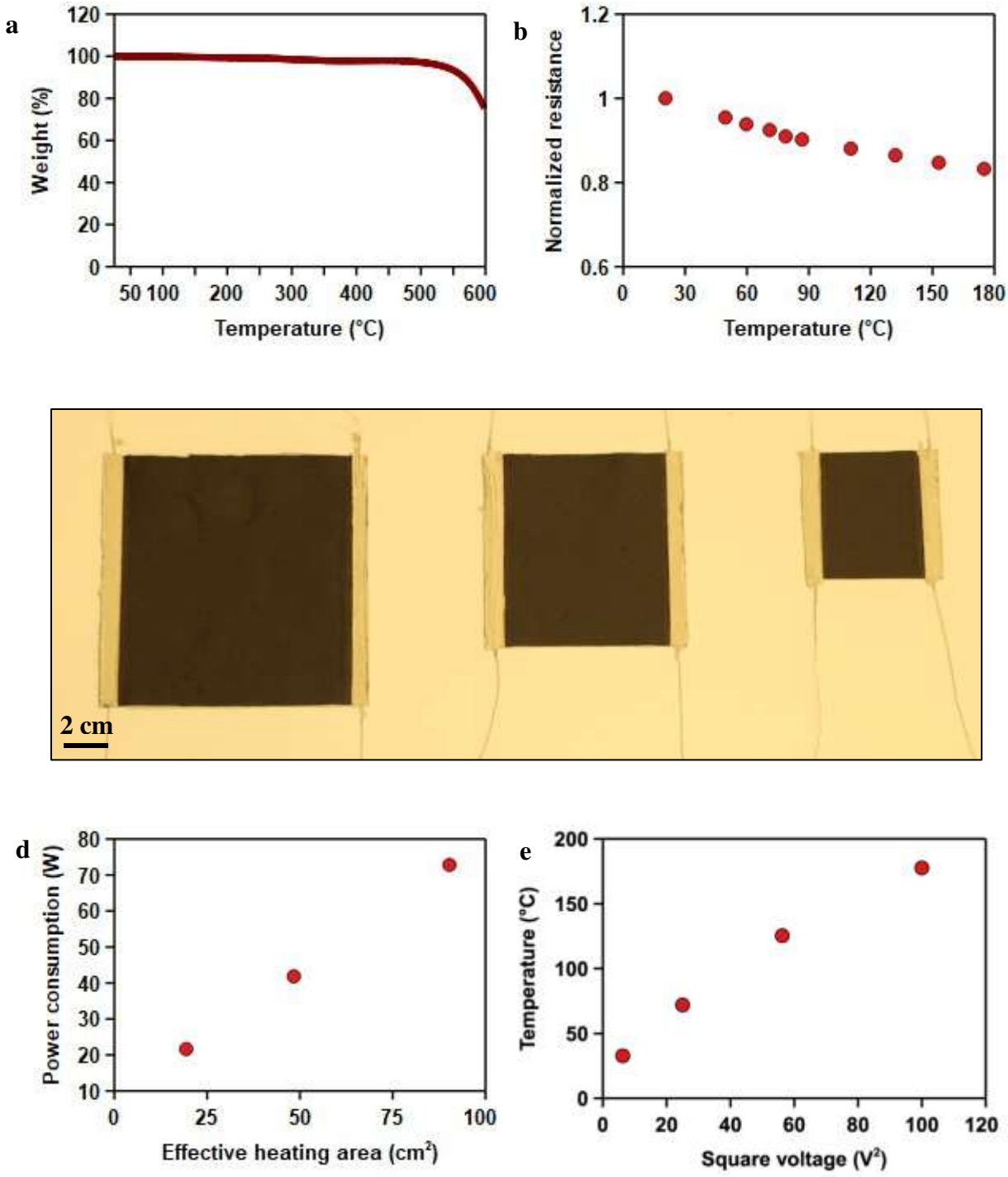

Figure A-2. Characterization of the buckypaper heater. (a) The TGA measurement evaluates the thermal stability of a buckypaper sample in an air atmosphere. (b) The electrical resistance of a buckypaper heater as a function of temperature. (c) The digital images of the buckypaper heaters of varying effective heating areas. (d) The relationship between the effective heating area and the power required to reach a target temperature. (e) The linear relationship between the square of the input voltage and the steady-state temperature.

Another important feature of buckypaper, which makes it an attractive choice as a resistive heater for initiating frontal polymerization, is that it maintains its heat generation capability under deformation (Figure A-3), allowing for manufacturing non-flat composite components.

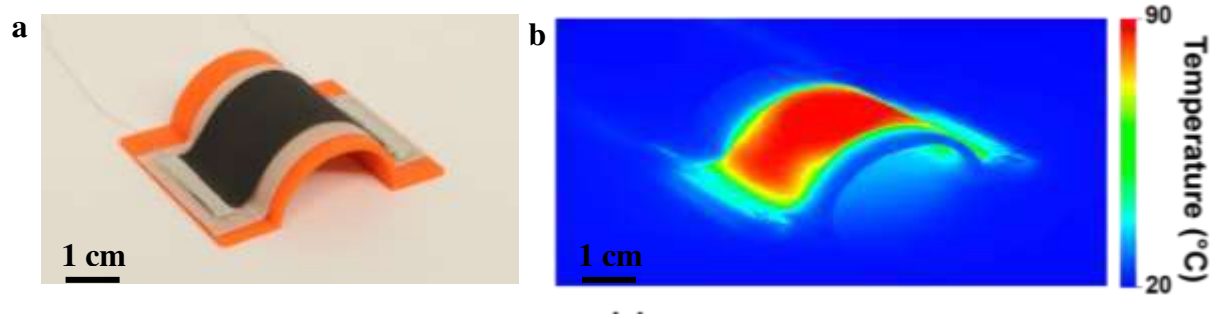

Figure A-3. The electrothermal performance of a deformed buckypaper heater. (a) Digital image of a deformed buckypaper heater. (b) Infrared imaging of a deformed buckypaper heater, showing uniform heat generation.

A.3 Processing challenges

This section will discuss the processing challenges of manufacturing carbon panels via the through-thickness FP manufacturing strategy using an integrated buckypaper heater. The issues related to the buckypaper heater, the VARTM process, and the resin system will be discussed.

The poor mechanical and handling properties of the buckypaper were significant issues that made manufacturing FRPCs difficult. Inadequate handling of the buckypaper during the heater fabrication, as well as the layup preparation processes, led to the formation of cracks in the buckypaper. Another cause of heater failure was the mechanical damage of the copper wire electrodes. Large alligator clips with sharp teeth can damage and even rupture the thin copper wire. In the case of using a metallic tool for composite manufacturing, any contact formed between the copper electrode and the tool leads to a short circuit, and no heat can be generated in the

buckypaper heater via the electrothermal effect. Metallic tools must be entirely covered by an electrically insulating material such as a Teflon sheet to eliminate the risk of forming a short circuit. Another cause of forming short circuits was using excessively thin glass fabric to isolate the carbon fabrics and the buckypaper layer electrically. Indeed, one layer of glass fabric with an areal weight of less than 100 g m^{-2} failed to completely isolate the two conductive materials, leading to the flow of electrons through the carbon fabric.

Manufacturing high-quality composite components with low void content using the conventional single-bagged vacuum-assisted resin transfer molding (VARTM) requires resin to slowly flow through the fabric reinforcement to fill the inter- and intra-tow spacing. The resin flow through the fabric can be described using Darcy's law:

$$Q = -\frac{K}{\mu L}\Delta P \qquad \text{(A-1)}$$

Q is the resin volumetric flow rate, K is the fabric permeability, L is the layup length, μ is the resin viscosity, and ΔP is the pressure difference between the resin inlet and outlet. Using the conventional single-bagged VARTM when processing dicyclopentadiene matrix composites led to making composite parts with very high void content due to the infusion speed being too quick. This issue mainly originates from the very low viscosity of DCPD resin. Several strategies were adopted to slow the infusion speed. First, the double-bagged VARTM approach was used to reduce the pressure difference between the inlet and outlet and achieve a slower infusion speed. This technique uses two vacuum pumps to slowly infuse and compact the composite layup separately. A low vacuum is applied on the inner bag to slowly infuse the fabric stack with the resin, while a

high vacuum is applied on the outer bag to compact the layup and achieve a high fiber volume fraction. While the double-bagged VARTM technique effectively slows the infusion speed to some extent, the infusion speed was still too fast due to the small size of the panels (10 cm × 10 cm). Another strategy for decreasing the infusion speed was using smaller tubes as resin inlets to reduce the volumetric flow rate of the resin. Several panels were prepared using inlet tubes of varying internal diameters, and the results showed that the optimum conditions were achieved when a tube with an internal diameter of 4 mm was used. The sufficiently low infusion speed allowed for manufacturing carbon panels with low void content, as displayed in Figure A-4.

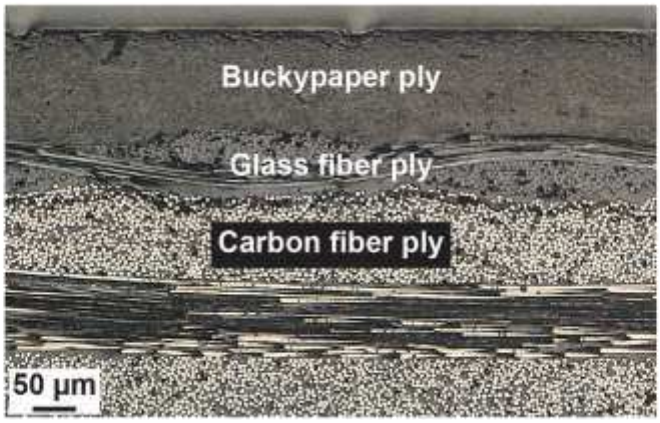

Figure A-4. The optical image of the cross-section of a carbon panel fabricated via the through-thickness FP manufacturing strategy using an integrated buckypaper heater.

It is important to note that although reducing the flow rate and the infusion pressure effectively reduced the infusion speed and enabled manufacturing panels with low void content, poor consistency of the infusion process due to the low viscosity of DCPD resin and the complexity of the double-bagged VARTM technique remained an issue throughout this study. For instance, race-tracking was a common issue, leading to the incomplete infusion of the fabric stack. Another common issue was the formation of a resin pool near the resin inlet due to leakage. The formation of a resin pool near the inlet led to the initiation of FP from the resin-rich area, followed by the in-plane front propagation.

Material-related issues were another source of failure. The FP resin system consisted of three main components: the dicyclopentadiene monomer, the second-generation Grubbs' catalyst, and the alkyl phosphite inhibitor. The dicyclopentadiene resin purchased from Sigma-Aldrich contained an impurity, which negatively affected the reactivity of the resin system. Complete removal of the impurity through filtration was essential to achieve a high front temperature. The Grubbs' catalyst and the alkyl phosphite inhibitor are hygroscopic, and their reactivities are greatly affected by absorbing moisture from the environment. One of the common issues in manufacturing carbon panels was measuring a front temperature that was too low due to the reduced reactivity of an aged catalyst. A less common issue was the thermal degradation of the matrix thermoset resin and the formation of large air bubbles due to the use of an aged inhibitor. The inhibitor bottle must be purged with an inert gas (e.g., Argon) and stored in a fridge. An unpurged inhibitor is good only for 48 hours.

A.4 Double-bagged vacuum-assisted resin transfer molding process

The low viscosity of DCPD resin makes fabricating high-quality composite parts using the conventional single-bagged VARTM difficult. Fabrication of high-quality composite panels with low void content using a DCPD resin system such requires a double-bagged VARTM process, in which two vacuum pumps control the infusion rate and volume fraction separately. This section outlines the procedure developed for manufacturing a composite panel using the double-bagged VARTM technique. Fabrics are first cut to the desired size using a specialty pair of scissors designed for cutting aramid fabric to minimize any possible damage to the fabric. A release film is taped down on the tool using flash tape to create a boundary between the composite and the tool, which is necessary for easy removal of the cured panel from the tool. Two pieces of peel ply are cut and taped on the release film using flash tape. The distance between the two layers of peel ply must be 1 cm shorter than the length of the fabric. This allows for the formation of a continuous path for air and resin to flow. Once all of the fabric plies are laid on the tool, two resin dams are created along the edges of the fabric using tacky tape to minimize the risk of race-tracking, which leads to the incomplete infusion of the fabric stack. Then, resin inlet and outlet tubes (ID = 4 mm and OD = 6 mm) are placed on the tool at a distance of 2 cm from the fabric stack. Sealant tape is placed around the layup, and a vacuum bag is sealed over the layup. A full vacuum is first applied on the layup, and a leak test is performed for 5 min to ensure the layup is entirely sealed. Afterward, a breather layer is placed on the first bag, and the second vacuum bag is applied. A full vacuum is applied on the outer bag using a second vacuum pump, and a leak test is performed. Once the leak test is completed, the vacuum in the inner bag is lowered to 42.3 KPa. The layup is debulked by being held under vacuum for 30 min to remove all the volatiles (e.g., moisture) from the composite layup.

The FP resin system used to manufacture the composite panels is based on DCPD and prepared according to the following procedure. Briefly, DCPD is first mixed with 5-ethylidene-2-norbornene at a 95:5 weight ratio to depress its melting point. Then, an appropriate amount of inhibitor is dissolved in Phenyl cyclohexane solvent, and the solution is added to a second container containing Grubbs' catalyst. Then, the mixture is sonicated for 20 minutes to achieve a uniform, transparent solution. Finally, the catalyst solution is mixed with resin using a magnet stirrer or thinky mixer. Once the resin solution is ready, the resin inlet tube is placed inside the resin container, allowing the resin to flow into the fabric stack. Just before the infusion front reaches the vacuum hose, the resin inlet is clamped, and heat is applied to trigger frontal polymerization. Just before the infusion front reaches the vacuum hose, the resin inlet is clamped, and heat is applied to trigger the frontal polymerization reaction. The vacuum is maintained for 30 min upon the completion of the cure cycle to allow for slow cooling of the layup.

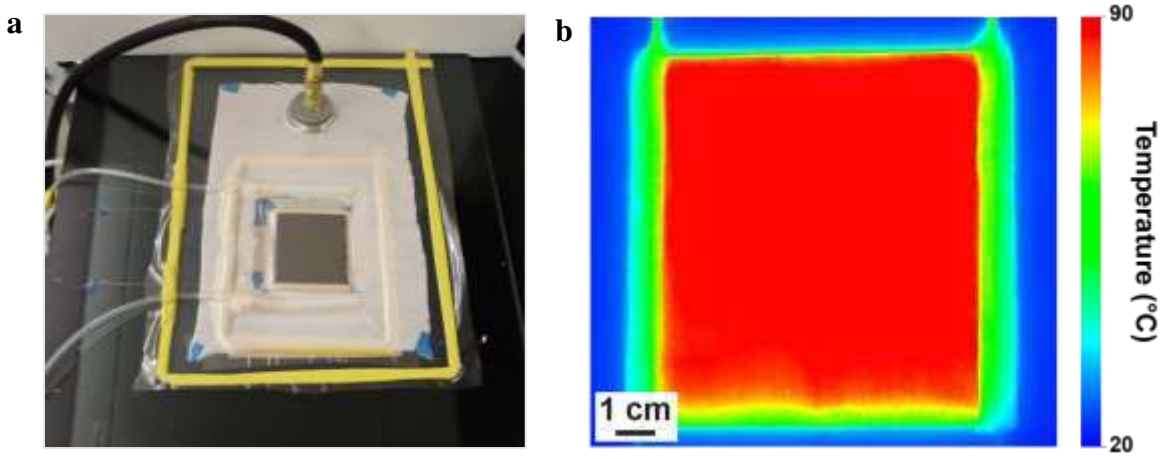

Figure A-5. Manufacturing of carbon panels via the through-thickness FP manufacturing method using an integrated buckypaper heater. (a) Digital image of a VARTM set up. (b) Infrared thermal image of a buckypaper heater embedded in a composite layup, showing the uniform heat generation in the buckypaper heater.

APPENDIX B: SUPPLEMENTARY DATA FOR CHAPTER THREE

B.1 Fabrication of LIG using a blue laser

In Chapter 2, it was demonstrated that the through-thickness frontal polymerization manufacturing strategy using an embedded buckypaper heater enables the rapid and energy-efficient manufacture of fully cured carbon composite panels using the conventional tooling materials typically utilized in the composite industry. However, the high cost and poor handling properties of buckypaper motivate the exploration of alternative resistive heating materials with better handling properties and lower costs for the manufacture of FRPCs. As discussed in Chapter 1, the excellent heat generation properties of laser-induced graphene and its scalable, inexpensive, and fast production process make LIG-based heaters an excellent choice for a heating solution in many applications. The quality of the LIG created on a precursor material depends on several factors, including the type of precursor material, the laser source, and the process parameters used to write the LIG. The commercial 10.6 μm CO_2 lasers have been widely used to write LIG on various precursors. When this study was started, the lack of access to a CO_2 laser was the motivation behind developing an in-house set-up to create LIG-based heaters. This study utilized a blue laser mounted on a robotic platform to write LIG on polyimide film and aramid fabric (Figure B-1). The electrothermal test results showed that the LIG-PI film created using the blue laser offers excellent heat generation properties, where a steady-state temperature of 100 °C can be reached when a low input voltage of only 5 V is applied across the heater (Figure B-1 b). However, although LIG-PI heaters exhibited

excellent electrothermal performance, the use of this material as a heating source to frontally fabricate FRPCs presented two challenges. The first was the warpage and shape distortion of the polyimide film during the lasing process, a significant issue that made fabricating large heaters quite challenging. The second issue with LIG-PI film heaters was the difficulty of integrating this material into a composite layup due to the solid nature of the polyimide substrate and lack of porosity.

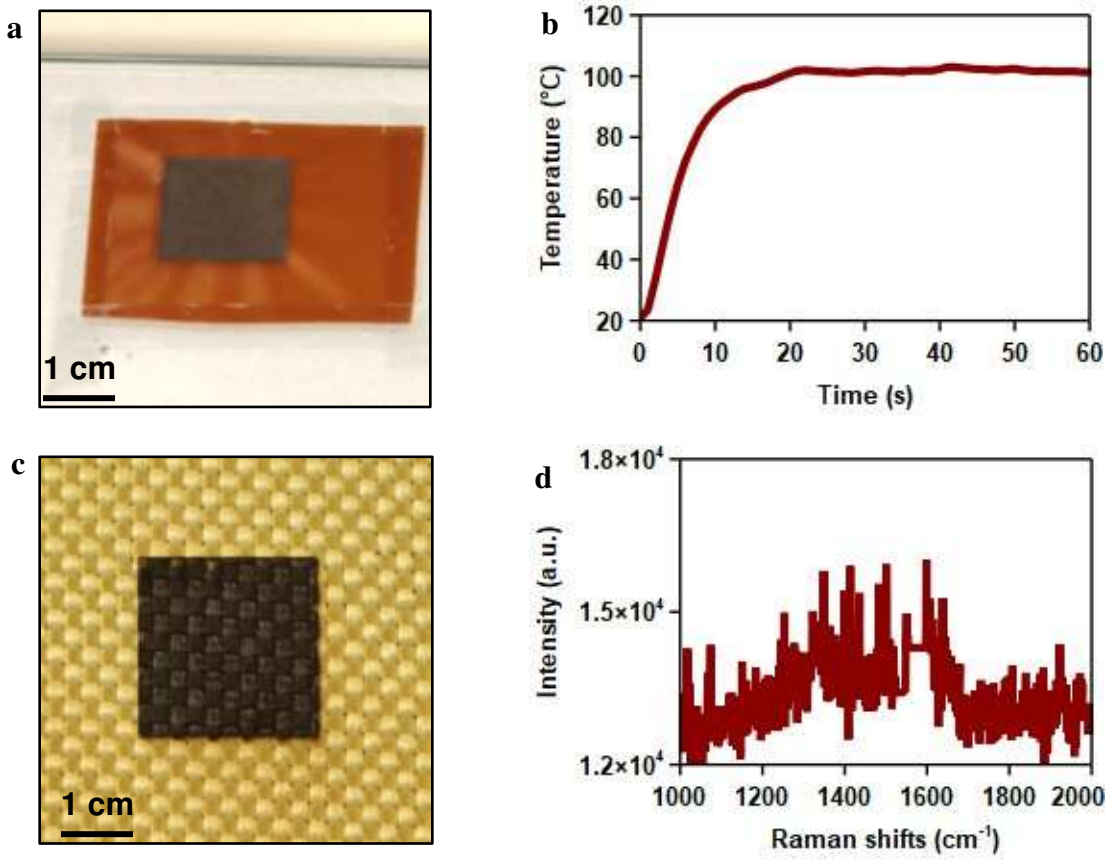

Figure B-1. Fabrication of LIG on polyimide film and aramid fabric using a blue laser. (a) The digital image of a LIG-PI film created using a blue laser. (b) The result of the electrothermal test performed on a 1 cm × 3 cm LIG-PI heater. (c) The digital image of an aramid fabric treated using a blue laser. (d) The Raman spectrum of the black layer formed on the aramid fabric.

Alternatively, LIG can be written on aramid fabric using a CO_2 laser. Aramid fabrics are less expensive substrate materials compared to polyimide films, provide a porous architecture for the easy infusion of solutions and resins, and are commonly used as fiber reinforcements in polymer composites. However, when the LIG-aramid fabric created using the blue laser (Figure B-1 c) was subjected to an electrothermal test, the results revealed that the lased material could not generate heat via the electrothermal effect. Raman spectroscopy was used to characterize the chemical composition of the black layer formed on the aramid fabric (Figure B-1 d). The lack of characteristic graphene bands in the Raman spectrum of the black layer demonstrated that the black layer is not LIG. Indeed, the blue laser only burned the aramid fabric and cannot supply the power required to convert the aramid fabric into graphene.

B.2 Fabrication of LIG-aramid fabric heaters using a CO_2 laser

Chapter 2 discussed creating and characterizing LIG-aramid fabric heaters using a commercial CO_2 laser. Figure B-2 shows the setup used for creating LIG-aramid fabric. The aramid fabric was taped down on a glass substrate using- heat-resistant tape to minimize the deformation of the fabric during the lasing process. Laser-induced graphene was then written on unidirectional and woven aramid fabrics to understand the effect of the architecture of the fabric on the quality of LIG-aramid fabric (Figure B-2 b, c). While the woven fabric maintained its integrity during the lasing process, the unidirectional aramid fabric fell apart due to the stresses induced in the fabric during the lasing process, making the unidirectional fabric an unsuitable precursor to create resistive heaters.

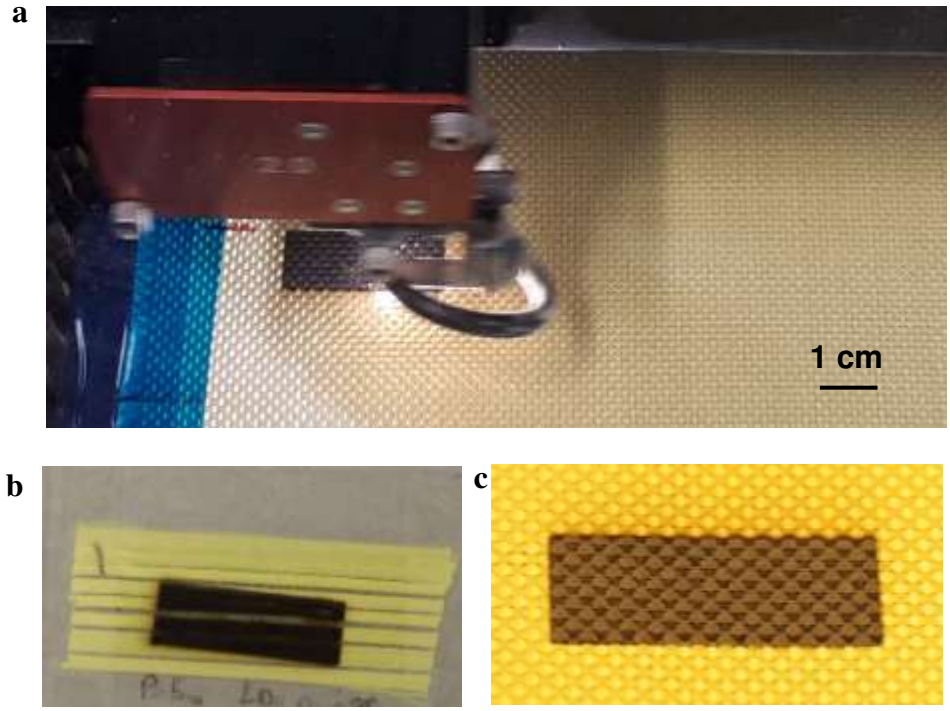

Figure B-2. Writing of LIG on aramid fabric using a CO_2 laser. (a) The set-up used to create LIG-aramid fabric. (b) Writing LIG on a unidirectional aramid fabric. (c) Writing LIG on a woven aramid fabric.

One of the unique advantages of LIG-based heaters is the ability to create patterned heaters, owing to the flexibility offered by the lasing platform. In this study, various complex LIG patterns were created on the aramid fabric (Figure B-3 a-c). However, the electrothermal test results showed poor electrothermal properties of the patterned heater (Figure B-3 d). Further experiments need to be conducted to address this issue, which was out of the scope of this study.

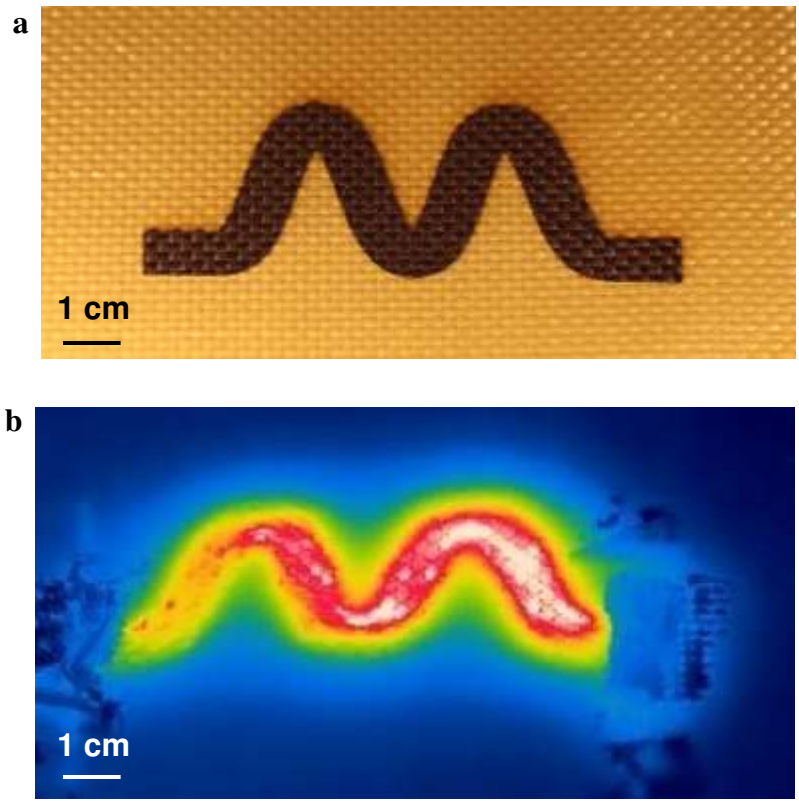

Figure B-3. Creation of an LIG patterns on aramid fabric. (a) The Digital image of the created pattern. (d) The infrared thermal image of the pattern shown in Figure B-3 a when an input voltage of 10 V was applied across the heater.